DESIGN AND DEVELOPMENT OF AN ELECTROSTATIC SEPARATOR FOR WASTE SEGREGATION

LAI KOON CHUN

DOCTOR OF PHILOSOPHY (ENGINEERING)

FACULTY OF ENGINEERING AND GREEN
TECHNOLOGY
UNIVERSITI TUNKU ABDUL RAHMAN
APRIL 2015

DESIGN AND DEVELOPMENT OF AN ELECTROSTATIC SEPARATOR FOR WASTE SEGREGATION

By

LAI KOON CHUN

A thesis submitted to the Department of Electronic Engineering,
Faculty of Engineering and Green Technology,
Universiti Tunku Abdul Rahman,
in partial fulfillment of the requirements for the degree of
Doctor of Philosophy (Engineering)
April 2015

ABSTRACT

DESIGN AND DEVELOPMENT OF AN ELECTROSTATIC SEPARATOR FOR WASTE SEGREGATION

Lai Koon Chun

Household solid waste is commonly disposed of in landfills, generating hazardous by-products such as leachate and methane gas from its organic contents. Thus, organics in landfills which consist mainly of food matter should be reduced. In this study, an electrostatic separator was designed and developed to segregate the organic food waste from waste mixtures. Principles of the electrostatic separation were discussed by referring to force models. Besides, the separation process of food waste was characterised with respect to both system and noise factors. The hard-to-control noise factors, i.e. size and moisture level of the feeding particles were then identified by employing a robust design based on Taguchi's method. Results revealed that the noise factors are key factors that should be properly selected so as to avoid undesirable sensitivity and variations of the separation process. The evaluation results confirmed that the system factors, i.e. rotation speed, electrical potential and electrodes interval are the most significant factors for the separation process. A statistical analysis with central composite design was conducted to analyse and model the performance of separation. Individual and interactive effects of independent factors on separation performance were assessed in terms of the recovery efficiency and purity of food waste matter.

For the system considered, the optimal operational conditions were deduced to be 60 rpm rotational speed, 30 kV applied voltage and 54 mm electrodes interval on particles with 4.0 mm size and 20 % water content. Under these conditions, food waste separation efficiency of 84.20% and purity of 93.00% were experimentally achieved. Separation efficiency and purity of non-food waste were respectively 88.70% and 98.50% under the same operational condition. These results fitted well with the predicted model. Results in this study concluded that the electrostatic separation could be an effective pre-treatment alternative in dealing with leachate and methane problems caused by landfilled organic wastes.

ACKNOWLEDGEMENTS

Acknowledgements are due to my supervisors, Associate Professor Dr. Lim Soo King and Dr. Teh Peh Chiong for their attention and support throughout this study. I am particularly grateful to Assoc. Prof. Dr. Lim, without whose advice this study would be harder to understand and appreciate. Thanks are also due to Dr. Teh, whose encouragement ensured the completion of the study.

Thanks are due to my employer, Universiti Tunku Abdul Rahman for funding the project. My sincere thanks to the Dean of Faculty of Engineering and Green Technology, Universiti Tunku Abdul Rahman for being supportive and understanding with the difficulties in working and studying at the same time throughout all these years.

I also would like to dedicate this thesis to my parents and colleagues. Many thanks are due to Professor Andrew Ragai Henry Rigit for his encouragement towards the end of the project, Dr. KH Yeap for the proofreading, Mr. Peter Chai and Mr. Michael Lee for their assistances and advices in fabricating and setting up the separator, Mr. Jiyuan Lee with the high voltage power source, and friends who have helped me in other ways especially Wymen and Christine. Last but not least, special thanks are due to my wife and my son, who have been very co-operative and also my source of inspiration.

APPROVAL SHEET

This dissertation/thesis entitled "***DESIGN AND DEVELOPMENT OF AN ELECTROSTATIC SEPARATOR FOR WASTE SEGREGATION***" was prepared by LAI KOON CHUN and submitted as partial fulfillment of the requirements for the degree of Doctor of Philosophy (Engineering) at Universiti Tunku Abdul Rahman.

Approved by:

_____
(ASSOC. PROF. DR. LIM SOO KING)
Date:
Associate Professor/Supervisor
Department of Electrical and Electronic Engineering
LKC Faculty of Engineering and Science
Universiti Tunku Abdul Rahman

_____
(DR. TEH PEH CHIONG)
Date:
Assistant Professor/Co-supervisor
Department of Electronic Engineering
Faculty of Engineering and Green Technology
Universiti Tunku Abdul Rahman

FACULTY OF ENGINEERING AND GREEN TECHNOLOGY

UNIVERSITI TUNKU ABDUL RAHMAN

Date: _____

SUBMISSION OF FINAL YEAR PROJECT /DISSERTATION/THESIS

It is hereby certified that **_LAI KOON CHUN_** (ID No: 10AED04870) has completed this ~~final year project/ dissertation~~/ thesis* entitled "*Design and Development of an Electrostatic Separator for Waste Segregation*" under the supervision of Assoc. Prof. Dr. Lim Soo King (Supervisor) from the Department of Electrical and Electronic Engineering, LKC Faculty of Engineering and Science , and Assist. Prof. Dr. Teh Peh Chiong (Co-Supervisor) from the Department of Electronic Engineering, Faculty of Engineering and Green Technology.

I understand that University will upload softcopy of my ~~final year project /dissertation~~/ thesis* in pdf format into UTAR Institutional Repository, which may be made accessible to UTAR community and public.

Yours truly,

_____
(*LAI KOON CHUN*)

*Delete whichever not applicable

DECLARATION

I hereby declare that the dissertation is based on my original work except for quotations and citations which have been duly acknowledged. I also declare that it has not been previously or concurrently submitted for any other degree at UTAR or other institutions.

Name   LAI KOON CHUN

Date _____

TABLE OF CONTENTS

LIST OF FIGURES

LIST OF TABLES

LIST OF NOMENCLATURES

Notation	Description	Unit
A	surface area	mm^2
B	Pareto percentage	%
C_{AD}	Air drag coefficient	-
d	Data dispersion	-
d_1	Corona electrode distance from roller	mm
d_2	Electrostatic electrode distance from roller	mm
D	Particle size	mm
E	Electric field strength	Vm^{-1}
F_{ad}	Air drag force	N
F_{ct}	Centrifugal force	N
F_e	Electrostatic force	N
F_g	Gravity force	N
F_i	Image force	N
FW_0	Mass of initial food waste in feeder	g
G_E	Electrodes gap	mm
k	Number of factor	-
K	Constant	-
m	Mass	g
m_{FW}	Mass in food waste tank	g
m'_{FW}	Mass of food waste in food waste tank	g
m_{NF}	Mass in non-food tank	g
m'_{NF}	Mass of non-food in non-food tank	g

n	Number	-
N	Rotation speed	min^{-1}
NF_0	Mass of initial non-food in feeder	g
P_{FW}	Separation purity of food waste	%
P_{NF}	Separation purity of non-food	%
Q	Particle charge	C
R	Radius of roller	mm
S_{FW}	Separation efficiency of food waste	%
S_{NF}	Separation efficiency of non-food	%
t	Thickness	mm
U	Supplied voltage	V
v	Number of level	-
v_r	Relative velocity	ms^{-1}
WC	Water content	%
y	Response	-

Greek

α_1	Corona electrode angle	deg
α_2	Electrostatic electrode angle	deg
β_0	Constant coefficient	-
β_i,	Coefficient of linear	-
β_{ii}	Coefficient of quadratic	-
β_{ij}	Coefficient of interaction equations	-
ε	Dielectric constant	Fm^{-1}
σ	Electrical conductivity	Sm^{-1}
ρ	Density	kgm^{-3}

ρ_c	Surface charge density	kgm^{-3}
ρ_r	Resistivity	Ωm
ω	Angular velocity	$rads^{-1}$

LIST OF ABBREVIATIONS

Notation	Description
ANOVA	Analysis of variance
CCD	Central composite design
DC	Direct current
ESD	Electrostatic discharge
FAO	Food and Agriculture Organization
FSC	Food supply chain
FW	Food waste
NF	Non-food waste
NIMBY	Not In My Back Yard
NSP	National Strategic Plan
OA	Orthogonal array
OVAT	One Variable At Time
PB	Plackett-Burman
PET	Polyethylene terephthalate
PS	Polystyrene
PTFE	Polytetrafluoroethylene
PVC	Polyvinyl chloride
RH	Relative humidity
RSM	Response surface methodology
SNR	Signal-to-noise ratio
SS	Sum of squares

CHAPTER ONE

INTRODUCTION

1.1   Research Background

Waste of food appears as a global dilemma in many countries. A study from Food and Agriculture Organization of the United Nations (FAO) reveals that 1.3 billion tonnes of food are wasted every year (FAOSTAT, 2012). Both the industrialised world and developing countries are suffered from this global threat (Gustavsson, 2010). Food loss and waste in different regions of the world is shown in Figure 1.1. Solid waste generation increases due to rural-urban migration, income per-capita increment and high demand of quality life from the citizens (Manaf, Samah and Zukki, 2009; Periathamby, Hamid and Khidzir, 2009). Rapid urbanisation and industrialisation in Malaysia make this country on a par as developed countries, which lead to increment of waste generation (Chua, Sahid and Leong, 2011).
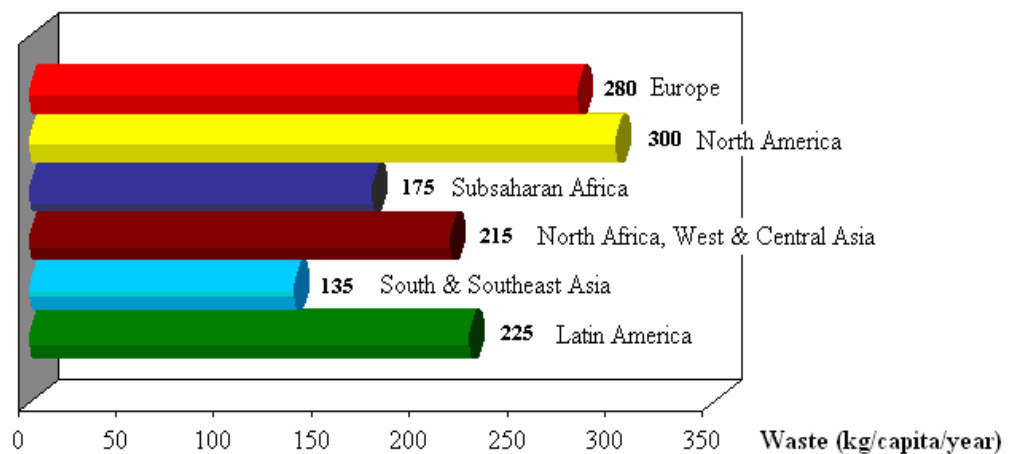
Figure 1.1: Food waste in different regions of the world (Gustavsson, 2010)

The solid waste generated per day in Malaysia has reached 17000 tonnes according to the National Solid Waste Management Department (2013). It is estimated that the daily wastes will increase to 30000 tonnes in 2020. The National Strategic Plan (NSP) for Solid Waste Management in Malaysia has introduced policy on waste management to prioritise waste reduction through processes of reducing, reusing and recycling since 2001. However, the policy does not lead to a positive result due to low awareness of citizens (Meen-Chee and Narayanan, 2006). Most food waste is disposed at the disposal site due to the lack of food waste recovery facilities, poor waste management in this country and NIMBY (Not In My Back Yard) syndrome (Saeed, Hassan and Mujeebu, 2009; Badgie et al., 2011). To date, source segregation of food waste is not commonly practised in Malaysia (Samsudin and Don, 2013).

In general, solid waste is disposed as landfills. Landfilling is the most general disposal method as compared to other approaches such as incineration and composting. This is highly attributed to its simplest and cheapest disposal procedures (Renou et al., 2008; Magdalena and Dana, 2014). Approximately 95% of collected municipal wastes are landfilled in Malaysia (Bashir et al., 2010). Although this could be the most practical waste treatment solution, landfilling does not seem to be the most rational approach to manage waste. Despite the inert solids, landfilling of food waste generates two main kinds of by-products, namely gaseous emission and fluidic leachate which can cause high contamination (Christensen et al., 2001; Desideri et al., 2003; Jaffrin et al., 2003). Landfill leachate is generally defined as a complex liquid

containing large amounts of organic (mainly food) and inorganic matter (Chian and De Walle, 1976). Landfill leachate becomes a hazardous source to groundwater aquifer and surrounding water sources for its high concentration of pollutants (Kjeldsen et al. 2002). Rainfall is the primary cause of leachate generation, followed by the biological decomposition activities taking place in the landfill. Besides, landfill gas such as methane and carbon dioxide due to the decomposition of biodegradable organic matter is a great source of pollution. It would pollute the air and cause public nuisance such as global warming and climate change (Tagaris et al., 2003).

Landfills in Malaysia are generally crowded and it is impractical to find new locations (Kathirvale et al., 2004). Therefore, proper food waste management is crucial in conserving a clean environment. It is not an uncommon practice to sort and reuse the waste materials. As shown in Figure 1.2, a high amount of organic material, particularly food waste (FW) (~45%) can be found in the municipal solid waste in Malaysia, followed by plastic (~24%), paper (~7%), metal (~6%), glass (~3%) and others (~15%).
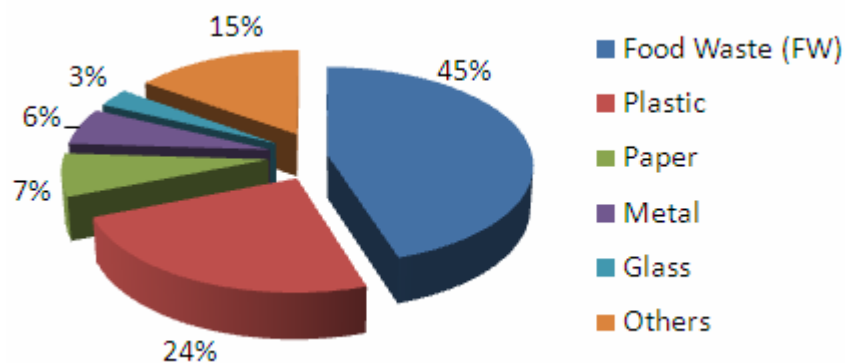
Figure 1.2: Solid waste composition (wt %) in Malaysia (National Solid Waste Management Department, 2013)

At present, studies of the recovery of plastic, glass and metal from solid waste have been widely carried out. However, to date, there is a lack of progress made for the FW recovery (Lin et al., 2013). The FW residues are in general turned into landfills or first generation recycling practices such as composting and animal feed (Kofoworola, 2007). Lately, researchers have placed high emphasis in food waste. This is because the high organic content in FW has the potential of being turned into highly added value end products, such as ethanol or a source of biofuel (Van Wyk, 2001; Le Man, Behera and Park, 2010; Moukamnerd, Kawahara and Katakur, 2013). Bioethanol is one of the most promising alternative energy sources to diminish the dependence on fossil fuel (McMilan, 1997). It can be produced by the fermentation of sugar-rich crops (e.g. sugar cane) and food wastes.

1.2   Problem Statements

Landfills consume large land area and it may cause undesired pollutions. Proper capturing and processing of landfills will turn the biogases emitted from landfills into renewable energy (Holm-Nielsen, Al Seadi and Oleskowicz-Popiel, 2009). The recovery of biogas from landfills can be profitable (Whalen, Reeburgh and Sandbeck, 1990). Incineration appears to be the lowest cost method, but the direct heavy metal emissions generated from the incineration process contribute significantly to human toxicity and environmental burdens (Tammemagi and Tammemagi, 1999; Xu, Chen and Hong, 2014). Hence, food waste contents from municipal solid waste are to be segregated in an environmental friendly way for the sake of independent

biogas production and landfill reduction. Source segregation is crucial for enabling the food waste to be reused and thus protecting the environment. Thus, the main aim of this study is to investigate the feasibility of an electrostatic separator in segregating non-food particles from the recoverable food waste.

Electrostatic separator is capable of separating particles based on the conductivities of the constituent components. It is widely used to sort out particles with high conductivities from those with relatively low conductivities. A number of studies have shown the capability of the separator in treating the electronic waste (Mohabuth and Miles, 2005; Yamane et al., 2011). Nevertheless, to the best of our knowledge, there is still a lack of research of electrostatic separator on the recovery of food waste being documented.

Food waste segregation with electrostatic separation process reduces the water and air pollutions and minimises the land usage for landfilling. Besides, the incineration of these landfill substances that are free from inorganic matters produces less residue and toxic gases. It contributes to less amount of landfill leachate with rare existence of organic matters in landfills. In addition to the environmental protection, the proposed segregation process indirectly enables the economical growth from biogas and potential biomass energy generation.

1.3 Objectives of the Thesis

Electrostatic separation of food waste still lacks of basic research, and it is crucial to carry out this study so as to increase the efficiency of the process. This project seeks to contribute to the fundamental knowledge that is required for future utilisation of practical sorting system. Therefore, the project is divided into the following steps:

i) developing an environmentally friendly way for waste segregation,

ii) characterising the performance of an electrostatic separator in terms of the separation efficiency and purity,

iii) designing a robust electrostatic separator which minimises random error, and

iv) modelling the separation process by determining the significant factors and the optimal operational conditions.

1.4 Outline of the Thesis

This chapter is the first of five chapters, which introduces the research background, problems and purposes of this study. Chapter 2 reports the general design of the electrostatic separator and the literature reviews. The electrostatic theory, various types of gas discharges, the separator applications and the descriptions of some related formulae are also described. The material and method required to run the experiment are qualitatively narrated in Chapter 3. The specifications of experimental equipment and the design parameters are elucidated using Taguchi's method. The mechanisms of the

6

corona formation process are introduced and the impact of the discharge of corona on various matters is described in this chapter.

Chapter 4 evaluates and discusses the electrical performances of the electrostatic separator with respect to its recovery efficiency and purity. The performance varies for different experimental designs. This phenomenon is thus studied in the same chapter by examining a number of potential influencing parameters. The optimal operational conditions are thus summarised by employing the optimisation method. Finally, Chapter 5 is devoted to conclusions and recommendations. The overall findings of this study are summarised and some recommendations are suggested for future improvement work.

CHAPTER TWO

LITERATURE REVIEW

2.1   Introduction

This review is intended to provide an up-to-date account of research on the electrostatic separation of wastes, with particular emphasis placed on the corona charging technique. The fundamentals of electrostatic such as discharge phenomena are introduced. In addition, information on typical designs and applications of electrostatic separator are reviewed. The former is becoming more important because of the knowledge required to predict charged granular waste dynamics. The design and construction of a robust separation system using Taguchi's method is discussed. Finally, the information essential for response surface methodology is briefly reviewed, in term of the selection of the design of the experiment and its applications.

2.2   Food Waste Overview and Treatment

Throughout the food supply chain (FSC), food loss can occur during the production stage and post-harvesting processes. Food waste is defined as the food loss at the retail and final consumption stages of the food chain, which relates to the behaviour of the retailers and consumers (Parfitt, Barthel and Macnaughton, 2010). In the retail stage, the foods include vegetables and

fruits which will be provided to wet markets, grocers and supermarkets. Before reaching the shelves, about 10-15% of them will be discarded for the reasons of improper handling, e.g. insufficient cooling storage. A large portion of crops is rejected before being distributed, due to the rigorous quality standards on the size, shape and appearance (Stuart, 2009). Upon reaching the consumption stage, wastage is once again generated from household, restaurants, hospitality sector, prisons, cafes and so on. Vegetables and fruits contribute the highest portion of food waste, if compared to cereal, roots and tubers, oilseeds and pulses, meat, fish and seafood, and milk. The waste of food does not only represent the waste of economic value, but also the waste of the limited natural resources such as water, nutrients, land and energy. Besides, the emission of greenhouse gases such as methane and carbon dioxide, due to the waste of food, it can cause global warming (Weitz et al., 2002).

Food waste in the consumption stage can be classified into two categories, namely pre-consumer food waste and post-consumer food waste. The pre-consumer waste gets its name for never being appeared in front of the consumer. For instance, overcooked, expired, contamination and trim waste contribute to this type of waste. Post-consumer waste, on the other hand, is mainly caused by the lack of awareness from both caterers and guests. The portion size and the behaviour of guests in the self-service buffet would lead to the waste of food (Garnett, 2006). Some authorities have started to put regulations on food waste management, before the food waste is sent for incineration or landfill. In Ireland, the Environmental Protection Agency and

the Clean Technology Centre published Waste Management (Food Waste) regulations 2009 to increase the recovery amount of food waste (Galway Country Council, 2013). Food waste from household must be source segregated, before being collected by an authorised waste collector. Source segregation refers to the waste segregation at source by the producers to avoid specified waste from being contaminated or mixed with others. Nevertheless, it strongly depends on the awareness of citizens and the continual enforcement from the policy authorities.

Pre-treatment of waste has recently received momentous interests. To date, researchers have studied the pre-treatment of organic waste with a number of processes. These include mechanical (Lindmark et al., 2012), thermo-chemical (Vavouraki, Volioti and Kornaros, 2014) and enzymatic (Taherzadeh and Karimi, 2008) treatments. However, very few studies were conducted using the electrostatic technique. Although electrostatic separation is not a common treatment for organic waste or food waste, it has received considerable attention for metal segregation from electronic waste (Veit et al., 2005).

Electrostatic separation provides an effective approach in recovering the reusable matter from solid wastes. It has been widely employed in applications involving dry separation process, e.g. to recover conductors from non-conducting mixtures (Lawver and Dyrenforth, 1973). The separation process sorts the charged bodies from the uncharged under an intensive electric field. It serves as an environmentally friendly way for recycling and

reusing the resources without giving negative impact to the surrounding (Kiewiet, Bergougnou and Brown, 1978).

2.3   Fundamental of Electrical Discharges

Upon energising by the high voltage electrical equipment, electrical discharge through the gaseous medium, or known as gas discharge, can be visible and audible. A gas discharge can be generated when the electrical energy passes through gas medium. A considerable amount of electrical charge should be created and stored. Studies show that gas discharges are formed by neutral and partially ionised particles. The negative charged particles (free electrons) drift in an opposite direction with the electric field. Owing to the elastic collisions with the molecules, the speed of the electrons is limited. When the field strength becomes larger and the collisions become inelastic, the ionisation effect happens and leads to an avalanche of charged particles. This process is known as gas discharging, where the electric field strength is higher than the electric breakdown of ambient gas at about 3 MV per meter. The constitution of electric current depends on the number of charges, the polarity and the speed with which they move. The interactions between particles have made the gas discharge a complex system which requires detailed investigations. Gas discharge phenomena can be classified typically into three categories, namely dark discharges (e.g. Townsend discharge), glow discharges and arc discharge. Various low pressure discharge modes between the parallel flat electrodes are schematically shown in Figure 2.1.
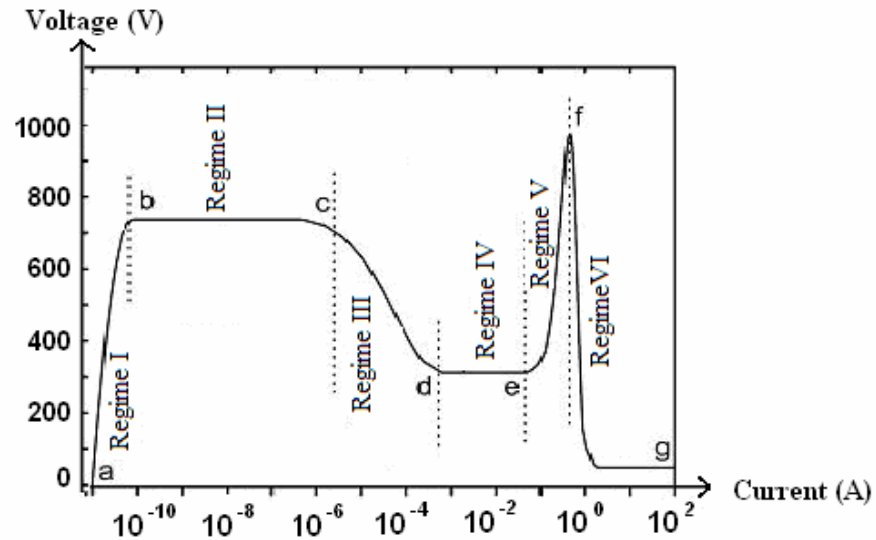
Figure 2.1: The voltage-current characteristic between parallel plate electrodes in a low pressure environment (Wagenaars, 2006)

There are six different discharge regimes, namely non-self-sustaining discharge (Regime I), Townsend discharge (Regime II), subnormal glow discharge (Regime III), normal glow discharge (Regime IV), abnormal glow discharge (Regime V) and arc discharge (Regime VI), which are described in the following subsections. It is clear that the observed voltage-current characteristic is highly non-linear.

2.3.1 Dark discharges

Dark discharge regions refer to the discharge regimes I and II as illustrated in Figure 2.1. The discharge is generally invisible to the eye, except for the corona discharges and the breakdown. By studying the voltage-current characteristic, different discharge modes or regimes can be thereafter recognised.

i) Regime I: Non-self-sustaining discharge

An extremely small current below 10^{-10} A can be measured when a low voltage of 200 to 500 V passes through an electrode gap with a few millimetres which containing gases such as oxygen and nitrogen. This is due to the fact that the cosmic rays or nearby UV lamp that generates the electrons in the gap. These few electrons produce a very small current and accelerate towards the anode by the potential difference. The applied voltage is not sufficient to ionise the atoms as observed in higher voltages. Therefore, it is not self-sustaining since the discharge requires external sources for the electrons generation. The discharge will cease when the electron source is removed.

ii) Regime II: Townsend discharge

The Townsend discharge is also named as dark discharge. This is because there is no substantial light emission from the discharge. Increasing in the applied voltage causes a changeover from a non self-sustaining discharge to a self-sustaining discharge. The electric field between the discharge gap enhances with the increasing of voltage. Electrons in the discharge gap ionise the neutral atoms and result in a multiplication of charged ions and electrons within the gap. Due to the impact ionisation, new electrons at the surface of the cathode experience a secondary emission into the gas. A sustainable current through the discharge gap is thus produced. The required voltage for

transition from a non self-sustaining to a self-sustaining discharge is called the breakdown voltage.

For Townsend discharge, the applied voltage of approximately 700 V is slightly higher than the breakdown voltage with a large resistance and a low current of 10^{-10} to 10^{-6} A. The space charge effect in the discharge gap is not significant as there are a limited number of charged particles. As it can be seen in Figures 2.1 (Regime II), the voltage-current curve for the Townsend discharge is consistently constant. This is due to the fact that the avalanche process takes its place in the gap. The increased voltage directs higher electron multiplication and produces more secondary emission of electrons at the cathode. The process results in a further multiplication of charges and electrons in the gap. In other words, the current rises considerably with a small increase in voltage.

2.3.1.1 Corona discharge

Corona discharge is a relatively weak luminous electrical discharge which takes place at or near the atmospheric pressure. The corona is created by a strong electric field using small needles or sharp edge on the electrode (Chang et al., 1995). Corona discharge may be considered as a Townsend discharge depending on field and potential distribution (Schütze et al., 1998). This discharge which emits from the electrode appears as a faint blue-violet filamentary discharge, differs from the applied field polarity and the geometrical configuration of electrodes. The coronas can be positive or

negative, depending on the potential polarity of the electrode. For instance, electrode with positive charge generates positive corona and vice versa.

Corona discharge has a relatively slower energy release compared with other gas discharges. The discharge does not leave any definite traces, but secondary effects such as wettability improvement of the directed material surface. Corona discharge can exist in two ways, i.e. passive and active, as illustrated in Figure 2.2. Passive corona in Figure 2.2 (a) refers to the conducting needle electrode connected to ground and exposed to an electric field by the sphere conductor. When the needle is moved towards the electric field until the field strength reaches the breakdown of ambient air, corona discharge is emitted in within the gap. On the other hand, the use of high voltage power supply denotes the active corona as shown in Figure 2.2 (b). The process is reversible to the passive corona, where the power supply applies a high potential to the needle for producing corona discharge. Active corona is widely used to charge objects electrostatically, such as powder coating, electrostatic copying and separation applications.
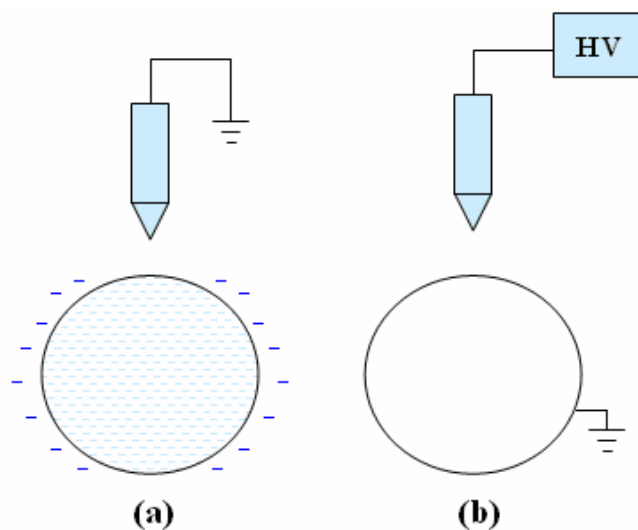
Figure 2.2: Type of corona discharges (a) passive corona, (b) active corona

As the ion-emitting plasma of one polarity will accumulate in the inter electrode space, the corona discharge is mostly limited by the space charge. Consequently, the corona has a positive resistance characteristic that a higher voltage is required with increasing current. As soon as the current in the discharge is adequately raised, additional current-carrying species will be produced and thus the spark discharge will be generated.

2.3.1.2 Spark discharge

Generally, if the source for a discharge is limited, the electrical discharge tends to manifest itself into a rapid impulse type filament discharge form known as spark. The existence of the spark discharge symbolises a complex physical phenomenon that relies on plentiful of variables such as pressure, electrode gap and electrode geometry. Spark can be formed when the applied electric field strength is higher than the dielectric field strength of air. This sporadically discharge redistributes charge and form regions of excess charge, which may create a highly conductive path from the electrode to the surrounding conductor. In electrostatic separation process, spark discharge is considered an undesired phenomenon as it may bring damage to the equipment and harm the operator.

2.3.2   Glow discharges

Discharges in regimes III, IV and V as illustrated by Figure 2.1 are classified as glow discharges, owing to the generation of luminous glow. Glow

discharge occurs once the breakdown voltage is reached. The discharges emit light due to the high enough electron energy of 1 to 5 eV and density, typically of the order of 10^6 to 10^{13} cm^{-3}, to generate excited gas atoms by collisions. Glow discharge is widely applied in various applications which include fluorescent lighting and plasma television.

i) Regime III: Subnormal glow discharge

Space charge effects are apparent in the discharge gap when the voltage further increases from that of previous regime II. The space charge is most likely positively due to the big mobility difference between the electrons and ions (Chang et al., 1995). As the positive space charge accumulates in front of the cathode, a cathode fall region is thus formed. Cathode fall, or known as cathode dark space, refers to the relative dark region near the cathode. The voltage drop in the cathode fall is almost equivalent to the voltage difference across the electrodes. Typically, the electron multiplication across the cathode fall enhances when the electron multiplication increases under a higher electric field. This has resulted in a lower required voltage in order to sustain the discharge. Hence, the voltage decreases with the increasing current as shown in the voltage-current curve in Figures 2.1 (Regime III). This mode is not stable and easily changed to the glow discharge mode.

ii) Regime IV: Normal glow discharge

In normal glow discharge mode, the minimum of sustaining voltage can be attained as the development of the cathode fall is completed. As there is a contact between the plasma with the cathode surface, the electrode current density remains with the current change. In other words, the increased current has no effect on the voltage change, but to spread the discharge over the surfaces of the electrode. The glow discharge regime stops when the entire electrode surfaces are covered by the discharge. The discharge voltage in this regime is consistent over a large variation range of current (10^{-3}-10^{-1} A).

iii) Regime V: Abnormal glow discharge

The discharge covers entire electrodes in this mode. The cathode fall increases with the increasing current and the voltage across the electrodes ascends sharply. Consequently, the average ion energy increases with enhancement of cathode current density. The ion bombarding the cathode surface generates thermionic emission and turns the glow discharge into the arc discharge.

2.3.3 Arc discharge

Arc discharge is the discharge regime VI shown in Figure 2.1. The transition of glow into arc discharge is observable when the current is further increased. An electric arc is a type of electric discharge which has the highest

current density, extending from an order of 0.1 to 1 A to a very large (10 kA) upper limit. Arc discharge is commonly used for industrial applications such as welding and plasma cutting. However, undesired arcing can bring harmful damages to the power stations, electrical transmission systems and equipment.

2.4   Electrostatic Separator

Electrostatic discharge (ESD) is one of the electrical discharges. It occurs when two electrically charged items contacting each other and generates a flow of electricity. The charge is typically applied in the electrostatic separator. Electrostatic separator sorts two items or substances based on the differences in electrical characteristics such as friction charges and surface resulting work function. This separation is a crucial manufacturing process in the ore beneficiation industry to remove the impurities. In general, the separation system does not only rely on electrostatic force, but also on the gravitational and centrifugal forces. As the electrostatic force is inversely proportional to the surface area, the separation works efficiently for the small and light-weight substances such as thin sheet and short wires.

2.4.1   Typical separation techniques

Electrostatic separator typically sorts two different types of substances (with different electrostatic characteristics) at once. Prior to the electrostatic separation, the substances are typically charged by friction charge, induced charge or corona charge before subjecting to the electrostatic and gravity

forces. Implementations of various charging methods are illustrated in Figure 2.3.
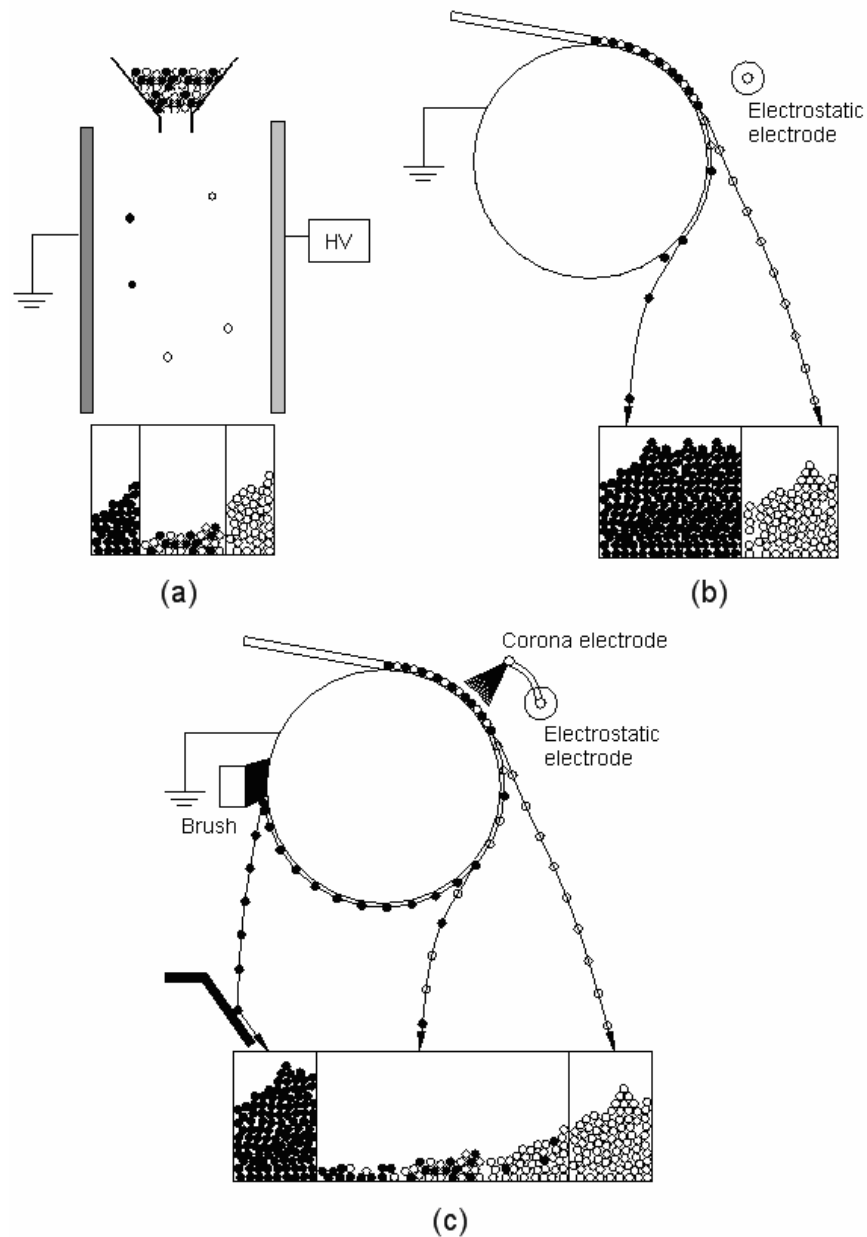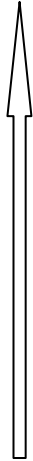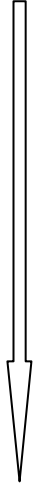
Figure 2.3: Typical electrostatic separation techniques (a) triboelectric (b) induction (c) corona charging (Chang, Crowley and Kelly, 1995)

Triboelectric charging equipment as shown in Figure 2.3 (a) consists of a vibration feeder, collection tanks and parallel plate electrodes connecting to high voltage supply. The charging activity takes place in the vibrating feeder

and turning the substances into either positively charged or negatively charged. The charging tendencies can be referred in the triboelectric series Table 2.1. The positively charged substance tends to move toward the negative electrode, whereas the negatively charged tends to move in an opposite direction.

Table 2.1: Triboelectric series (Harper, 1967)

Human hands	Positively charged
Glass	
Nylon	
Human hair	
Wool	
Aluminium	
Food	
Paper	
Cotton	Neutral
Steel	
Wood	
Hard rubber	
Brass	
Polyester	
Polyethylene	
PVC (Vinyl)	
Teflon	Negatively charged

This separation technique relies on the magnitude of supplied voltage and the gravitational force. Thus, it is suitable for applications with large gravity difference, such as removing impurities (ashes) from ore particles. In addition, it can be combined with the cyclone type separator, as shown in Figure 2.4, to provide better separation efficiency.
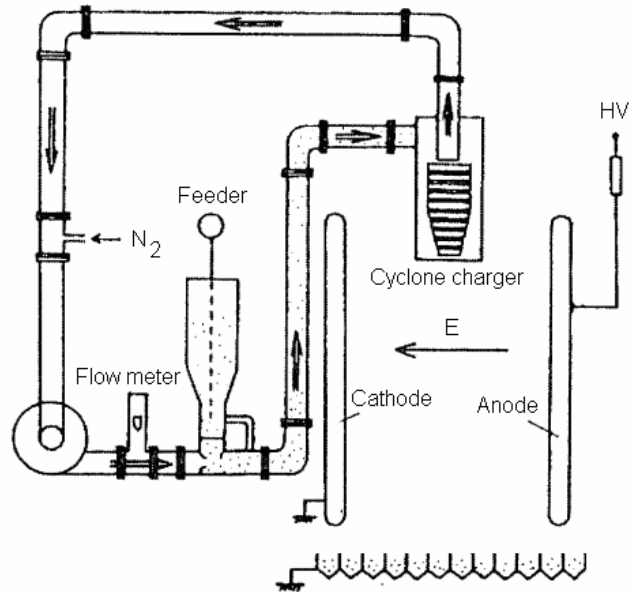
Figure 2.4: Cyclone electrostatic separator (Toraguchi and Haga, 1982)

Induction charging separator can be applied in the food processing industry to remove the impurities such as hair, plastics and waste straw. The food is placed on a vibrating conveyor belt under multiple high voltage electrodes, as shown in Figure 2.5. The charged impurities are to be moved toward the electrodes and carried away by a suction pump. This technique ensures the foods are not in contact with the electrodes due to hygienic purposes.
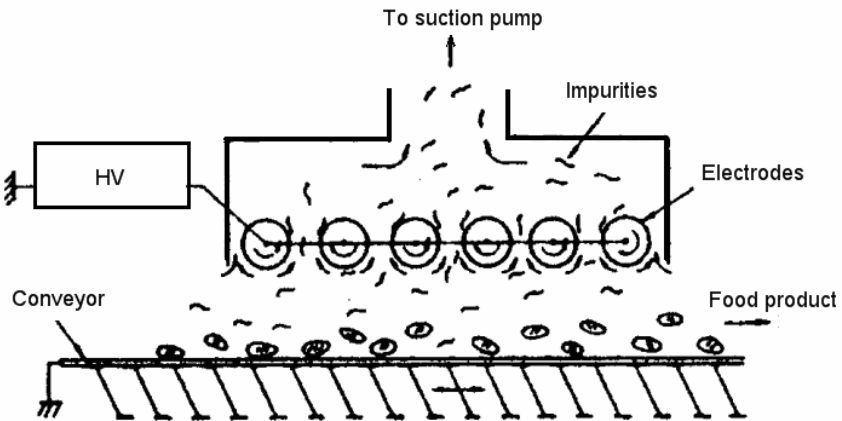
Figure 2.5: Induction type electrostatic separator (Masui, 1982)

In the waste processing industry, the corona charging separator can be used to recover copper from used electrical wire, or to separate scrap papers from the paper-plastic mixture. This technique is free from pollution as it does not involve burning or chemical reaction. As demonstrated in Figure 2.6, the substances on the roller surface are subjected to an electric charge, ionised from the needle corona electrode and eventually separated due to the differences in conductivity and electrostatic properties.
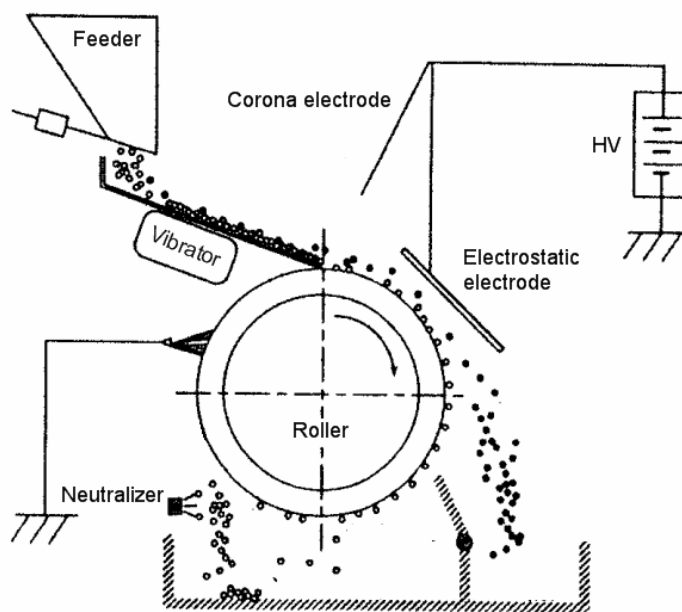
Figure 2.6: Corona charging type electrostatic separator (Masui, 1982)

2.4.2   Applications and design consideration

Electrostatic separation has long been applied in the mining industry. For instance, the ores with good conductivity such as iron and magnesium can be separated from quartz and silica which have poorer conductivity. Back in 1982, Murata et al. (1982) has utilised the method to separate copper particles ranging from 37 to 840 μm in diameter. The particles were put on an inclining plate electrode under a non-uniform electric field. The results revealed that the particles could be sorted to the collecting boxes, and the sorting efficiency increases with increasing particle size difference as the forces exerted on the smaller particle could be easily differentiated from that of larger particle.

In the past decade, Iuga et al. (2001) applied the technique in processing granular wastes of chopped electrical wires to remove polyvinyl chloride (PVC) wires insulation from the copper conductor. Moreover, they utilised the electrostatic force for feldspar extraction from pegmatite which contains quartz and muscovite mica. It was summarised that electrostatic separation is a better way for mineral beneficiation techniques, as compared to flotation method and magnetic sorting, especially for small granular sizes (i.e. < 0.5 mm) (Iuga et al, 2004).

Recently, Ravishankar and Kolla (2009) stated that the separation efficiency is not only affected by particle sizes, but also other factors such as humidity and temperature. Inline with the arguments, several studies had been made to analyse the different electrostatic separation processes. Elder et al.

(2003) concluded the separation efficiency of mineral sand relies on the rotation speed, electrodes configuration, temperature of granule and other parameters. Besides, Aman et al. (2004) identified that the supply potential and electrode position to be the key factors for metal recovery. A study from Calin et al. (2008) revealed that the different compositions may affect the separation results in separating plastic mixtures. In short, electrostatic separation is a multi-factorial process which requires simultaneous control of both mechanical and electrical forces on the granular mixtures (Samuila et al., 2005). Various parameters could affect the performance of the separation process.

2.5   Taguchi's Method

In order to make the process less sensitive to the effects of random variability, one may classify various design factors into two groups, namely system factor and random (or noise) factor. A robust design should be made to reduce the variations of the process conditions caused by the random factors, such as manufacturing variation and component deterioration. Robust design refers to a proper experimental arrangement that makes the process insensitive to the sources that are hard to control in practical conditions. This design, implemented by using Taguchi's method (1986), is a statistical technique in enhancing the manufactured goods' quality. It identifies the dominant process parameters and determines the appropriate operational environment in which an experiment is to be performed. Given a general model of control system as shown in Figure 2.7, Taguchi's method can be employed to:

(i) determine which factors are influential on the response output y

(ii) determine where to set the influential controllable system factor x so that the variability in y is small

(iii) determine where to set the influential controllable x so that the effects of the uncontrollable noise factor z are minimised
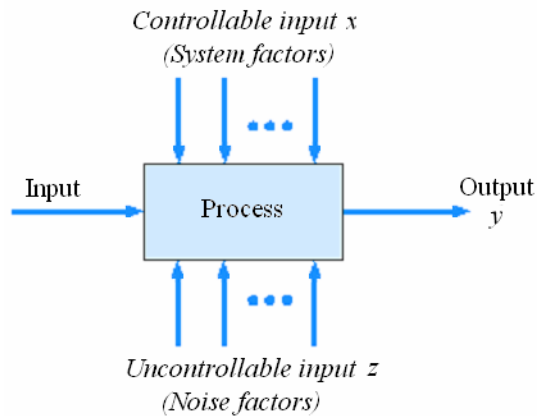
Figure 2.7: General model of control system.

Taguchi's method has been applied in the industries and it has been proven to be a critical success in controlling the quality of process (Dascalescu, 2008). Basavarajappa et al. (2008), Davidson et al. (2008), Hsu et al. (2009) and Mahapatra et al. (2008) have utilised Taguchi's method in analysing the impacts caused by various parameters such as speed of the experimental tools. The interactions between the empirical factors and responses were discussed. Chiang and Hsieh (2009), Comakli et al. (2009), Keles (2009) and Lin et al. (2009) have employed the same approach in process optimisation and performance evaluation. The aim was to identify the optimal operational conditions. Taguchi's experimental design, which is based only on a minimum number of experiments, provides a reliable model for criterion selection and decision making (Chou, Ho and Huang, 2009).

2.5.1　Array design

Taguchi's method is a robust parametric analysis technique with reduced the number of experiments (Senthilkumar, Senthikumaar and Srinivasan, 2013). Taguchi's methodology of experimental design is based on an orthogonal array (OA) arrangement, where the inner array and outer array are respectively the system factors and random factors. In a typical design, a total of four factors were varied by three different levels. In the full factorial design, a total of 3^4 or 81 set of experiments are required to be performed and studied. However, only nine experiments (L-9 orthogonal array) were required for this four-factor-three-level system by using Taguchi's method. This has reduced the time and cost to acquire the same necessary results. Given a process with four factors (A, B, C and D) and three levels (L1, L2 and L3), the responding L-9 OA was thus formed, as tabulated in Table 2.2.

Table 2.2: L-9 orthogonal array design

| Experiment | Factors | | | |
No.	A	B	C	D
1	L1	L1	L1	L1
2	L1	L2	L2	L2
3	L1	L3	L3	L3
4	L2	L1	L2	L3
5	L2	L2	L3	L1
6	L2	L3	L1	L2
7	L3	L1	L3	L2
8	L3	L2	L1	L3
9	L3	L3	L2	L1

The L-9 orthogonal array is equivalent to a 2-(v, k, 1) array, or a set of (k-2) mutually Latin squares of order v, where v and k respectively denote the number of levels and number of factors. In other words, the L-9 orthogonal array in this study is a 2-(3, 4, 1) array, resulting in a 3^{4-2} fractional factorial design. The first (indexing) column of the table is an array on v-set and other columns appeared as square arrays of order k. The first square array is a transpose array of the indexing column, whereas the resulting square is the Latin squares of order v. Latin square is a $v \times v$ array in which each entry occurring exactly once in each row and each column.

2.5.2   Signal-to-noise ratio

A signal-to-noise ratio (SNR) is used as the objective function to determine the robustness. It relies on the orthogonal array output, which specifies the effects of various factors on the response formation. There are three different types of objective functions, namely nominal-is-best, larger-is-better and smaller-is-better. Nominal-is-best type of objective function can be used to determine the characteristics that are needed to be drawn as close as possible to a nominal response value, which is shown in equation (2.1):

$$\text{SNR} = 10\log\left(\frac{\overline{y}}{\overline{s}}\right)^2 \qquad\qquad (2.1)$$

where $\overline{y}$ is the mean of responses and $\overline{s}$ is the standard deviation. Larger-is-better type of objective function identifies the characteristics for the response

to have its maximised value. Similarly, smaller-is-better type targets for the minimised value of the response.

Larger-is-better type of objective function is defined as:

$$SNR = -10\log\left(\frac{1}{n}\right)\sum_{i=1}^{n}\frac{1}{y_i^2} \qquad (2.2)$$

whereas smaller-is-better type of objective function is calculated by:

$$SNR = -10\log\left(\frac{1}{n}\right)\sum_{i=1}^{n}y_i^2 \qquad (2.3)$$

where n is the number of sample and y_i is the response collected in each evaluation. The relative significance of the factors on the response can be analysed by studying the percentage (%) impact that determined by:

$$\%impact = \frac{\left(SNR - \overline{SNR}\right)^2}{\sum\left(SNR - \overline{SNR}\right)^2} \qquad (2.4)$$

where $\overline{SNR}$ is the mean value of SNR.

2.6   Response Surface Methodology

Response surface methodology (RSM) is an effective way to use with multivariable system to determine the interactions among system factors and to predict the response. It has been successfully employed to several optimisation processes such as nickel removal (Aravind et al., 2013) and wastewater denitrification (Srinu Naik and Pydi Setty, 2014).

2.6.1 Operational design

A number of factors can be analysed simultaneously with proper design of experiments (Rezouga et al., 2009). Besides, the optimisation results deduced from the statistical analysis reduce the computing effort and cost (Vlad et al., 2014).

In order to identify the critical points in RSM, the response is expressed as a quadratic model according to the following polynomial function:

$$y = \beta_0 + \sum_{i=1}^{p} \beta_i X_i + \sum_{i=1}^{p} \beta_{ii} X_i^2 + \sum_{1 \leq i \leq j}^{p} \beta_{ij} X_i X_j + e_i \qquad (2.5)$$

where β_0 is a constant coefficient, X_i, X_j are independent variables, β_i, β_{ii}, β_{ij} are the coefficients of linear, quadratic and interaction equations, and e_i is the error. Equation (2.5) can be rewritten as:

$$y = \beta_0 + \beta_1 X_1 + \beta_2 X_2 + \beta_3 X_3 + ... + \beta_p X_p + \beta_{11} X_1^2 + \beta_{22} X_2^2 + \beta_{33} X_3^2$$
$$+ ... + \beta_{pp} X_p^2 + \beta_{12} X_1 X_2 + \beta_{13} X_1 X_3 + \beta_{23} X_2 X_3$$
$$+ ... + \beta_{p-1p} X_{p-1} X_p + e \qquad (2.6)$$

2.6.2 Analysis of variance

Analysis of variance (ANOVA) was employed to assess the fitted quality of model and statistical significance of regression coefficients. ANOVA compares the change of variable levels and the variation due to

random errors of response measurement (Lee and Lee, 2012). The data dispersion (d) for each observation (x) is obtained using the equation:

$$d = (x - \bar{x})^2 \tag{2.7}$$

The total sum of square (SS_{tot}) adds all observation dispersions:

$$SS_{tot} = SS_{reg} + SS_{lf} + SS_{pe} \tag{2.8}$$

$$SS_{reg} = \sum_i^m \sum_j^n \left(\tilde{x}i - \bar{x} \right)^2 \tag{2.9}$$

$$SS_{lf} = \sum_i^m \sum_j^n \left(\tilde{x}i - \bar{x}i \right)^2 \tag{2.10}$$

$$SS_{pe} = \sum_i^m \sum_j^n \left(x_{ij} - \bar{x}i \right)^2 \tag{2.11}$$

where SS_{reg}, SS_{lf}, SS_{pe}, m, n and $\tilde{x}$ are the sum of error due to regression, sum of error due to loss of fit, sum of error due to pure error, number of level, number of observation and estimated value, respectively. The model quality is evaluated by values of the significance of regression test (F-value,$_{reg}$) and the lack of fit test (F-value,$_{lf}$). A significant regression and a non-significant lack of fit imply that the model could be fitted well to empirical data. The values of the mentioned tests can be determined by using equations (2.12) and (2.13):

$$F_{reg} = \frac{n-k}{k-1} \cdot \frac{SS_{reg}}{SS_{lf} + SS_{pe}} \tag{2.12}$$

$$F_{lf} = \frac{n-m}{m-k} \cdot \frac{SS_{lf}}{SS_{pe}} \tag{2.13}$$

31

where k is the number of parameters of the model.

Accuracy of the model can be measured by the coefficient of determination, or known as R^2:

$$R^2 = 1 - \frac{SS_{lf} + SS_{pe}}{SS_{tot}} \qquad (2.14)$$

A larger value of R^2 is desirable as it means higher accuracy. The optimum conditions of the quadratic model can be determined by calculating the critical points. The quadratic function, equation (2.6) for three variables can be described as the first grade system in equations (2.15) to (2.17):

$$\frac{\partial y}{\partial X_1} = \beta_1 + \beta_{12} X_2 + \beta_{13} X_3 + 2\beta_{11} X_1 \qquad (2.15)$$

$$\frac{\partial y}{\partial X_2} = \beta_2 + \beta_{12} X_1 + \beta_{23} X_3 + 2\beta_{22} X_2 \qquad (2.16)$$

$$\frac{\partial y}{\partial X_3} = \beta_3 + \beta_{13} X_1 + \beta_{23} X_2 + 2\beta_{33} X_3 \qquad (2.17)$$

In order to obtain the optimum values, partial differentiations of output response y with respect to X_1, X_2 and X_3 are set to zero. The critical point, i.e. the maximum and minimum coordinates of X_1, X_2 and X_3, can be obtained by satisfying equations (2.15) to (2.17) and solving the system.

2.7 Force Model

Electrostatic separation process relies on the forces act on the particles, allowing to be sorted out from a mixture. A number of forces exist in the process. This includes the pinning force induced by the corona electrode and the mechanical centrifugal force due to rotation. Figure 2.8 illustrates the forces that act on a particle during the separation process.
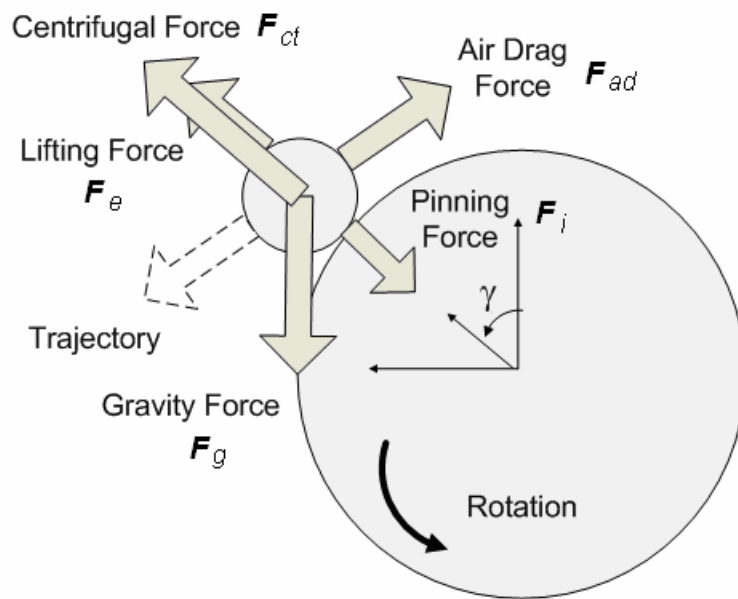
Figure 2.8: Forces act on particles (magnitude not according to scale)

The five forces were summarised as (i) centrifugal force due to the rotation, (ii) lifting force due to the attraction by electrostatic electrode, (iii) gravity force, (iv) pinning force due to the ion generation from the corona electrode on the insulative particles, and (v) air drag force due to air friction. The deposition of particles from the feeder was set to 12 g/min in order to form a monolayer on the surface of the roller.

The particles that pass through the corona ionising zone are subjected to ionising and pinning effects generated by the corona electrode. According to Lu et al. (2008), the induced pinning force, or known as image force, F_i correlates to the size of the particles and is defined as:

$$F_i = \frac{Q^2}{4\pi \cdot t^2 \varepsilon_1} \tag{2.18}$$

where Q is particle charge, t is the particle thickness and ε_1 is dielectric constant of particle. The electrostatic electrode located downstream the corona electrode induces a lifting force, the strength of which relies on the electric field. The lifting force, also known as electrostatic force, F_e, applied on the particles was calculated by:

$$F_e = QE = K\varepsilon_1 E^2 \rho_c \tag{2.19}$$

where K is a constant, E is the electric field strength and ρ_c is the surface charge density. The gravity force, F_g, acted on the mass, m, of the particles was defined as:

$$F_g = mg = \rho At \cdot g \tag{2.20}$$

where A is the surface area of particle and ρ is the density of the particle.

The centrifugal force applied on the particles is generated by the roller which rotates in counter-clockwise angular direction. This force, F_{ct}, is always at an opposite direction to that of the pinning force and computed as (Younes et al., 2007):

$$F_{ct} = \rho A t \omega^2 R \tag{2.21}$$

where R is the radius of separator roller, ω is the angular velocity and ρ, A, t are the density, surface area, thickness of the particle respectively. An air drag force, F_{ad} in an opposite direction from the rotational trajectory provides friction to the particles. It can be determined by:

$$F_{ad} = \frac{1}{2} C_{AD} \cdot A \rho v_r{}^2 \tag{2.22}$$

where C_{AD} is the air drag coefficient and v_r is the relative speed of particle.

2.7.1 Food waste

Due to the dissimilarity of surface resistivity, the charges acted on food waste particles differed from that of on non-food particles. For instance, when both food and non-food particles were moved into the corona ionising zone, the more conductive food particles discharged rapidly to the grounded roller if compared to the non-conductive plastic and glass particles. Figure 2.9 illustrates the combination of forces applied on the food particles.
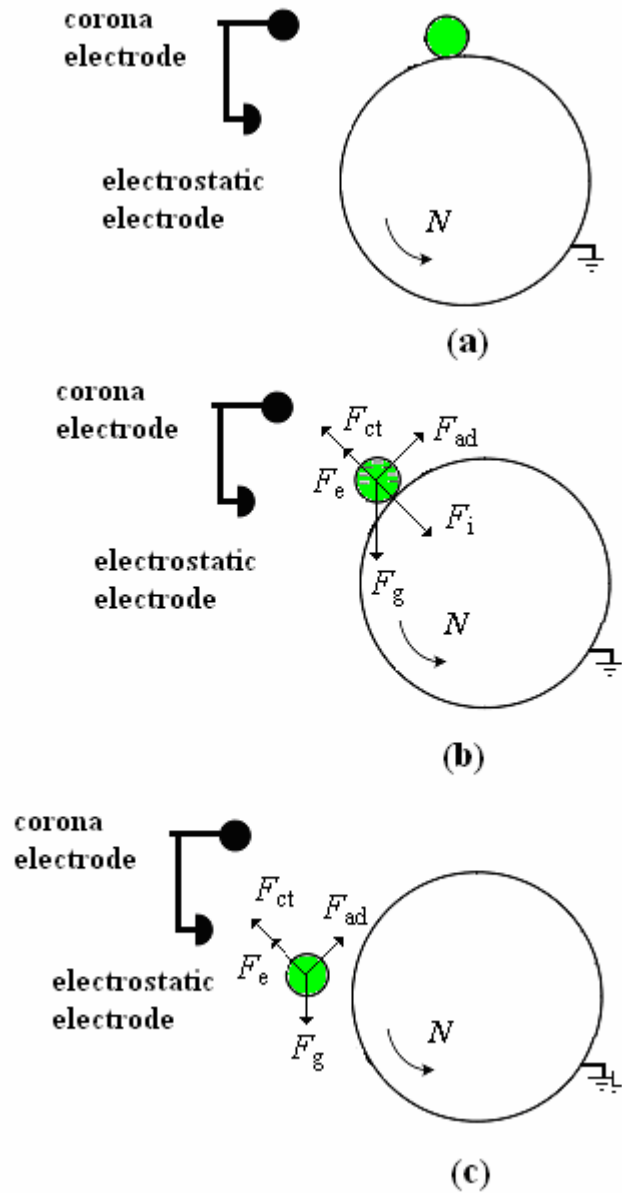
Figure 2.9: Forces exerted on food particles in (a) feeding, (b) ionising and (c) detaching stages (Li et al., 2007)

Figure 2.9 (a) shows the food particle being deposited onto the surface of the roller rotating in a counter-clockwise direction. When the food particle passed by the ionising zone as shown in Figure 2.9(b), it experienced a combination effect of air-drag force, centrifugal force, electrostatic force, pinning force and gravity force. However, since the food particle is

dissipative, the charges on it were discharged through the grounded electrode and the effect of pinning force was weakened. Dissipative particle allows the charges to flow to ground more slowly than the conductive particle. The resulting force equilibrium state can be hence determined as:

$$F_g \cos\gamma = F_{ct} + F_e \qquad (2.23)$$

and

$$F_g \sin\gamma = F_{ad} \qquad (2.24)$$

In order to detach from the ground rotating roller towards the food collection tank as shown in Figure 2.9(c), the mechanical and electrical forces exerting on the conductive food particle have to be satisfied,

$$F_{ct} + F_e \geq F_g \cos\gamma \qquad (2.25a)$$

or

$$\rho A t \omega^2 R + k \varepsilon_1 E^2 \rho_c \geq \rho A t g \cos\gamma \qquad (2.25b)$$

It is noticeable in equation (2.25b) that the process relies on the properties of the particle (i.e. density, area, and thickness), roller configuration (i.e. rotation speed and roller radius), electric field strength, particle surface charge and position of corona electrode (angle γ). In this study, properties of the particles were set to have small variability (further discussion in chapter 3). Impact of these variables on the separation performance was insignificant if compared to the rotational speed and electric field strength. The two parameters were then defined as the system factors in this study for the parametric studies and the assessment of system robustness in chapter 4.

2.7.2 Non-food waste

Unlike dissipative particles, electrostatic force is absent in insulative non-food particle. Non-food particle experiences only air-drag force, centrifugal force, pinning force and gravity force, as shown in Figure 2.10.
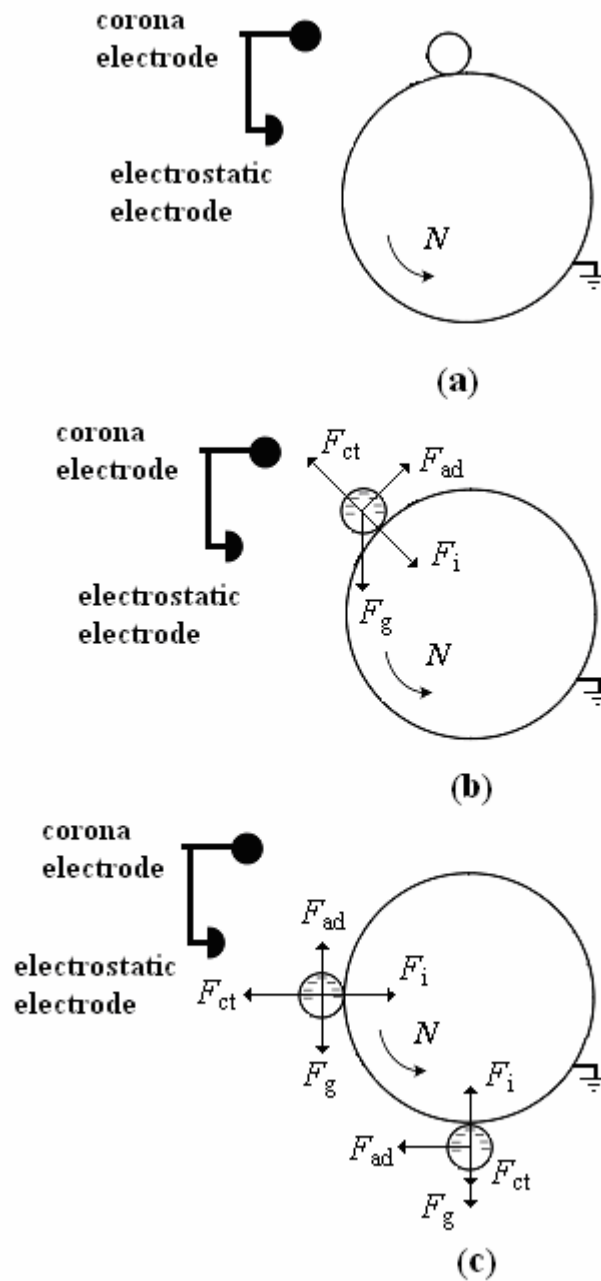
Figure 2.10: Forces exerted on non-food particles in (a) feeding, (b) ionising and (c) detaching stages (Li et al., 2007)

As shown in Figure 2.10(b), the force equilibrium state can be calculated by:

$$F_{ct} = F_i + F_g \cos \gamma \qquad (2.26)$$

and

$$F_g \sin \gamma = F_{ad}$$

In contrast with food particle, the non-food particle was to be kept attached to the roller surface before reaching the brush. This ensures the particle to drop into the non-food collection tank. Thus, the following conditions have to be satisfied:

$$F_i + F_g \cos \gamma \geq F_{ct} \qquad (2.27a)$$

or

$$\frac{K\varepsilon_2 E^2 \rho^2{}_c}{t^2} + \rho A t g \cos \gamma \geq \rho A t \omega^2 R \qquad (2.27b)$$

where K is a constant and ε_2 is dielectric constant of the non-food particle. As the non-food particle travelled to a point that $\gamma = \pi$, equation (2.27a) can be rewritten as:

$$F_i \geq F_{ct} + F_g \quad , \text{ when } \gamma = \pi \qquad (2.28a)$$

or

$$\frac{K\varepsilon_2 E^2 \rho^2{}_c}{t^2} \geq \rho A t \omega^2 R + \rho A t g \qquad (2.28b)$$

It was apparent that a high electric field strength, E was required to generate large pinning force on the non-food particle. Alternatively, the slow rotation speed of the separator could ensure that the condition stated in

39

equation (2.28) can be satisfied and it maintains a minimised usage of electricity. However, slow separation process was undesirably for productive outputs and hence the moderate range of speed should be therefore selected. By observing equations (2.25) and (2.28), it seems that electric field demonstrated the synergistic effect to the separation efficiency for both food and non-food particles. Effect of rotation speed, on the other hand, appeared as synergistic to food particle separation and antagonistic to non-food separation. Nevertheless, some essential evaluations ought to be performed and analysed in order to confirm their influences on the performance of waste separation.

2.8   Summary

Electrostatic separation has been widely used for impurity removal and waste recycling. Its comparatively simple configuration has gained a wide acceptance. Charging of the substances can be achieved by means of triboelectric charge, induction charge and corona discharge. The spark discharge can be generated if the current in the discharge is adequately raised. However, spark discharge produces erosion and degrading traces at the electrodes. The energy released by the discharge should be maintained to prevent the undesired spark effect.

The separation process is sensitive to the effects of random variability. Taguchi's method which based on an orthogonal array arrangement can be employed to provide robustness to the process. Signal-to-noise ratios are used in the robust parametric analysis technique. The robust process reduces the

variations of the process conditions caused by the random factors such as manufacturing variation and component deterioration.

The efficiency of the separation relies on the uniform electric field and the separator configuration. As the separation process relates to the system parameters such as applied voltage and position of electrodes, the evaluation of these parameters should thus be performed. Research on the optimum electric field and equipment construction for a complete separation system should also be carried out by employing respond surface methodology along with ANOVA analysis. The review on development of waste separator and review on design consideration were summarised in Table 2.3 and 2.4, respectively.

Table 2.3: Summary of review on development of waste separator

Authors and Year	Description	Major Findings
Lawver and Dyrenforth (1973)	• Recover conductor from non-conducting mixtures	• Sorting of solid particles by means of electrical forces that exerted on charged bodies
Kiewiet, Bergougnou and Brown (1978)	• Sort the very fine particles in fluidised base with electrostatic fields	• Recovery of iron of 60 % can be achieved. • Recovery increases with increasing voltage
Masui (1982)	• Remove impurities in food processing industry with induction type and corona charging type separators	• Non-invasive separation with high voltage, together with either suction pump (induction) or neutraliser (corona charging)
Toraguchi and Haga (1982)	• Remove ashes from ore particles with cyclone type separator	• Suitable for applications with large gravity difference
Iuga et al. (1993)	• Propose an improve design over the traditional with corona electrodes	• Compared various electrodes • Uniformity of space-charge distribution on the surface of electrode
Chang, Crowley and Kelly (1995)	• Separation using triboelectric separator with parallel electrodes	• Charging tendencies of substances are referred in triboelectric series
Veit et al. (2005)	• Recover metal from printed circuit boards scraps	• Combine magnetic and electrical forces for metal recovery
Wu, Li and Xu (2008)	• Propose an improve design with double rotating roller	• Improved recovery if compared to single roller design separator

Table 2.4: Summary of review on design consideration

Authors and Year	Parameters and Description	Major Findings
Murata et al. (1982)	• Particle size: 37 - 840μm	• Sorting efficiency increases with increasing size difference
Iuga et al. (2001)	• Particle size decreases	• Separation efficiency increases
Elder et al. (2003)	• Electric field increases • Uniform particle size • Rotation speed	• Separation efficiency increases • Better separation efficiency • Affects the efficiency
Aman et al. (2004)	• Corona electrode angle increases	• Separation efficiency decreases (conductor only) • Effective when angle > 25°
Iuga et al. (2004)	• DC electric filed • Mineral size decreases	• Better than AC electric field • Separation efficiency increases
Samuila et al. (2005)	• Corona electrode angle increases	• Separation efficiency decreases
Li et al. (2007)	• Particle size	• Optimum value of 0.6 – 1.2 mm for industrial application
Bendaoud et al. (2008)	• Corona electrode distance decreases	• Separation efficiency decreases
Calin et al. (2008)	• Mixture composition	• Affects the separation efficiency
Lu et al. (2008)	• Particle shape	• Affects the falling trajectory
Ravishankar and Kolla (2009)	• Particle size, humidity and temperature	• Affects the separation efficiency
Xue, Li and Xu (2012)	• Rotational speed	• Optimum value of 50 – 70 rpm

CHAPTER THREE

MATERIALS AND METHODS

3.1   Introduction

This chapter describes the properties of test sample and the operational concept of the electrostatic separator, as well as, the experimental techniques performed for validation. It also summarises the electrode construction, separator design and calculation, calibration and quantification of errors for the experimental work. The evaluation analysis presented in chapter 4 includes the separation characterisation, the robustness assessment of the separator and the process optimisation. The experimental work started with waste samples preparation. Characterisation of the separation system was then carried out by analysing the parameters of the separator under various operational conditions, followed by the robustness assessment using Taguchi's method, where the L-9 orthogonal array design was applied to limit the random errors caused by noise factors. Larger-is-better and smaller-is-better types of objective functions were employed for the yield of food waste and middling respectively. System performance optimisation technique was then applied to determine the optimal working conditions by utilising response surface methodology. The proposed methods in this study are summarised into a flowchart as shown in Figure 3.1.
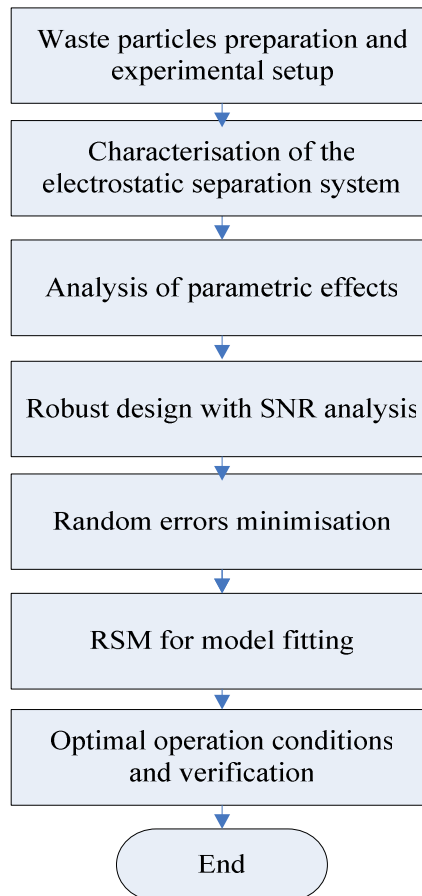
Figure 3.1: Flowchart of the proposed method

3.2　　Waste Granule Preparation

The objectives of the project are to electrostatically treat the waste mixture. Thus, the commonly available wastes were used. The sample of test was typically a mixture of food waste particles, FW (fruits peel, 40 wt%) and non-food waste particles, NF (glass, 10 wt% and plastic, 50 wt%) per each experimental run. The fruit peel refers to the peel from carrot and apple with water content ranged from 10% to 30%, whereas the plastic refers to the polystyrene (PS) food box and polyethylene terephthalate (PET) mineral water bottles. All particles were cut manually into sizes within 1.0 mm to 4.0 mm. The physical and electrical properties of the samples are given in Table 3.1.

Table 3.1: Typical properties of test samples

Properties	Symbol	Unit	FW	Glass	Plastic
Density	ρ	kgm^{-3}	1200 - 1400	2000 - 2500	1050 - 1360
Particle thickness	t	m	2.0×10^{-4} - 5.0×10^{-4}	1.0×10^{-3} - 2.0×10^{-3}	3.0×10^{-4} - 3.0×10^{-3}
Electrical Conductivity	σ	Sm^{-1}	$>1\times10^{-4}$	1×10^{-11} - 1×10^{-15}	$<1\times10^{-20}$
Resistivity	ρ_r	Ωm	$<1\times10^{4}$	1×10^{11} - 1×10^{15}	$>1\times10^{20}$

The density ρ was calculated by weighting a known area of sample. The volume was obtained by multiplying the measured area with the measured thickness. In order to validate the calculation of volume, a known mass of sample was put into a container filled with liquid medium and the liquid height was measured. A total of 10 measurements were taken and the range of density was determined. The resistivity was measured with a megaohm meter and the electrical conductivity was the reciprocal of resistivity. All samples were not reused in the electrostatic characterisation as the electrical properties may change once being used. The corona in the vicinity of the electrode tip may cause large molecules in the samples to break down to molecular fragments, which produces smaller fragments with bigger ionic mobility and thus changing the electrical conductivity. Note that the sample of test was mixed with fruit peel with the highest electrical conductivity, plastic with the largest thickness and glass with the largest density, thus it is impractical to employ triboelectrostatic or cyclone type separator. The rotating roller type separator was suggested instead, for its capability in treating the glass and

plastic independently. However, there is lack of literatures to treat these samples at the same time and with mixture of food waste. To the best of our knowledge, this is the first report of food waste-glass-plastic separation process using roll-type separator.

Figure 3.2 shows the difference in conductivities of the waste particles, when being put on a ground plate electrode exposed to a corona needle electrode. It is apparent that the fruit peel is conductive as the corona discharge penetrates through the particle to the grounding, whereas the glass is relatively non-conductive (dissipative) and plastic (PS) is absolutely insulative.

Figure 3.2: Different conductivities of particles (a) food, (b) plastic and (c) glass

3.3 Electrostatic Separator Design and Setup

In this study, a roll-type electrostatic separator has been utilised to segregate the food waste from a mixture of plastic and glass environmentally friendly. The food appears more conductive for its high water content (Wang et al., 2008), making it detachable from others during the rotational separation process. The separator sorts the more conductive matter and less conductive

matter to different locations. However, some matter may fall in between as middling product, resulting in a decline in separation efficiency (Wu, Li and Xu, 2008). The main objectives of present study focus on determining the efficiency of waste recovery by electrostatic process, identifying the dominant empirical factors and building up the equations for optimal separation results with respect to operational conditions.

3.3.1 Test rig

The test rig was constructed with the objective of producing continuous corona discharges and to examine qualitatively and quantitatively its efficiency for waste separation. A schematic of the experiment layout and electrical connections of the experimental work is shown in Figure 3.3.
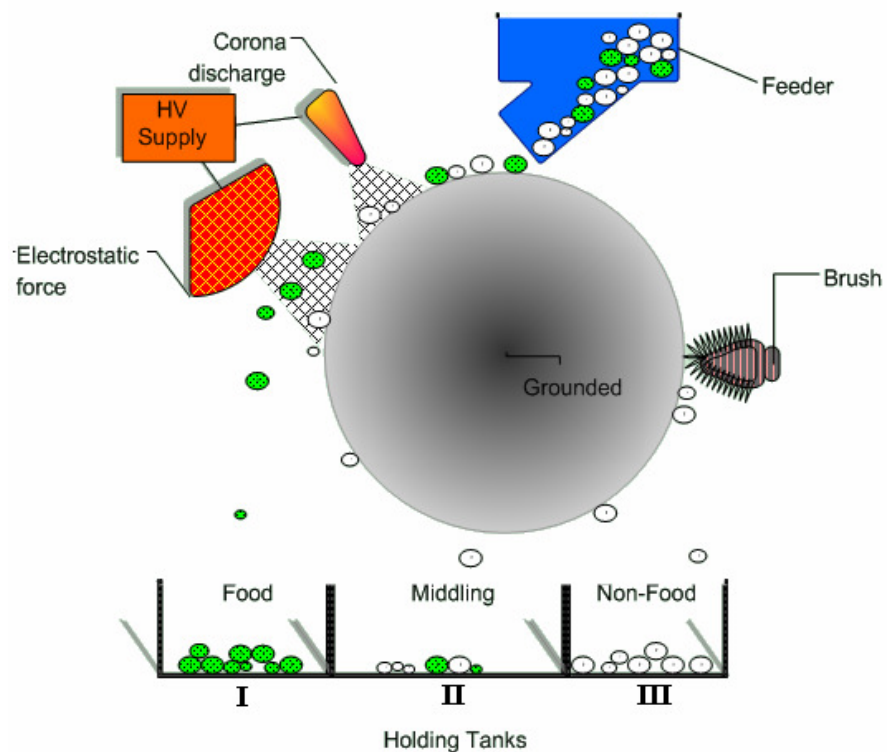
Figure 3.3: Diagram of electrostatic separator

The separation process utilised an earth-grounded roller type electrostatic separator rotating in counter-clockwise direction. The samples in the feeder were deposited onto the roller surface. An ionising needle electrode powered by a high voltage direct current (DC) power supply (InformationUnlimited, USA) with rated output up to 35 kV was placed at one side of the separator for corona discharge generation. The connection from power supply to the electrode was housed inside a polytetrafluoroethylene (PTFE) tube for electrical insulation purpose. A set of insulated retort stand was used to hold the needle electrode and provide flexibility to change the electrode displacement. An electrostatic plate electrode was connected downstream, providing the non-discharging electrostatic field. A non-conductive brush was placed at another side to remove particles left on the roller and to provide a clean roller surface for the next rotation cycle.

The output of high voltage power supply was calibrated using a purpose built voltage divider with a 1: 301 ratio, forming by three 10 MΩ resistors and a 100 kΩ resistor. The actual value of the resistors was measured using a digital Multimeter model 8145 (GW-Instek, Taiwan), with rated accuracy of $\pm$ 0.25% in the 20 MΩ resistance range and $\pm$ 0.10% in the 200 kΩ range. The resistors were connected in series and the output voltage across the 100 kΩ resistor was measured, with rated accuracy of $\pm$ 0.03% in the 200 V range. The measurements were conducted one hour after the units were switched on so that the equipment have sufficient time to warm up and were carried out in triplicate as to assess the magnitude of random error sources. The magnitude of the percentage error for the calibrated voltage due to the

accuracy of measuring instrument was calculated to be 0.38%.

The speed of the roller was controlled by a geared motor with a power consumption of 40 W (PeeiMoger, Taiwan). Output of the motor was controlled by an electronic speed controller to provide a speed range of 0 – 120 rpm. In order to avoid electromagnetic wave interference, the motor controller was shielded with a metal plate and placed away from the power source. The experiment was run in a ventilation room and the ambient was recorded to be 24 – 28 °C with relative humidity (RH) of 55 – 65 %.

3.3.2   The separator design

A lab scale roll type separator, used as the starting point of the design of the corona charge type separator as described by Figure 2.3 (c), was fabricated. The separator in this study has a better control of rotary speed as driven by the electronic speed controller, which marks the key improvements over the traditional design. The roller surface, corona electrode and electrostatic electrode were made of stainless steel. Stainless steel was chosen over other cheaper electrical conductors such as aluminium since the latter tends to form an oxide layer that is highly electrical resistant. The photo and schematic of the separator design are shown in Figures 3.4 and 3.5, respectively. Note that the metal plate that used as the shield has been removed while preparing Figure 3.4.
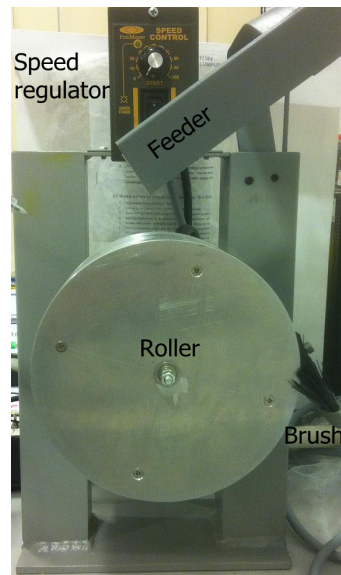
Figure 3.4: Photograph of the separator
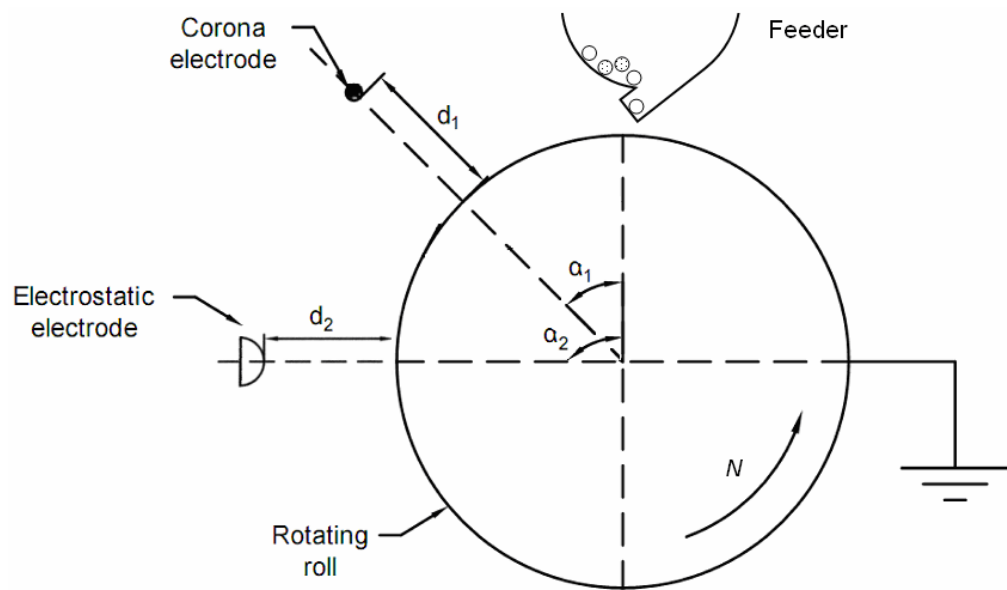
Figure 3.5: Design schematic of the separator

During the electrostatic separation process, various factors may affect the separation performance. Referring to the section 2.7 discussed previously, the factors included the rotation speed and electrode position. The system parameters involved in this study are summarised in Table 3.2 and the effects will be discussed in the following chapter.

Table 3.2: System parameters and their range

Variables	Min. value	Max. value
Voltage level, U (kV)	20	30
Rotation speed, N (rpm)	60	90
Corona electrode angle, α_1 (°)	25	50
Corona electrode distance, d_1 (mm)	50	60
Electrostatic electrode distance, d_2 (mm)	40	50

Note: Electrostatic electrode angle, $\alpha_2 = 90°$, feed rate = 12 g/min.

The range of voltage level was selected based on the constraint of the high voltage supply, which provides a maximum rated voltage of 35 kV. The range of rotation speed was summarised in Table 3.2 by referring to the literatures. The maximum speed of the motor can achieve to be 120 rpm. The corona electrode must not be placed too close to the feeder outlet as the charge may affect the feeding rate. Direct corona may also dispel the particles to another side of the roller before they can travel along the counter-clockwise rotational direction, thus resulting in a poor separation performance.

The electrostatic electrode was set at an angle of 90 degrees. The interval between two electrodes was varied in a range of 25 – 50 degrees, or approximately 31 – 61 mm on surface of the roller with a radius of 70 mm. The distance of the corona electrode is preferred to be further away from the roller surface in order to generate a wider pinning zone. It is to be noted, however, that placing it too far may lead to a weak space charge on the granules (Samuila et al., 2005). Thus, the range of corona electrode distance d_1 was set as shown in Table 3.2. On the other hand, the distance for electrostatic electrode d_2 should be set within a range of 1.0 to 2.5 times of voltage level U

(Xu et al., 2009). These values were calculated to be sufficient for falling trajectory deviation resulted from electrostatic force and prevention of high risk spark discharge. Detailed calculation work will be described in Chapter 4.

3.4   Analytical Procedures

During the electrostatic separation process, the air surrounding the ionising electrode was ionised by a high intense corona discharge, thus forming an ionising zone. When the roller delivered the particles through the zone, the more conductive food particles dissipated their charge through the grounded roller, avoiding them from being pinned for a longer time than the less conductive one. With the continuous rotation from the roller, the more conductive particles were subjected to higher difference between centrifugal force and pinning force, and thrown off the roller. The electrostatic electrode induced an evenly distributed electric field and deviated the more conductive particles from their natural falling trajectory. The less conductive particles remained pinning onto the roller due to the larger pinning force applied on them and they subsequently fell off at different locations. In chapter 4, the separation mechanisms were analysed by referring to the force model. The potential system factors were identified and effects of these factors on the separation performance were determined during the characterisation process.

Nevertheless, some low moisture (<10% moisture content) food particles may not able to detach from the roller to food tank due to poor conductivity. Similarly, some oversize or overweight non-food particles may

drop earlier before falling into the non-food tank, when the centrifugal force surpassed the pinning force. These hard-to-control factors, e.g. uniform size/area of granule due to machinery constraint, limit the system performance and affect the accuracy of the analysis. The unsorted particles tend to fall as middling products (Figure 3.3). Thus, in addition to the characterisation, a robust design created by employing Taguchi's method is utilised to analyse the robustness of the separation process control and to minimise the unwanted effects of random factors. The characterised results were further evaluated by employing response surface methodology as to identify the optimal conditions.

3.4.1 Efficiency and purity determination for OVAT evaluations

In electrostatic separation, food waste and non-food waste were separated by electrostatic processes. However, misclassification may occur undesirably as discussed earlier in section 3.4. Thus, OVAT evaluations were necessary to analyse the efficiency and purity of the separation results. The test sample of waste mixture was deposited onto the roller surface and eventually dropped into three collection tanks, namely food waste tank, non-food waste tank and middling (M) tank. The mass from each tank was measured by a digital precision balance with a resolution of 0.01 g after each run. The separation efficiencies, S (%) of food waste, S_{FW} and non-food waste, S_{NF} were calculated by:

$$\%SFW, S_{FW} = \frac{m_{FW}}{FW_0} \times 100\% \tag{3.1}$$

$$\%SNF, S_{NF} = \frac{m_{NF}}{NF_0} \times 100\% \tag{3.2}$$

where m_{FW}, FW_0, m_{NF} and NF_0 are the mass in FW tank, initial food waste mass in the feeder, mass in NF tank and initial non-food waste mass in the feeder, respectively. Similarly, the purities of the food waste tank (P_{FW}) and non-food waste tank (P_{NF}) were determined by:

$$\%PFW, P_{FW} = \frac{m'_{FW}}{m_{FW}} \times 100\% \tag{3.3}$$

$$\%PNF = P_{NF} = \frac{m'_{NF}}{m_{NF}} \times 100\% \tag{3.4}$$

where m'_{FW} and m'_{NF} are the food waste mass in FW tank and non-food waste mass in NF tank, respectively. Both m'_{FW} and m'_{NF} were determined by manuall sorting.

3.5   Robust design with Taguchi's method

Robust design is an engineering approach for reliable productions under various controllable circumstances. The design enhances the quality and diminishes the negative noise impact on the products. Robust design may not produce the most optimal result. However, implementation of the design improves the process and quality of the products (Camposeco-Negrete, 2013).

This study employed Taguchi's method to assess the robustness of food waste segregation process from the solid waste mixtures. The four factors, namely voltage level, rotation speed, water content and particle size were considered based on reports found in the literature. A signal-to-noise ratio (SNR) was used as the objective function to determine the robustness.

SNR is viable for replicated experiments to facilitate the data filtration and noise reduction process. It has been widely employed in stochastic screening and optimisation problems as a performance measure (Besseris, 2014). In this study, larger-is-better type of objective function was applied for maximal food waste recovery, whereas smaller-is-better type of objective function was used to yield minimal middling product.

In the robust design, voltage level and roller rotation speed were selected as system factors (Dascalescu et al., 2005), whereas the water content and size of food waste particles were defined as hard-to-control random factors. Water content in food waste decides its conductivity and likelihood to be moved to the food collection tank. However, this parameter is hard to control in practical conditions (Hou et al., 2010). The size of particles, on the other hand, varied due to the machinery limitation. This noise factor may eventually lead to low recovery efficiency (Wu, Li and Xu, 2008). Robust design using Taguchi's method in present study targeted to limit the negative impact of these hard-to-control random factors (i.e. water content and particle size) on the separation process.

Four factors which varied within three levels have been selected as: particle size (1.0 mm, 2.5 mm and 4.0 mm), moisture or water content (10 %, 20 % and 30 %), roller rotation speed (60 rpm, 70 rpm and 80 rpm) and supplied voltage level (20 kV, 25 kV and 30 kV). Table 3.3 tabulates the factors and their corresponding levels. The recovered waste and middling product were selected as the responses. The maximisation of waste recovery

and meanwhile the minimisation of middling product are desirable in enhancing the separation efficiency of the electrostatic separator.

Table 3.3: Factors and their levels

Factor	*Level*		
	1	**2**	**3**
Particle size, D (mm)	1.0	2.5	4.0
FW water content, WC (%)	10	20	30
Rotation speed, N (rpm)	60	70	80
Voltage level, U (kV)	20	25	30

As this is a design of four factors with three levels, an orthogonal array was built as shown in Figure 3.6. The orthogonal array was designed to understand the impact of each factor by assuming that there is no interaction between any two factors. A total of nine design points were selected for the Taguchi's method to form an L-9 array, as previously discussed in Table 2.2.

In general, the system factors (rotation speed, voltage level) have significant effects on the average output of the process, whereas the random factors (particle size, water content) may or may not have influences on the values around the average of output. Effect of these factors was evaluated by analysing the mean value of each array and the respective signal-to-noise ratio (SNR) value. The parameters of the orthogonal array design were shown in Table 3.4. Analytical discussion based on these parameters was performed in the chapter 4.
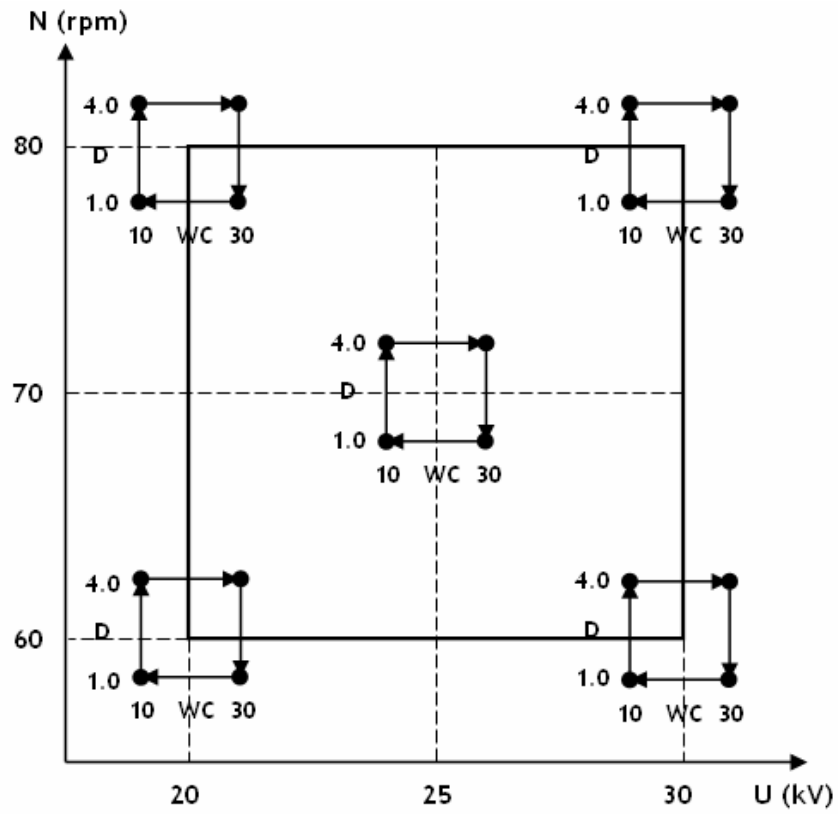
Figure 3.6: Inner and outer arrays by Taguchi design

Table 3.4: L-9 orthogonal array and the factors

Exp. no.	Particle size (mm)	FW water content (%)	Rotation speed (rpm)	Voltage level (kV)
1	1.0	10	60	20
2	1.0	20	70	25
3	1.0	30	80	30
4	2.5	10	70	30
5	2.5	20	80	20
6	2.5	30	60	25
7	4.0	10	80	25
8	4.0	20	60	30
9	4.0	30	70	20

3.6 Separation Process Optimisation using Response surface methodology

Design of experiments and analysis of the variables were performed by employing RSM using Design Expert 8.0.5 software (Stat-Ease Inc., USA). A Plackett-Burman (PB) factorial design was applied as a screening experimental design approach to navigate an n-dimensional design space with $n + 1$ experiments. In present study, 11 factors with high/low values were selected and led to a total of 12 experiments. Eight of them were practical factors including applied voltage (F1), rotation speed (F2), corona electrode angle (F3), corona electrode distance (F4), electrostatic electrode distance (F5), %FW content in mixture (F6), mixture volume (F7), ambient temperature (F8), and three of them were dummy factors (D1, D2 and D3). The high and low values of each practical factor were determined by referring to the discussion in Table 3.2 and OVAT (one variable at time) parametric analysis in the following chapter.

Based on the PB design outputs, central composite design (CCD) was employed for modelling. CCD is a factorial design with a central point and an α-distance ($\alpha = 1.68$) star topology. As CCD requires the extension of range due to the α-distance, it comes as a consideration in choosing the appropriate operational range and not exceeding the maximal rated output of the machines. Separation efficiency and purity of both food and non-food waste, as discussed previously in section 3.4, were used as responses in evaluating the influence of the mentioned practical factors. In order to identify the main effects, the Pareto

analysis was applied to calculate the vital percentage of each significant factor towards the response as follows:

$$B_i = \left(\frac{\beta_i^2}{\sum \beta_i^2} \right) \times 100 \qquad\qquad (3.5)$$

where B_i represents the importance level of each variable and β_i represents each polynomial coefficient.

Optimisation process was started with the mathematical and statistical analyses of the experimental data. The polynomial models and the fitness of the models were evaluated, in addition to the tests of significance. The optimal operational conditions would thus be determined with respect to the optimum values for each factor (Aggarwal et al., 2008).

3.7   Summary

The test rig and the electrostatic separator have been described and the characteristics of the waste were defined in this chapter. The high voltage power supply was calibrated by using a purpose built voltage divider. During the separation process, an electrostatic field was produced by the corona and electrostatic electrodes. Conductive food particles in this field are highly subjected to electrostatic charge, whereas non-food particles are mainly subjected to corona charge.

The selection of factors and their range were justified in this chapter. The range of the applied voltage, U (20 - 30 kV) was selected based on the output constraint of the high voltage supply at 35 kV. The range of rotation speed (60 - 90 rpm) was chosen on the same reason. Distance of corona electrode from the roller surface was set within a range of 50 and 60 mm, so as to provide a wide pinning zone and meanwhile maintaining a strong space charge on the particles. A simple rule was applied in determining the distance of the electrostatic electrode, i.e. $1.0*U <$ distance (mm) $< 2.5*U$. The distance was calculated to be sufficient for falling trajectory deviation and for sparks prevention.

Performance of the separator was affected by the system factors, e.g. applied voltage. However, the performance may also be influenced by some hard-to-control random factors. A robust design employing an L-9 orthogonal array was employed to minimise the negative impact from these random factors. The system factors were analysed to identify their effects on the separation efficiency and purity. Response surface methodology was then employed to predict the optimal separation performance.

CHAPTER FOUR

RESULTS AND DISCUSSION

4.1   Characterisation of Recovery Efficiency

The theoretical discussion in the literature review suggested a number of factors that could influence the separation performance of the separator. It is equivalently critical to recognise their effects which govern the separation process. The one-variable-at-time (OVAT) analytical method was employed to assess the impacts of these effects. In an attempt to make a comprehensive understanding on the process, this section explores the influence of the operating conditions in terms of the applied voltage, roller rotation speed, position of the electrodes and composition of the mixture. The waste samples throughout the parametric study were prepared in 100 g and the size of each particle was in average 4.0 mm.

4.1.1   Effect of applied voltage

The extent of electrostatic separation caused by applied voltage could be quantified in terms of food waste recovery and yield of middling product. The corona discharge from the corona electrode is generated continuously once the power supply is turned on, and ceased immediately as soon as the power is cut off. As illustrated in Figure 4.1, the separation and recovery of

food waste were related significantly to the applied voltage. A drastic increment of purity (%PFW) along with a distinct rise of separation efficiency (%SFW) was noted at the voltage level of above 15 kV. For instance, the purity was improved from 51% to 89% when the voltage increased from 5 kV to 15 kV. The observation suggests that the voltage can be set (i.e. 15 kV) as a threshold for the parametric studies throughout section 4.1. Although high separation efficiency can be observed at 5 kV, it in fact resulted in a very low purity and consequently poor food waste recovery as shown in Figure 4.2, mainly due to the weak electric field.
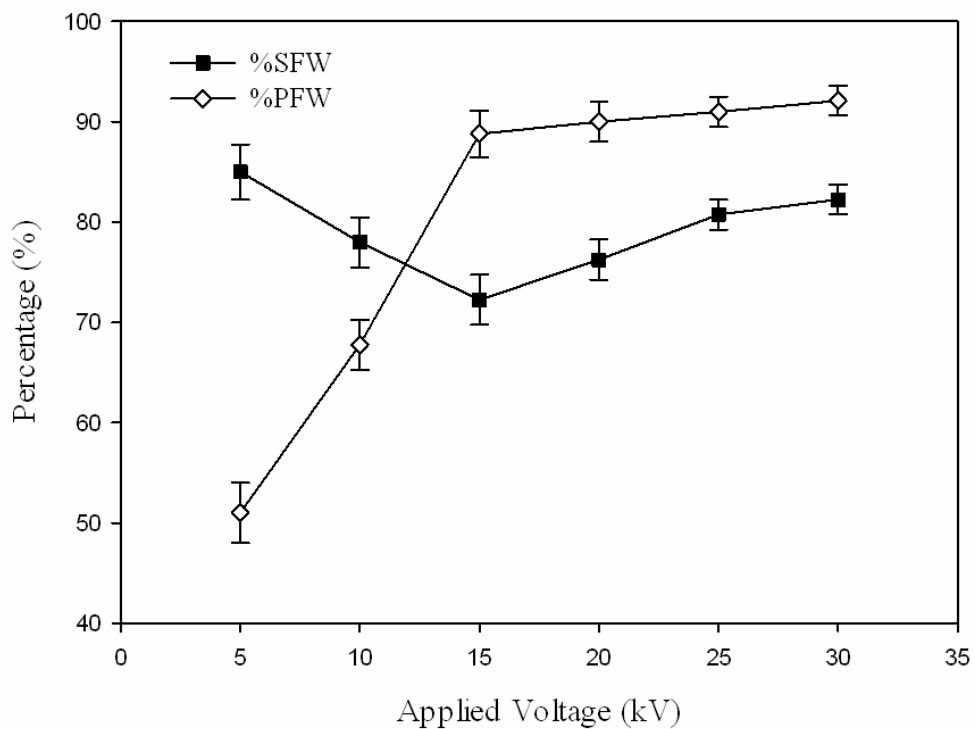
Figure 4.1: Effect of applied voltage on food waste recovery and purity (rotation speed = 70 rpm; feed content FW:NF = 40:60)

To better understand the extent of applied voltage on separation process, the weight of middling products and the recovered food waste were

measured. Recovered food waste (FW) refers to the multiplication product of separation efficiency (%SFW) and purity (%PFW). As shown in Figure 4.2, it can be observed that the recovered food waste increases with the increase of applied voltage and reduction of middling products. This can be interpreted that a stronger electric field enhances the detachment of food waste to the FW tank and as well the separation purity, thus reducing the mass in the middling collection tank. It has been established that the separation process is attributed to the electrostatic force. As expressed by equation (2.19), the electrostatic force F_e is directly proportional to the square of electric field. It can be deduced that the higher the electric field, the higher the electrostatic force acted to deviate food particles from falling trajectory which leads to better separation efficiency and food recovery (Bendaoud et al., 2008).
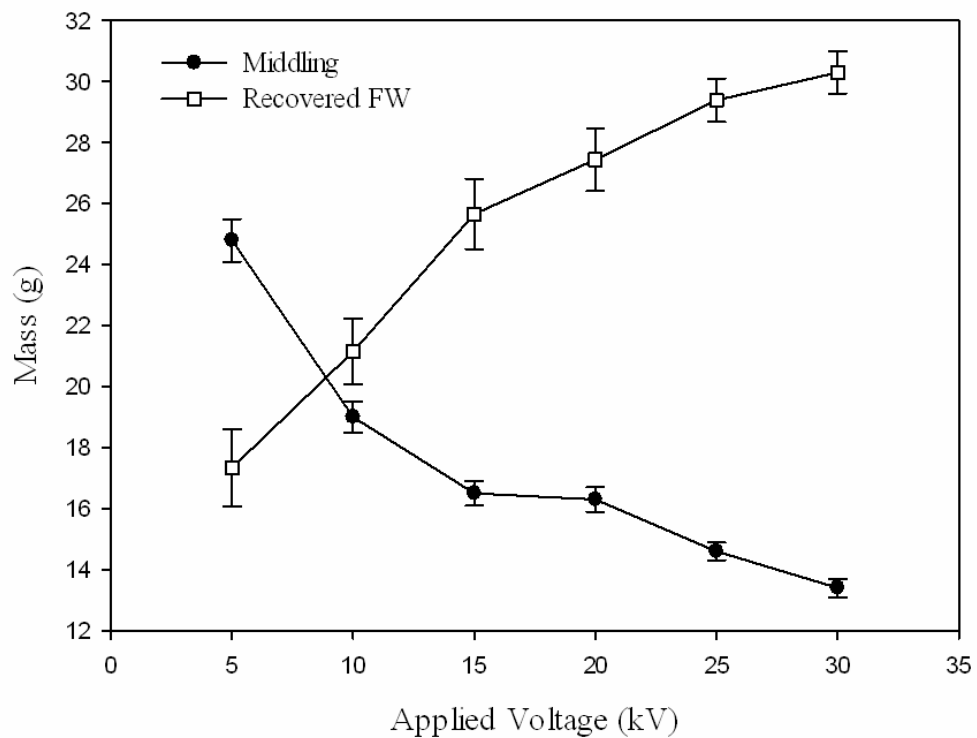
Figure 4.2: Effect of applied voltage on mass of recovered food waste and middling (rotation speed = 70 rpm; feed content FW:NF = 40:60)

Figure 4.3 illustrates the effect of applied voltage on the non-food particles. It shows that high purity of non-food particles, more than 90% in this case, was found inside the NF collection tank with insignificant impurities. However, the recovered mass of NF, which derived from the multiplication product of NF separation efficiency (%SNF) and purity (%PNF), exhibited a comparatively low output when the applied voltage was below 15 kV. This was due to the fact that the low electric field is insufficient to generate strong pinning force to move NF particles into NF tank, as previously expressed by equation (2.28). Besides, the results verified the previous discussion that the minimal required voltage level should be set to obtain effective separation results.
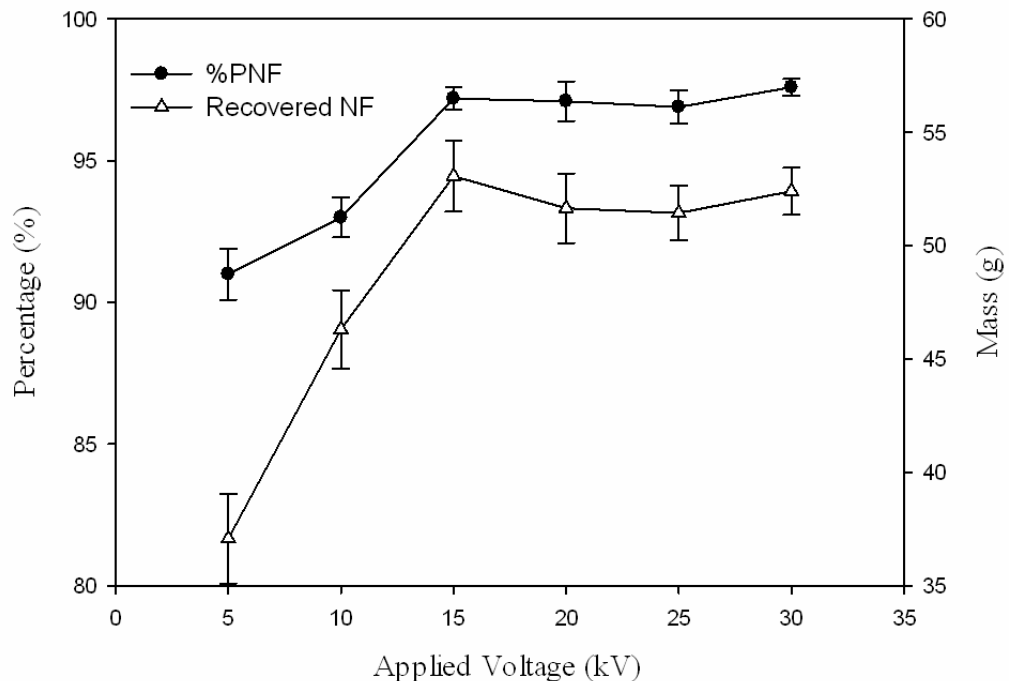
Figure 4.3: Effect of applied voltage on purity and recovered mass of non-food waste (rotation speed = 70 rpm; feed content FW:NF = 40:60)

4.1.2 Effect of roller rotation speed

The relationship between the voltage and the separation efficiency at different rotation speed is depicted in Figure 4.4. Interestingly, the separation of food waste at slower rotation speed was found to be more effective. For instance, at the same applied voltage of 30 kV, the FW separation efficiency can reach about 87% at a speed of 20 rpm if compared to 77% at 80 rpm. It appeared that the lowest level of rotation speed can prolong the time of waste particles to stay within the ionising zone. Nevertheless, the slow processing speed is impractical for energy cost optimisation. As such, the speed range of 40 rpm to 80 rpm could be considered for a rapid separation process on one hand, and for maintaining a high recovery of waste on the other hand.
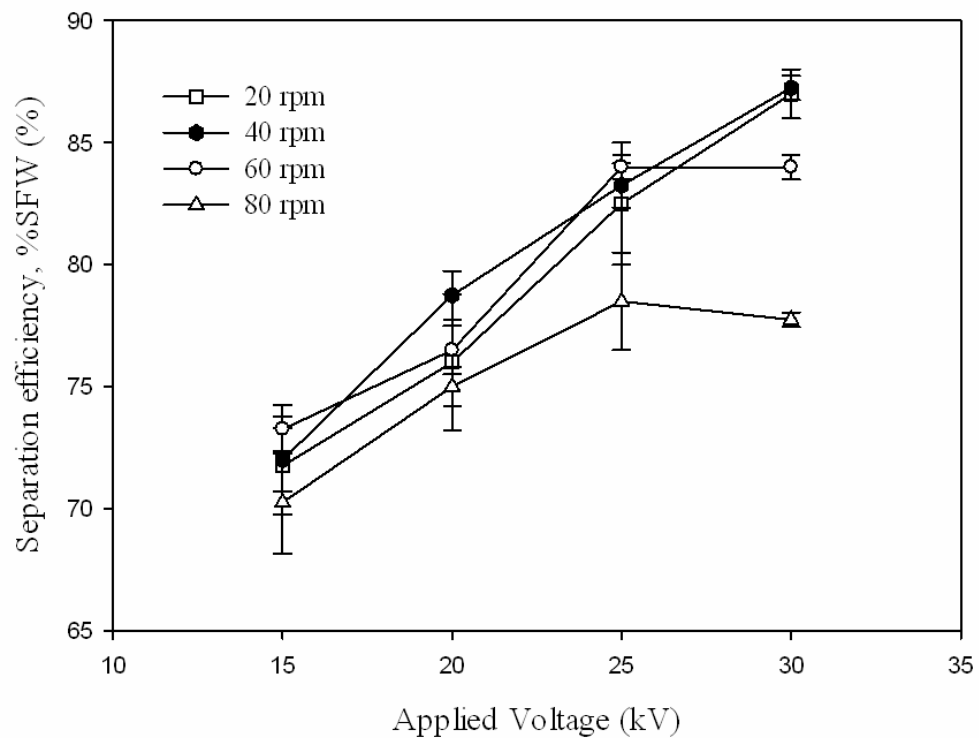
Figure 4.4: Effect of roller rotation speed on FW separation efficiency (feed content FW:NF = 40:60)

As shown in Figure 4.5, in general, the middling mass reduced with faster roller rotation, indicating an enhancement to the separation efficiency. It is in contrast to the previous discussion. From equation (2.21), the centrifugal force F_{ct} relates positively to the rotation speed. A higher rotation speed implies a larger centrifugal force to deviate the food particles to FW tank. Nevertheless, results in this section exhibited that a slower rotation process can also contribute to an effective separation. The separation performance in this case can be regarded as a competition between centrifugal force and the ionising time (Elder, Yan and Raiser, 2003; Xue, Li and Xu, 2012). There is likely a critical roller rotation speed level, and it should be determined specifically via an optimisation methodology, which would be discussed in the section 4.3.
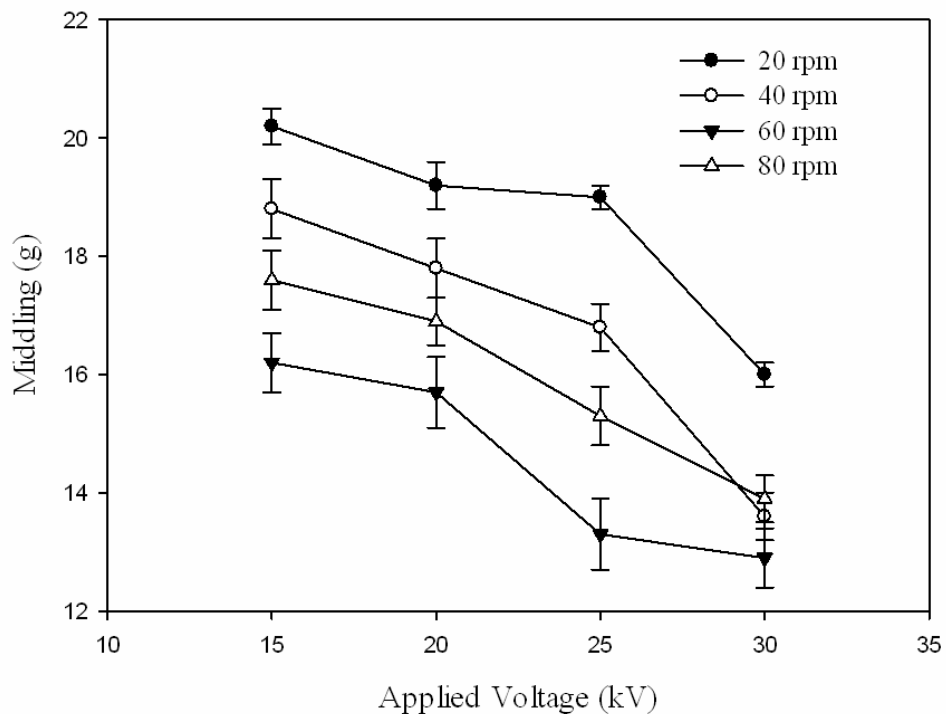
Figure 4.5: Effect of roller rotation speed on middling (feed content FW:NF = 40:60)

4.1.3 Effect of angular position of electrodes

The corona electrode and the electrostatic electrode are the essential elements in the process of electrostatic separation. In most applications, these electrodes are regularly characterised by different angles and positions, owing to the different natures and properties of the waste particles. As previously shown in Figure 3.5, placement of the electrodes depends on a number of parameters and investigation on their interactions could be an intricate task. In order to simplify the complexity, the distances of the corona electrode and electrostatic electrode from the roller surface was set as 50 mm and 40 mm, respectively. This study also suggested a definition of electrodes gap G_E, which reflects the relationship between the two electrodes, was termed. As the corona electrode angle was set by referring to the fixed electrostatic electrode angle ($\alpha_2 = 90°$), this parameter measured the interval (mm) between the two electrodes according to the following equation:

$$G_E = \frac{2\pi R}{360}(\alpha_2 - \alpha_1) = 1.222(90 - \alpha_1) \tag{4.1}$$

The value of the electrodes gap corresponds to various angles of the corona electrode (see Figure 3.5). These values were calculated using equation (4.1) and it was summarised in Table 4.1.

Figure 4.6 shows the results for the change of the FW separation efficiency with different electrodes gap designs under various applied voltages. A significant separation was noticed for a small gap of 50 mm, whereas a large gap of 80 mm exhibited marginal improvement of efficiency.

Influence of electrodes gap on the separation process is also reflected from the measurement of middling mass. As depicted in Figure 4.7, great reduction in middling was accomplished with the electrodes gap of 50 mm at the same applied voltage compared to that of 65 mm and 80 mm. When the corona electrode was moved further from the electrostatic electrode, the gap increased to 80 mm and the efficiency deteriorated below that with a smaller gap.

Table 4.1: Corona electrode angle and corresponding electrodes gap

α_2 (°)	Corona electrode angle, α_1 (°)	Electrodes gap, G_E (mm)
90	25	80
90	37	65
90	50	50
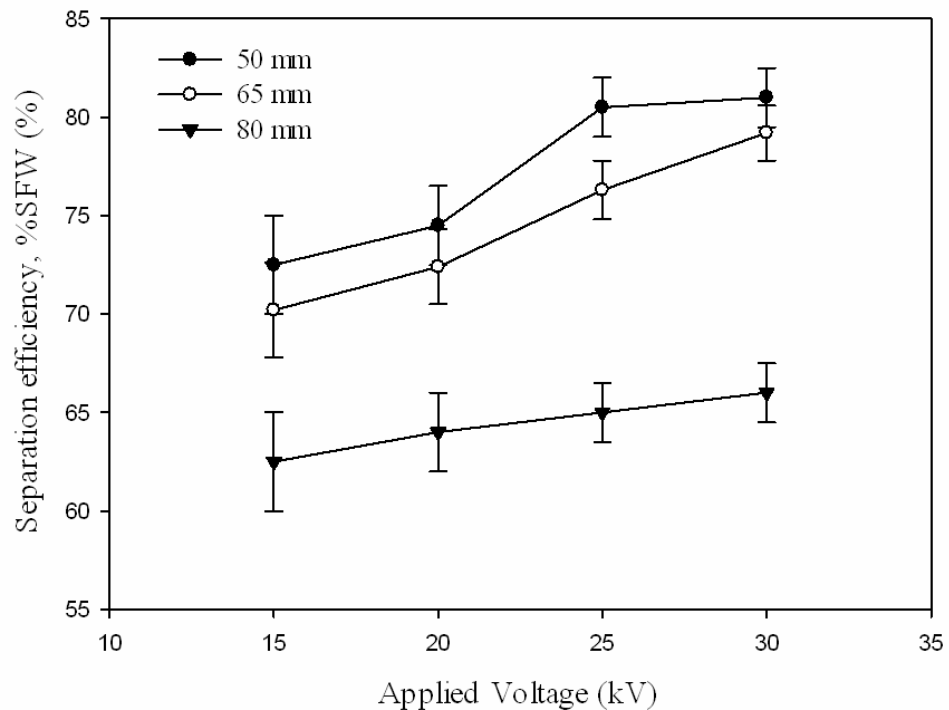
Figure 4.6: Effect of electrodes gap on separation efficiency (rotation speed = 70 rpm; feed content FW:NF = 40:60)

It appears that the separation efficiency would enhance in term of reduction of middling with small electrodes gap. Set on a basis that the intensity of space charge between the electrodes increases with a closer distance would yield higher efficiency. However, it is also possible that if the electrodes are located too close, charge would gather around the electrodes and to cause localised high electric field and pressure. This can lead to operational interruption and a decline in machine lifespan. It is hence desirable to establish an optimisation model for effective separation.
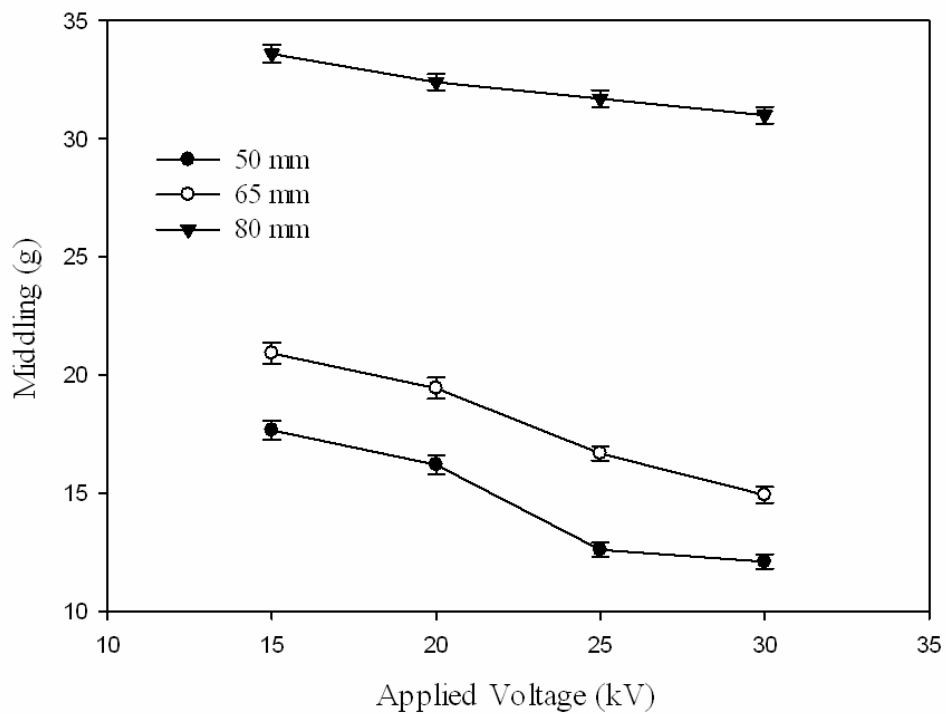
Figure 4.7: Effect of electrodes gap on middling (rotation speed = 70 rpm; feed content FW:NF = 40:60)

Figure 4.8 shows the purity and mass of samples for FW and NF along with the mass of middling under an applied voltage of 25 kV. It is noticeable that the purity and separation efficiency decreased with the increment of gap

distance between the electrodes. It could be due to the fact that the corona electrode is placed too close to the feeder output. Based on the experimental observation when the angle of corona electrode was set at 25 degrees, the large coverage of the induced ionising charge interfere the particles coming out from the feeder. The charge repels the particle undesirably instead of pinning it onto the surface of the roller. In other words, with electrodes gap of 80 mm, the particle could be eventually fallen into the NF tank or classified as middling if fallen outside any tank, thereby increasing the mass of middling and affecting the purity of the NF collection.
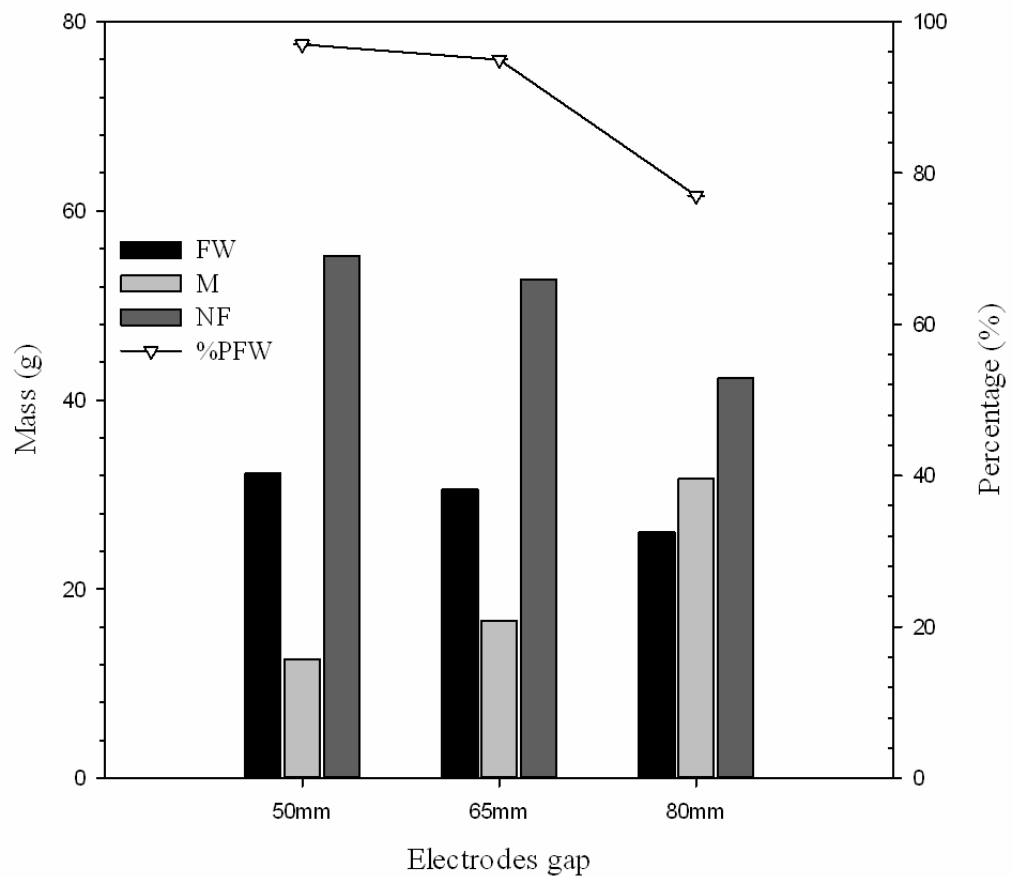
Figure 4.8: Mass and purity with different electrodes gap (rotation speed = 70 rpm; feed content FW:NF = 40:60, applied voltage = 25 kV)

4.1.4 Effect of mixture composition

Besides the separator parameters discussed previously, the efficiency of separation is also affected by the type of mixture in terms of mixing ratios. Mixed samples derived from mixing the food (moisture 10% - 30%) and non-food particles at different ratios as tabulated in Table 4.2 were investigated. The groups G1, G2, G3, G4 and G5 for the FW:NF mixtures consisted of mixing ratios of 50:50, 40:60, 30:70, 20:80 and 10:90 by volume, respectively.

Table 4.2: Mixture with different mixing ratios (particles were in same size)

Group	Mixture	
	FW (%)	NF (%)
G1	50	50
G2	40	60
G3	30	70
G4	20	80
G5	10	90

Figure 4.9 illustrates the separation efficiency and purity of the mixed FW-NF samples. The outcomes indicated that the mixture in G5 exhibited the most prevalent NF separation in term of purity. On the contrary, the FW separation purity turned out to be highest. The result could be explained by the fact that the separation purity is highly dependent on the mixing ratio. For instance, the higher the mixing ratio of particular particles, the higher the respective separation purity, and vice versa. On the other hand, small variance of the separation efficiencies, for both FW and NF particles, signified the trivial effect of the mixing ratio in this study.
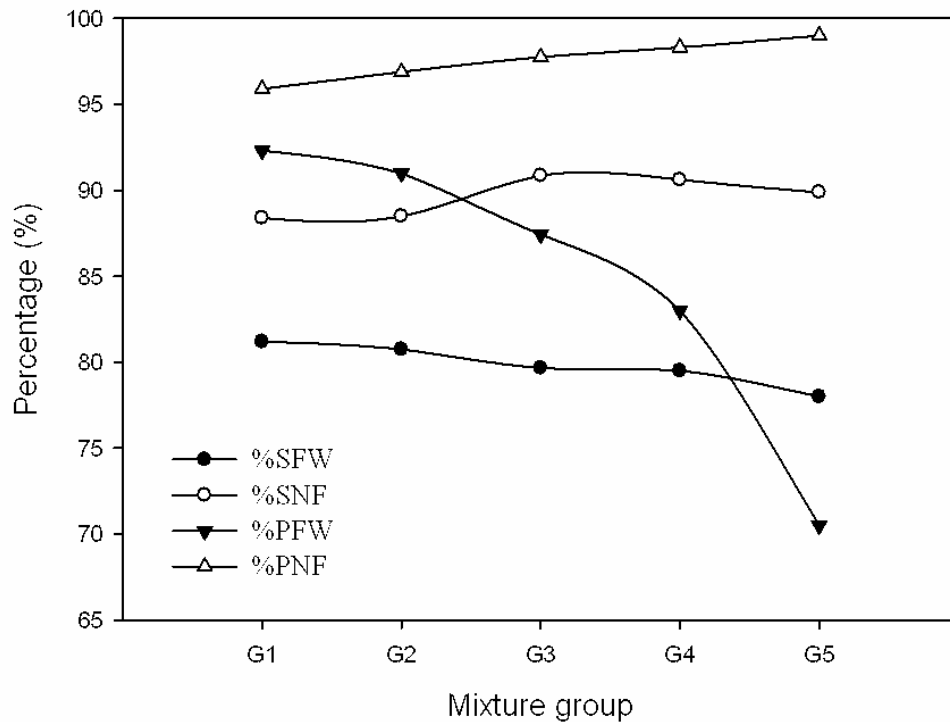
Figure 4.9: Effect of mixing ratios on separation efficiency and purity (rotation speed = 70 rpm; applied voltage = 25 kV)

Effect of the mixing ratio on the mass of middling and recovery is depicted in Figure 4.10. As discussed previously, the influence of mixing ratio on the separation efficiency of FW particle was insignificant. However, with the drastically decline of purity from mixture G1 to G5, the recovered FW particles were between the mass of 37.5 and 5.5 g out of the FW collection tank with mass ranging from 40.6 to 7.8 g, respectively. Similarly, the NF mass between 42.4 g (out of 44.2 g) and 80.1 g (out of 80.9 g) can be extracted. The mass of middling lies in the range between 15.2 and 11.3 g. It is likely that the high amount of NF particles in mixture G5 contributes to frequent tribocharging activities, causing a great repellent effect which improves the separation efficiency.
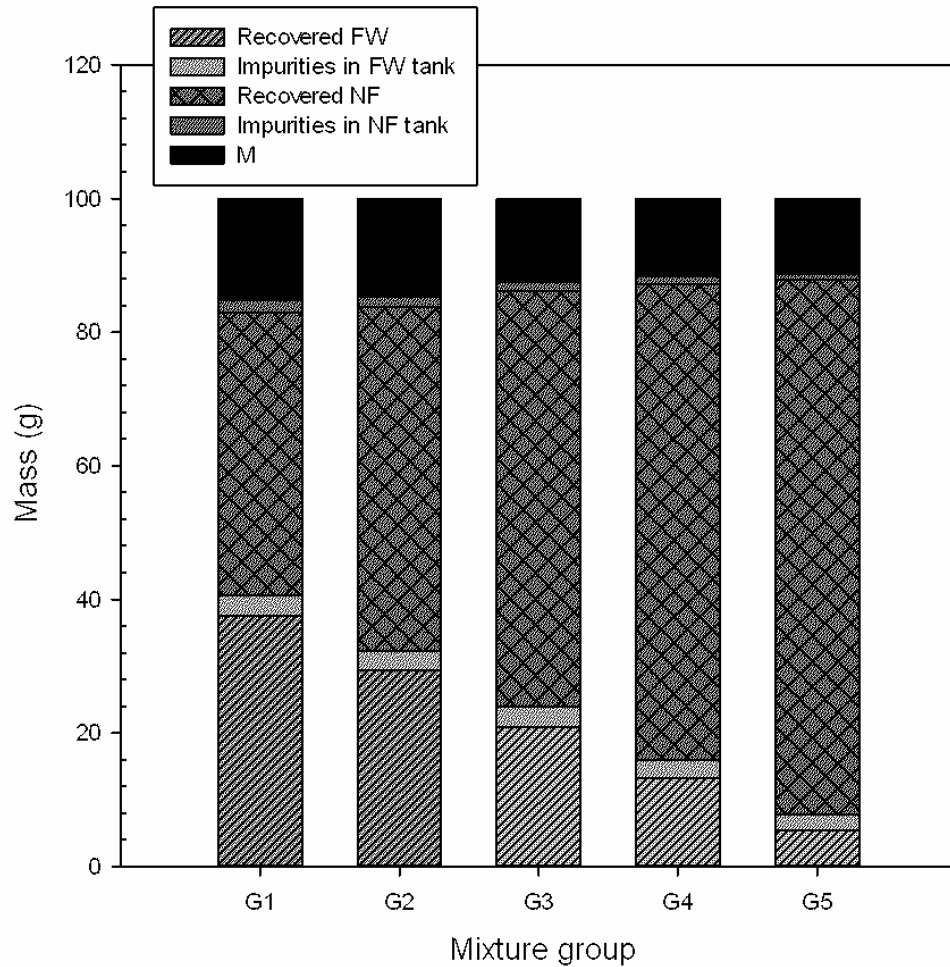
Figure 4.10: Effect of different mixing ratios (rotation speed = 70 rpm; applied voltage = 25 kV)

4.1.5 Summary

The applied voltage, roller rotation speed, angular position of electrodes and composition of the mixture were examined on their impacts to the separation process. It can be summarised from the parametric studies and theoretical consideration that the most superior effect of electrostatic separation was associated with test sample under a high voltage level. The separation process can be enhanced by determining the optimum values of

rotation speed and electrodes gap for creating an intensive charging coverage, while keeping the process time short to save energy. The optimisation model should be established as it would provide a comprehensive analysis on separation efficiency and purity.

4.2   Robust Design

In addition to the influencing factors previously discussed, the electrostatic separation process was sensitive to the effects of random variability. Characteristic variation of samples and any source of natural occurring were considered as random noise factors (Dascalescu et al., 2005). Taguchi's method provides an approach to assess the robustness of the separation processes. The main purpose of robust design using Taguchi's method is to limit the variations of the hard-to-control random errors. The L-9 array design in this study consisted of two types of factors, namely dominant design factors (i.e. applied voltage and rotation speed) and random noise factors (i.e. size and water content of the particles).

4.2.1   Experimental results

The mass of the recovered food waste and middling products collected from the tanks were used as the experiment responses of the L-9 array design. This study was to decide the effective separation configurations for maximal food waste recovery and meanwhile minimal middling products. Thus, larger-is-better type and smaller-is-better type of objective functions were applied,

respectively. The former type is generally aligned with a positive sign, whereas the latter type has a negative SNR. The recorded responses were tabulated in Table 4.3 with their corresponding SNRs calculated using equations (2.1) and (2.2).

Table 4.3: Experimental response and the corresponding SNR.

Exp. no.	Food waste, FW (g)	% SFW	SNR (FW)	Middling, M (g)	% Recovery	SNR (M)
1	28.9	72	29.22	16.0	27	-24.08
2	32.3	81	30.18	15.1	25	-23.58
3	30.1	75	29.57	14.5	24	-23.23
4	31.4	79	29.94	13.7	23	-22.73
5	30.0	75	29.54	16.8	28	-24.51
6	32.5	81	30.24	14.9	25	-23.46
7	31.5	79	29.97	15.1	25	-23.58
8	34.0	85	30.63	13.4	22	-22.54
9	31.3	78	29.91	15.3	26	-23.69

Table 4.4 shows the percentage impacts of the design factors. The impact of each factor on the food waste recovery and the middling was calculated using equation (2.4). It is noticeable that the voltage level has the maximum effect (39.44 %) on effective recovery of food waste, followed by the particle size (26.93 %), water content (17.90 %) and rotation speed (15.73 %) within the design range. On the other hand, the minimal middling product was mostly influenced by the voltage level (79.78 %). The water content has a negligible effect (0.78 %) compared to rotation speed (12.07 %) and particle size (7.37 %).

Table 4.4: Percentage impact of different factors on food waste and middling.

Factor	Level	Food waste, FW			Middling, M		
		SNR	$\overline{\text{SNR}}$	%impact	SNR	$\overline{\text{SNR}}$	%impact
D (mm)	1	29.67			-23.64		
	2	29.91	29.92	26.93	-23.60	-23.51	7.37
	3	30.18			-23.29		
WC (%)	1	29.71			-23.48		
	2	30.13	29.92	17.90	-23.58	-23.51	0.78
	3	29.91			-23.46		
N (rpm)	1	30.05			-23.39		
	2	30.01	29.92	15.73	-23.35	-23.51	12.07
	3	29.69			-23.79		
U (kV)	1	29.56			-24.10		
	2	30.13	29.92	39.44	-23.54	-23.49	79.78
	3	30.06			-22.84		

It is not surprising at all that the applied voltage appears as a key factor for electrostatic separation. High level of applied voltage implies that a large number of food waste particles can be attracted towards food waste collection tank. Meanwhile, the non-food waste particles were effectively pinned and moved to the non-food waste tank. Therefore, the middling product dropped within was consequently minimised. Similarly, high recovery rate and low middling were observed on the particles with large size of 4.0 mm as shown in Tables 3.4 and 4.3. This was due to the fact that particles with large surface area were subjected to more attraction and pinning effects by ionisation process, thus making them to drop to their respective collection tanks effectively (Ruan and Xu, 2012).

Besides, it is worth noting that water content improves the conductivity of food waste particles. Hence, this factor has much larger impacts on the results of food waste recovery than that on middling. The rotation speed of the separator also demonstrated perceptible influences on both responses. This can be explained by the centrifugal force generated by the rotating roller. Centrifugal force plays a certain role to detach the wastes at the right point, in addition to the attraction and pinning forces induced by the electrodes.

4.2.2 SNR analysis

The graphical representation of the SNR effect of design factors on the maximal food waste recovery was shown in Figure 4.11. It showed that the best situation happened at large particle size (4.0 mm) with 20 % water content under a 60 rpm rotation speed and 25 kV of applied voltage. Similarly, by analysing the graphical representation of the effect of design factors on the minimal middling product shown in Figure 4.12, it was observed that large particle size is preferable for its highest SNR value within the experimental range. However, the water content of 20 % is not good for middling minimisation, though it contributes to the maximal recovery of food waste. Considering the water content does not have much influence on the middling product as shown in Table 4.4, 20 % water content of food waste is an optimum selection.
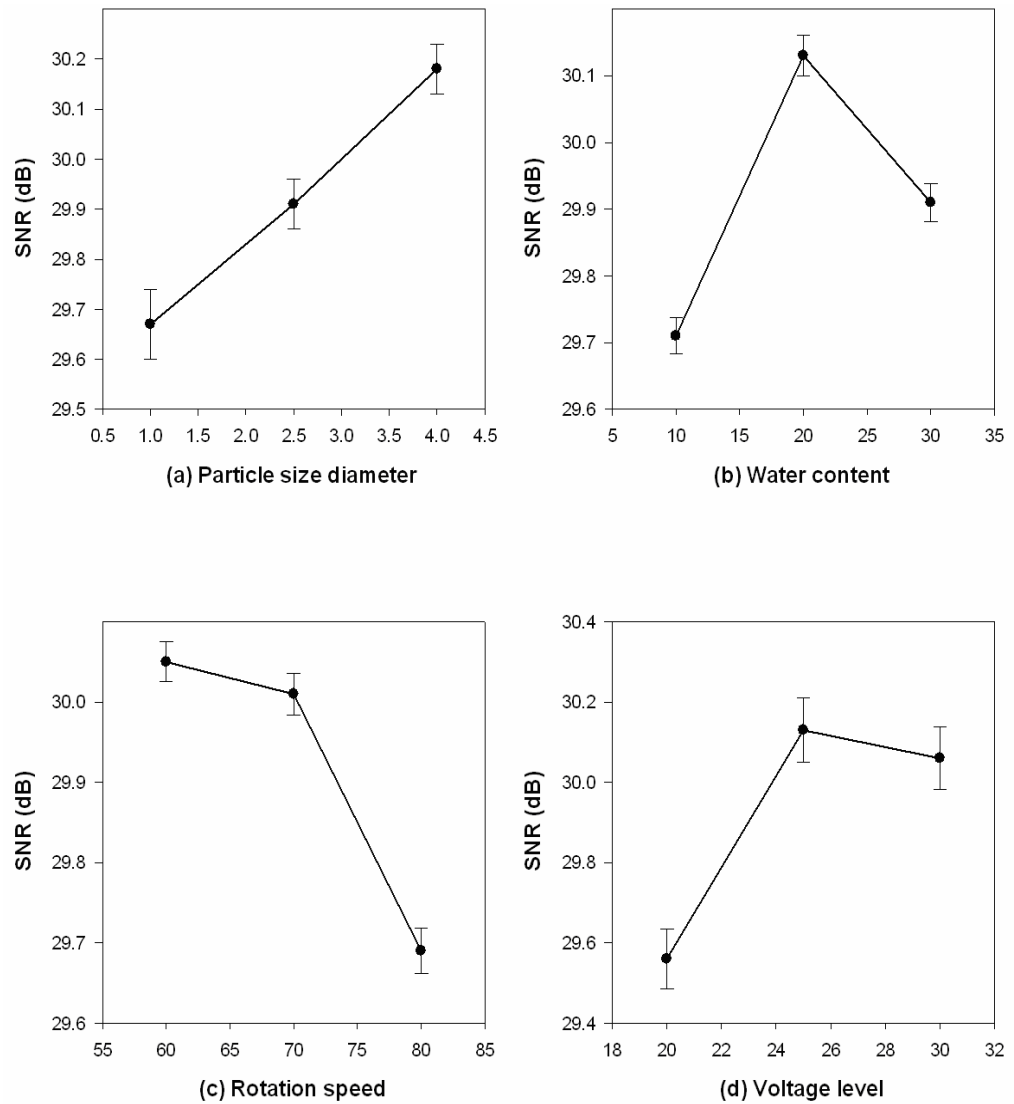
Figure 4.11: Effect of factors on SNR for maximal food waste recovery.

By studying the system factors in Figures 4.11 and 4.12, it can be seen that a applied voltage of 25 kV and rotation speed of 60 rpm yield the best maximal food waste recovery. Likewise, an applied voltage of 30 kV produces the minimal middling product at rotation speed of 70 rpm. Therefore, a robust design of food waste separation process can be achieved at an applied voltage of 25-30 kV at the roller rotation speed of 60-70 rpm with particles of 4.0 mm in size and 20% of water content. Having this set of condition achieved using

Taguchi's method, the variations from random factors can be minimised and the separation efficiency can be eventually enhanced.
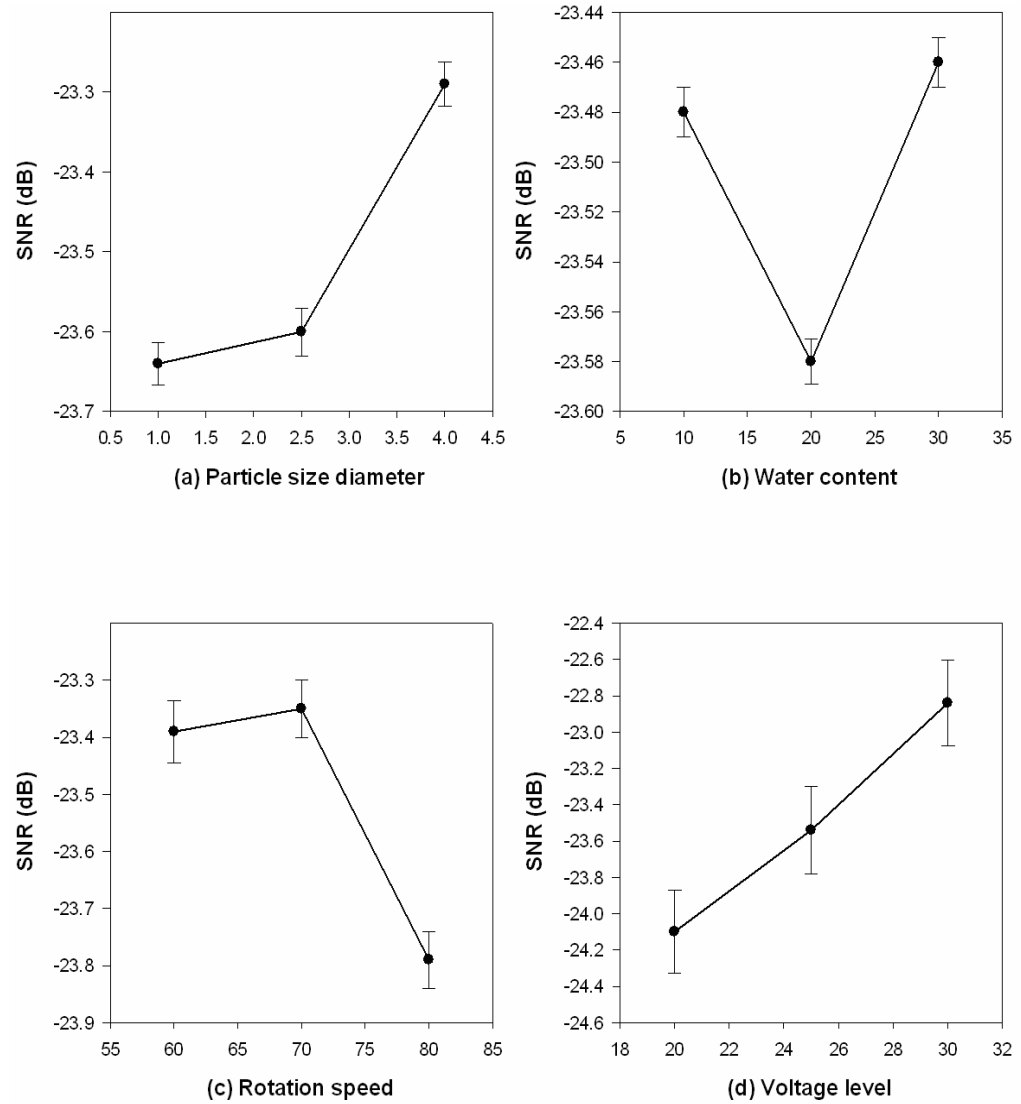
Figure 4.12: Effect of factors on SNR for minimal middling product.

4.2.3 Summary

The robust design targets to limit the negative impact of the hard-to-control random factors. The impacts of four factors, namely applied voltage, rotation speed, water content and particle size diagonal were determined. It

was noticeable that the applied voltage has a significant impact on effective recovery of food waste and reduction of middling product within the design range. Besides, the SNR analysis revealed that the abovementioned functions can be attained with 4.0 mm particle size of food waste and 20 % water content, which to result in less error from the variations of noise.

4.3   Optimisation and Modelling

The parametric studies described in previous section have been used to examine a number of system parameters of the electrostatic separator along with different mixing ratio. Nevertheless, it is impractical to study every potential parameter as it would be time-consuming and not cost-effectively. Optimisation plays a role for such purposes in this section so as to examine the parameters with great reduction of required experimental work.

A screening procedure by applying Plackett-Burman (PB) factorial design was performed to minimise the number of experiments for optimisation, and to indicate the significant parameters which influence the efficiency of the responses. The parameters of eight practical factors, namely potential level (F1), rotation speed (F2), corona electrode angle (F3), corona electrode distance (F4), electrostatic electrode distance (F5), %FW content in mixture (F6), mixture volume (F7), ambient temperature (F8), and three dummy factors (D1, D2 and D3) were depicted in Table 4.5. The responses of the FW separation efficiency (R1), middling product (R2) and NF separation efficiency (R3) were also tabulated in the table.

Table 4.5: Screening with PB factorial design

F1 (kV)	F2 (rpm)	F3 (°)	F4 (mm)	F5 (mm)	F6 (%)	F7 (g)	F8 (°C)	D1	D2	D3	R1 (%)	R2 (g)	R3 (%)
20	90	50	60	40	40	100	28	-1	1	1	74.5	18.5	86.2
30	60	50	60	50	40	100	24	1	-1	1	83.8	13.1	89.0
30	90	30	50	40	60	100	28	1	-1	1	59.7	36.7	68.8
20	90	30	60	50	40	200	28	1	-1	-1	57.5	37.1	66.6
20	90	50	50	50	60	200	24	-1	-1	1	74.8	20.6	86.4
30	60	50	60	40	60	200	28	-1	-1	-1	83.6	14.2	89.1
30	60	30	50	50	40	200	28	-1	1	1	64.5	33.2	68.4
20	60	30	50	40	40	100	24	-1	-1	-1	61.3	32.9	71.0
20	60	30	60	40	60	200	24	1	1	1	61.1	35.1	70.6
20	60	50	50	50	60	100	28	1	1	-1	76.5	18.3	89.5
30	90	50	50	40	40	200	24	1	1	-1	77.9	15.4	89.2
30	90	30	60	50	60	100	24	-1	1	-1	59.5	36.6	69.3

In order to identify the main effects on the responses, Pareto analysis was used to determine the influence of the independent factors (Zarei et al., 2010). As can be seen from the Pareto chart shown in Figure 4.13a, three factors were found to be statistically significant and above the t-value limit of the FW separation efficiency, i.e. the corona electrode angle, rotation speed and potential level. Likewise, the results for the middling product and NF separation efficiency were deduced. As shown in Figure 4.13b, the Pareto chart showed that the corona electrode angle, rotation speed and potential level account for majority of the total effect on the middling mass. The Pareto chart for the NF separation efficiency demonstrated that only two factors, namely the corona electrode angle and rotation speed, were significant and lied above the t-value as shown in Figure 4.13c. The ANOVA tables (Table 4.6 – 4.8) confirm the significance of the model for each response and its significant

factors at *p*-value less than 0.05 (Bashir et al., 2010). No outliers were found in the normal probability test.
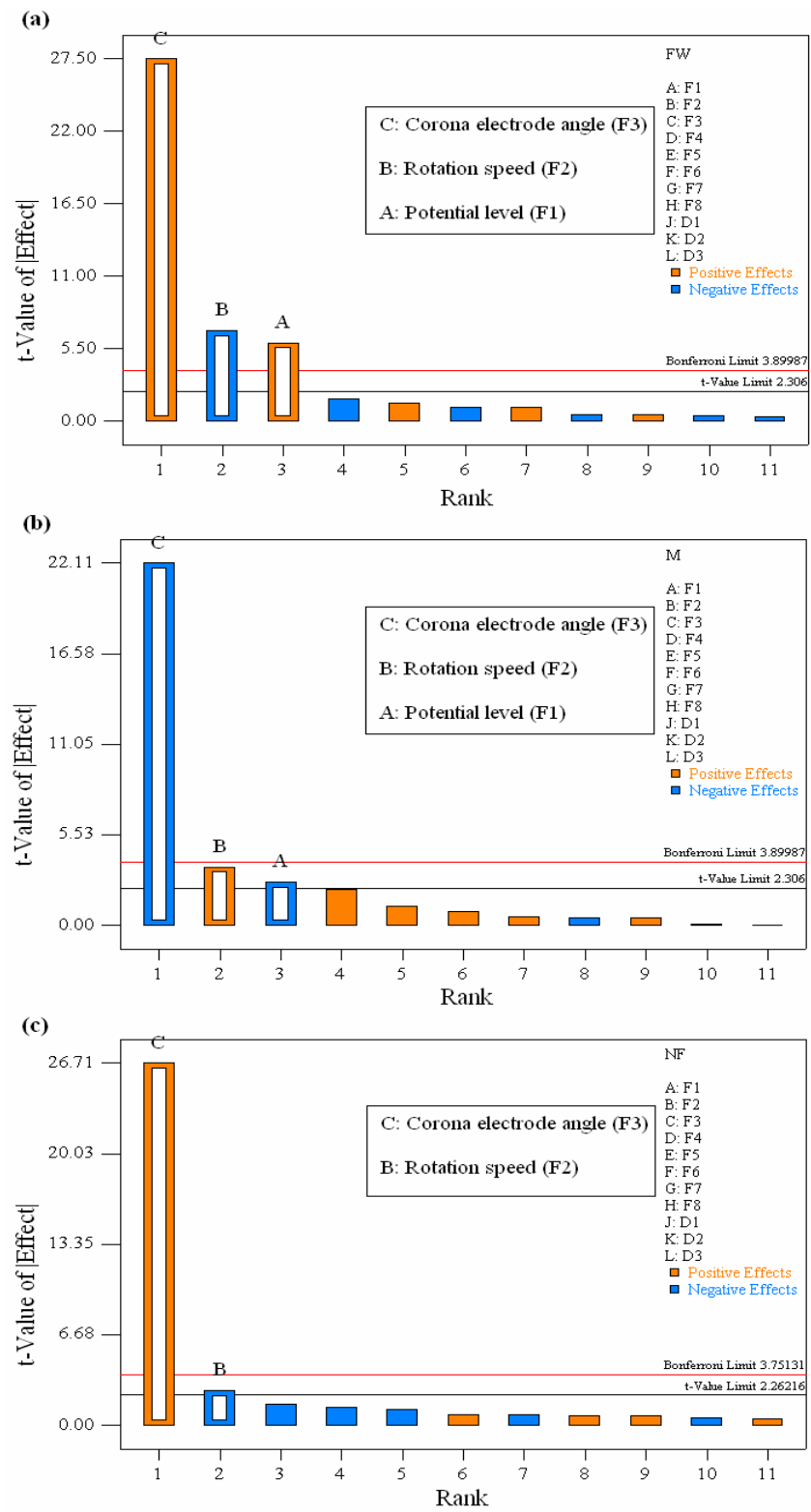
Figure 4.13: Pareto charts for (a) FW separation efficiency; (b) middling; (c) NF separation efficiency.

Table 4.6: ANOVA table for FW separation efficiency in PB design.

Source	Sum of squares	Degree of freedom	Mean square value	F-value	p-value
Model	1068.56	3	356.19	279.73	<0.0001
F1	45.24	1	45.24	35.53	0.0003
F2	60.30	1	60.30	47.36	0.0001
F3	963.02	1	963.02	756.30	<0.0001

Table 4.7: ANOVA table for middling product in PB design.

Source	Sum of squares	Degree of freedom	Mean square value	F-value	p-value
Model	1078.06	3	359.35	169.51	<0.0001
F1	14.74	1	14.74	6.95	0.0299
F2	27.30	1	27.30	12.88	0.0071
F3	1036.02	1	1036.02	488.69	<0.0001

Table 4.8: ANOVA table for NF separation efficiency in PB design.

Source	Sum of squares	Degree of freedom	Mean square value	F-value	p-value
Model	1106.61	2	553.30	359.96	<0.0001
F2	10.27	1	10.27	6.68	0.0295
F3	1096.34	1	1096.34	713.24	<0.0001

In particular, the potential level and corona electrode angle provided positive effect whereas the rotation speed gave the negative effect to the separation efficiency as shown in Figure 4.13a. However, in Figure 4.13b, the three factors exhibited an overall opposite effect on the middling product, and it indicated that the separation efficiency can be enhanced by minimising the middling product. It is in close agreement with our experiments which show

that the recovery of food waste increases with decreasing amount of unsorted middling for a given amount of each test sample. Therefore, the middling response is not included for further discussion, whereas separation efficiency is focused in the next section for performance optimisation.

4.3.1 Operational process design analysis and optimisation

The PB factorial design identified three significant factors to be optimised. The five factors that were not considered significant in the PB design were set to low level when performing the experiments for optimisation. A total of four responses was measured, namely FW separation efficiency (S_1), NF separation efficiency (S_2), FW separation purity (P_1) and NF separation purity (P_2). This study focused on optimising the separation conditions by employing the central composite design (CCD) approach.

Three independent variables, namely, electrical potential (A), rotation speed (B) and electrodes gap (C) were selected for the optimisation process. The CCD design of the experiment was used to evaluate the influence of the variables in 20 experiments, which consisted of 8 factorial points, 6 replica center points and 6 axial points. Table 4.9 shows the levels and ranges of the three independent variables involved. The CCD design matrix and the corresponding experimental results were summarised in Table 4.10.

Table 4.9: Experimental levels of independent process factors.

Levels	Variable		
	A: Potential level (kV)	B: Rotation speed (rpm)	C: Electrodes gap (mm)
$-\alpha$	16.59	49.77	39.77
Low (-1)	20.00	60.00	50.00
Center (0)	25.00	75.00	65.00
High (+1)	30.00	90.00	80.00
$+\alpha$	33.41	100.23	90.23

The CCD approach extends the α-distance to both low and high levels. These critical values of the potential level and rotation speed are still within the capability of experimental apparatus, whereas the electrodes gap is adjusted accordingly. Table 4.10 lists the experimental design matrix with the corresponding evaluated values for the separation efficiency and purity. The ANOVA results for quadratic models of S_1, S_2, P_1 and P_2 were tabulated in Tables 4.11 – 4.14, respectively, whereas the polynomial equations were deduced as equations 4.13 – 4.16.

Table 4.10: CCD for various experimental conditions.

Run	Factor			Response			
	A	B	C	S_1	S_2	P_1	P_2
	(kV)	(rpm)	(mm)	(%)	(%)	(%)	(%)
1	20.00	60.00	50.00	76.5	89.5	90.0	97.1
2	20.00	90.00	50.00	74.7	86.4	88.7	97.0
3	30.00	60.00	50.00	84.0	89.2	92.7	97.6
4	30.00	90.00	50.00	77.9	89.2	90.1	97.7
5	20.00	60.00	80.00	58.6	68.5	68.9	74.3
6	20.00	90.00	80.00	57.2	66.6	68.0	74.3
7	30.00	60.00	80.00	64.3	68.3	71.0	74.8
8	30.00	90.00	80.00	59.7	68.9	69.3	74.7
9	25.00	49.77	65.00	80.4	82.5	87.7	93.4
10	25.00	100.23	65.00	72.9	83.9	85.7	93.2
11	16.59	75.00	65.00	69.6	85.5	85.4	93.7
12	33.41	75.00	65.00	75.9	89.1	88.9	94.3
13	25.00	75.00	39.77	71.6	81.4	82.5	88.5
14	25.00	75.00	90.23	41.6	47.3	47.9	51.4
15	25.00	75.00	65.00	76.7	87.1	88.4	94.8
16	25.00	75.00	65.00	75.4	85.7	86.8	93.2
17	25.00	75.00	65.00	74.7	84.8	86.0	92.3
18	25.00	75.00	65.00	76.7	87.2	88.0	94.9
19	25.00	75.00	65.00	74.9	84.8	85.9	92.1
20	25.00	75.00	65.00	75.5	85.7	86.5	93.2

In order to demonstrate the empirical correlation between response S_1 and the independent factors, a second-order equation was deduced as follows:

$$S_1(\%) = -41.912 + 3.324A - 0.244B + 3.206C - 0.013AB$$

$$-0.034A^2 + 2.387 \times 10^{-3} B^2 - 0.029C^2 \qquad (4.13)$$

where S_1 was the separation efficiency of FW in terms of actual factors.

Besides, a polynomial equation was deduced for response S_2:

$$S_2(\%) = 1.364 - 1.715A + 3.599C$$

$$+ 0.024A^2 - 3.745 \times 10^{-3} B^2 - 0.033C^2 \qquad (4.14)$$

where S_2 was the separation efficiency of NF in terms of actual factors.

The purity of the FW separation, P_1 was represented by a quadratic polynomial in terms of the actual factors:

$$P_1(\%) = -9.914 + 0.130A - 0.0362B + 3.647C - 0.034C^2 \qquad (4.15)$$

Concerning the purity of the NF separation, P_2, the suggested model was quadratic and the final equation in terms of actual factors was determined as:

$$P_2(\%) = -1.784 + 3.981C - 0.036C^2 \qquad (4.16)$$

The factors with either synergistic or antagonistic effect on the response were decided based on the positive or negative signs of the regression coefficients. Tables 4.11 to 4.14 summarised the ANOVA results for the efficiency and purity of the models. The model F-values of 258.17, 242.32, 373.69 and 332.84 for responses S_1, S_2, P_1 and P_2 respectively, implied all the models were significant. The p-values were <0.0001 indicated the adequacy of the models. The predicted R-Squared value of 0.9796 was in close agreement with the adjusted R-Squared value of 0.9919 for S_1. The signal to noise ratio (adequate precision) of 65.257 indicated that the model

can be applied to navigate the design space. Like S_1, the predicted R-Squared of 0.9805 for S_2 was close to the adjusted R-Squared of 0.9913. Adequate precision of 58.178 (greater than 4) implied that the model S_2 could also be used in the design space navigation (Olmez, 2009). Regarding purity responses P_1 and P_2, not much difference was observed between the R-Squared values for both models.

Table 4.11: ANOVA results for quadratic model of S_1.

Source	Sum of squares	Degree of freedom	Mean square value	F-value	p-value	Remarks
Model	1885.29	9	209.48	258.17	<0.0001	Significant
A	63.70	1	63.70	78.51	<0.0001	Significant
B	51.47	1	51.47	63.44	<0.0001	Significant
C	1121.41	1	1121.41	1382.10	<0.0001	Significant
AB	7.03	1	7.03	8.67	0.0147	Significant
A^2	10.21	1	10.21	12.59	0.0053	Significant
B^2	4.15	1	4.15	5.12	0.0471	Significant
C^2	618.60	1	618.60	762.40	<0.0001	Significant
Residue	8.11	10	0.81			
Lack of fit	4.36	5	0.87	1.16	0.4370	Not significant
Pure error	3.75	5	0.75			
Cor Total	1893.41	19				

R-squared: 0.9957; Adj R-Squared: 0.9919; Pred R-square: 0.9796; Adeq precision: 65.257.

Table 4.12: ANOVA results for quadratic model of S_2.

Source	Sum of squares	Degree of freedom	Mean square value	F-value	p-value	Remarks
Model	2274.32	9	252.70	242.32	<0.0001	Significant
A	8.31	1	8.31	7.97	0.0181	Significant
C	1421.86	1	1421.86	1363.45	<0.0001	Significant
A^2	5.31	1	5.31	5.09	0.0477	Significant
B^2	10.23	1	10.23	9.81	0.0106	Significant
C^2	812.17	1	812.17	778.80	<0.0001	Significant
Residue	10.43	10	1.04			
Lack of fit	4.80	5	0.96	0.85	0.5672	Not significant
Pure error	5.63	5	1.13			
Cor Total	2284.75	19				

R-squared: 0.9954; Adj R-Squared: 0.9913; Pred R-square: 0.9805; Adeq precision: 58.178.

Table 4.13: ANOVA results for quadratic model of P_1.

Source	Sum of squares	Degree of freedom	Mean square value	F-value	p-value	Remarks
Model	2351.64	9	261.29	373.69	<0.0001	Significant
A	13.12	1	13.12	18.76	0.0015	Significant
B	7.12	1	7.12	10.19	0.0096	Significant
C	1486.68	1	1486.68	2126.16	<0.0001	Significant
C^2	823.34	1	823.34	1177.49	<0.0001	Significant
Residue	6.99	10	0.70			
Lack of fit	1.56	5	0.31	0.29	0.9016	Not significant
Pure error	5.43	5	1.09			
Cor Total	2358.63	19				

R-squared: 0.9970; Adj R-Squared: 0.9944; Pred R-square: 0.9917; Adeq precision: 74.855.

Table 4.14: ANOVA results for quadratic model of P_2.

Source	Sum of squares	Degree of freedom	Mean square value	F-value	p-value	Remarks
Model	2718.60	9	302.07	332.84	<0.0001	Significant
C	1729.68	1	1729.68	1905.90	<0.0001	Significant
C^2	959.35	1	959.35	1057.09	<0.0001	Significant
Residue	9.08	10	0.91			
Lack of fit	1.89	5	0.38	0.26	0.9158	Not significant
Pure error	7.19	5	1.44			
Cor Total	2727.68	19				

R-squared: 0.9967; Adj R-Squared: 0.9937; Pred R-square: 0.9910; Adeq precision: 68.008.

The good correlations R^2 value for the efficiency and purity models shown in Figures 4.14 and 4.15, respectively, indicated that there are only minor difference between the real values and the theoretical values. The p-values indicated the significance effect of the model, particularly when p-value is less than 0.05. It is apparent that all the models were highly significant as the p-values were <0.0001 (Tables 4.11 to 4.14). In addition, the quantitative impact of three independent factors was determined by their p-values. In the S_1 model, the significant model terms were identified as A, B, C, AB, A^2, B^2, C^2 with p-values <0.05 (Table 4.11). All the independent factors, i.e. A-potential level, B- rotation speed, C-electrode gap and second-order effect of C-electrode gap have high significance effect on the separation efficiency for p <0.0001. On the other hand, the parameters of A, C, A^2, B^2, C^2

are significant variables for the S_2 model. This model was mainly influenced by the second-order but less significantly by the first-order effect of B-rotation speed. The significant model terms for the P_1 model were found as A, B, C, C^2, whereas the significant terms for the P_2 model were C, C^2. It is worth to note that the purity models were mostly influenced by the C-electrode gap and its second-order effect, but not the interaction effects amongst A-potential level, B-rotation speed and C-electrode gap.

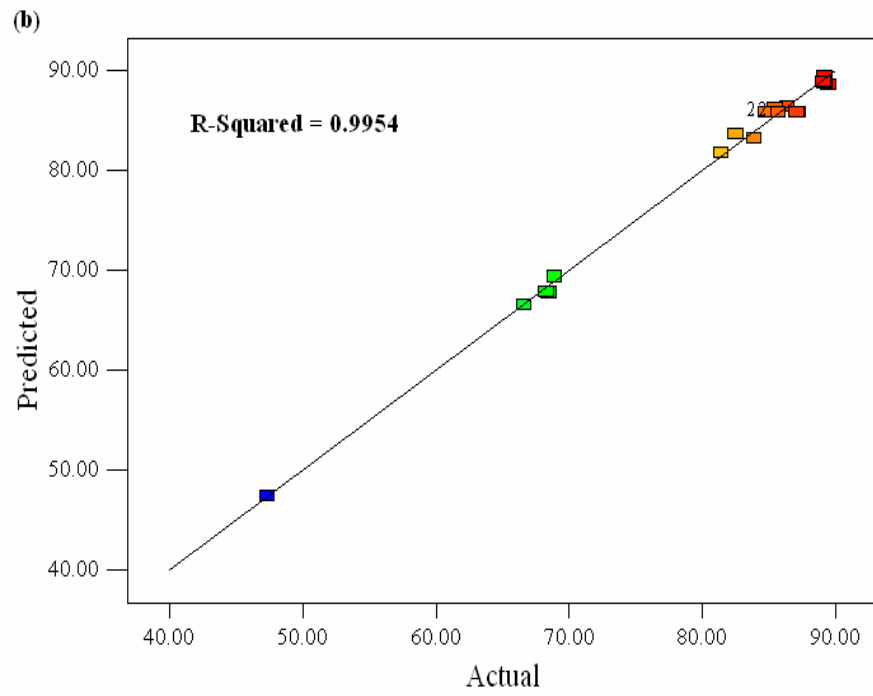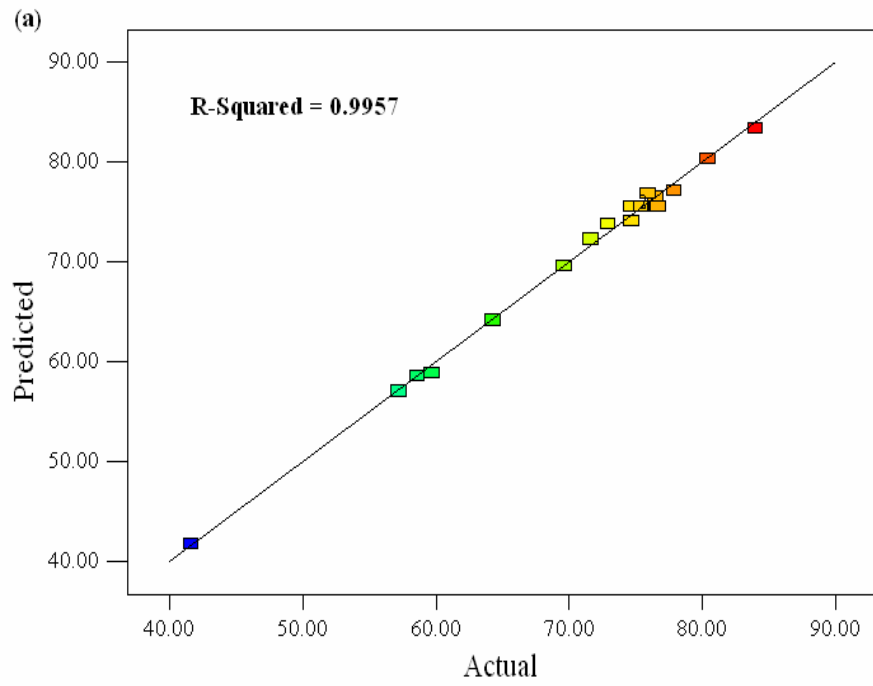Figure 4.14: Predicted values versus actual values. (a) FW separation
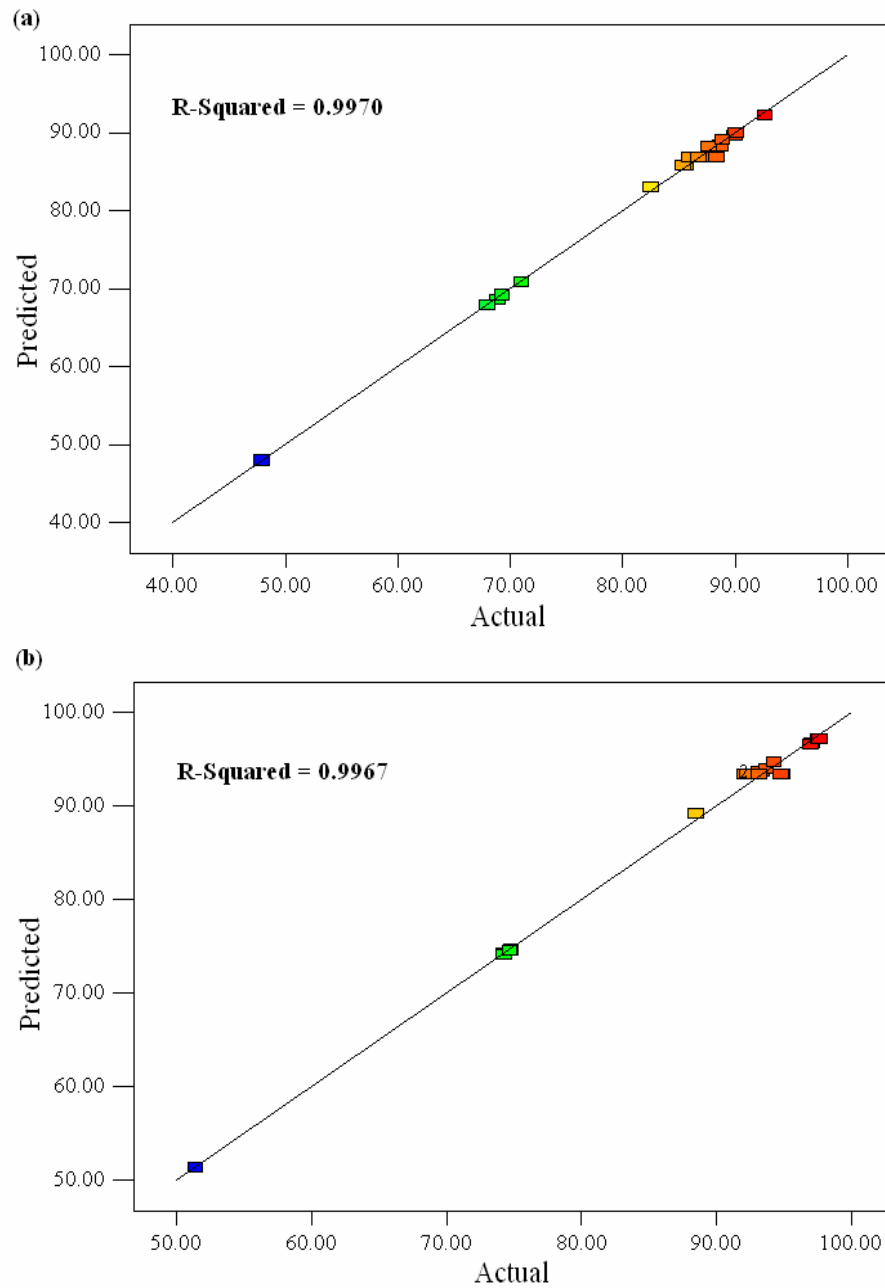efficiency; (b) NF separation efficiency.

Figure 4.15: Predicted values versus actual values. (a) FW separation purity; (b) NF separation purity.

4.3.2   Surface plot analysis

Three-dimensional surface plots were generated to further study the interactions between the independent factors *A*, *B*, *C* and the separation

conditions of the waste. The combined effects of factors *A* and *B* on the FW separation efficiency was shown in Figure 4.16a. It showed that at an electrode gap of 65 mm the separation efficiency increases with an increasing magnitude of potential level and decreases with an increasing speed of roller rotation. The surface plot indicated that the potential level has a synergistic effect on corona charging of the waste granules. For instance, the separation efficiency enhances from 69.6% to 76.7% with the increasing magnitude of potential level from 16.59 kV to 25.0 kV when the rotation speed is maintained at 75 rpm. The reason of this observation is that the size of the particle test sample is not uniform, and thus a larger coulomb force is required to treat the larger particles. It is generally known that Coulomb force relates positively with potential supplied. Compared with the potential level, the rotation speed demonstrated an antagonistic effect on the separation performance. It was noted that the separation efficiency decreased from 80.4% to 72.9% when the rotation speed increased from 49.77 rpm to 100.23 rpm and the potential level was maintained at 25 kV. The reason is that the value of the middling product increased with the increasing rotation speed (see Figure 4.13). The observed relation between the middling and rotation speed was in a good agreement with the work from other researchers (Wu et al., 2008). The highest value of separation efficiency of waste was obtained at the minimum rotation speed and potential level closed to 30.0 kV.

Figure 4.16b demonstrates the correlated effects of factors *A* and *B* on the FW separation efficiency with a constant speed of 75 rpm. It was obvious that the separation efficiency increased with increasing potential level,

indicating a stronger electrostatic field enhances the induction charging of conductive particles. For the electrode gap, the percentage of separation efficiency firstly rose with increasing gap from 50 mm to 60 mm, and then dropped progressively when the gap was beyond 60 mm. It indicated that 50 mm to 60 mm was the proper spacing to yield a uniformly extensive charge distribution to enhance the separation efficiency (Xu et al., 2009). Therefore, the efficiency dropped once it exceeded the proper range. Figure 4.16b also demonstrates that the potential level and electrode gap have the synergistic effect on the separation efficiency, and the highest value of efficiency could achieve at the maximum potential level with a proper spacing of electrodes approximately closed to 60 mm.

With a fixed potential level of 25 kV, the combined effects of factors B and C on the FW separation efficiency was shown in Figure 4.16c. It was apparent that the separation efficiency of waste decreased with increasing rotation speed when the electrode gap was less than 60 mm. The reason is that the unsorted middling increased with the rotation speed as discussed above. Moreover, Figure 4.16c shows that the separation efficiency decreased with increasing electrode gap after reaching the mentioned proper gap of 60 mm. It is attributed to the weaker charge on the test particles. The highest value of the FW separation efficiency was achieved at the minimum rotation speed with an electrode gap of approximately closed to 60 mm.

Comparatively, surface plots for models S_2, P_1 and P_2 were shown as respective three-dimensional diagrams in Figures 4.17 - 4.19. The diagrams

exhibited how each of the models varied as a function of two-factor (*A*-potential level and *B*-rotation speed, *A*-potential level and *C*-electrodes gap, *B*-rotation speed and *C*-electrodes gap) interaction. It was apparent in Figure 4.17a that the NF separation efficiency did not increase continually with increasing magnitude of potential level and rotation speed. This implies that the optimal design points should be identified in order to determine the optimal separation conditions.

Figure 4.16: Surface plots for combined effects of two independent factors on FW separation efficiency. (a) Potential level and rotation speed (electrodes gap = 65 mm); (b) Potential level and electrodes gap (rotation speed = 75 rpm); (c) Rotation speed and electrodes gap (potential level = 25 kV)

Figure 4.17: Surface plots for combined effects of two independent factors on

NF separation efficiency (a) Potential level and rotation speed (electrodes gap

= 65 mm); (b) Potential level and electrodes gap (rotation speed = 75 rpm); (c)

Rotation speed and electrodes gap (potential level = 25 kV)

Figure 4.18: Surface plots for combined effects of two independent factors on FW separation purity (a) Potential level and rotation speed (electrodes gap = 65 mm); (b) Potential level and electrodes gap (rotation speed = 75 rpm); (c) Rotation speed and electrodes gap (potential level = 25 kV)
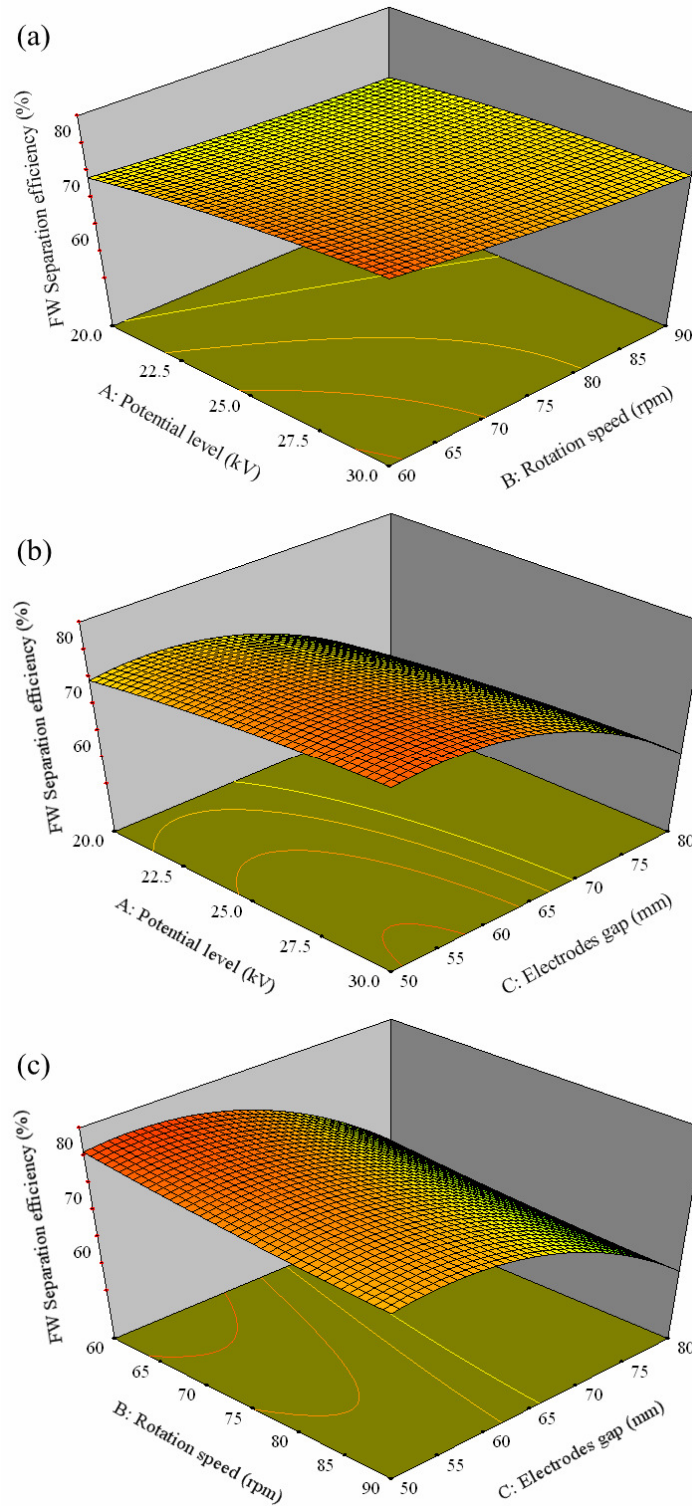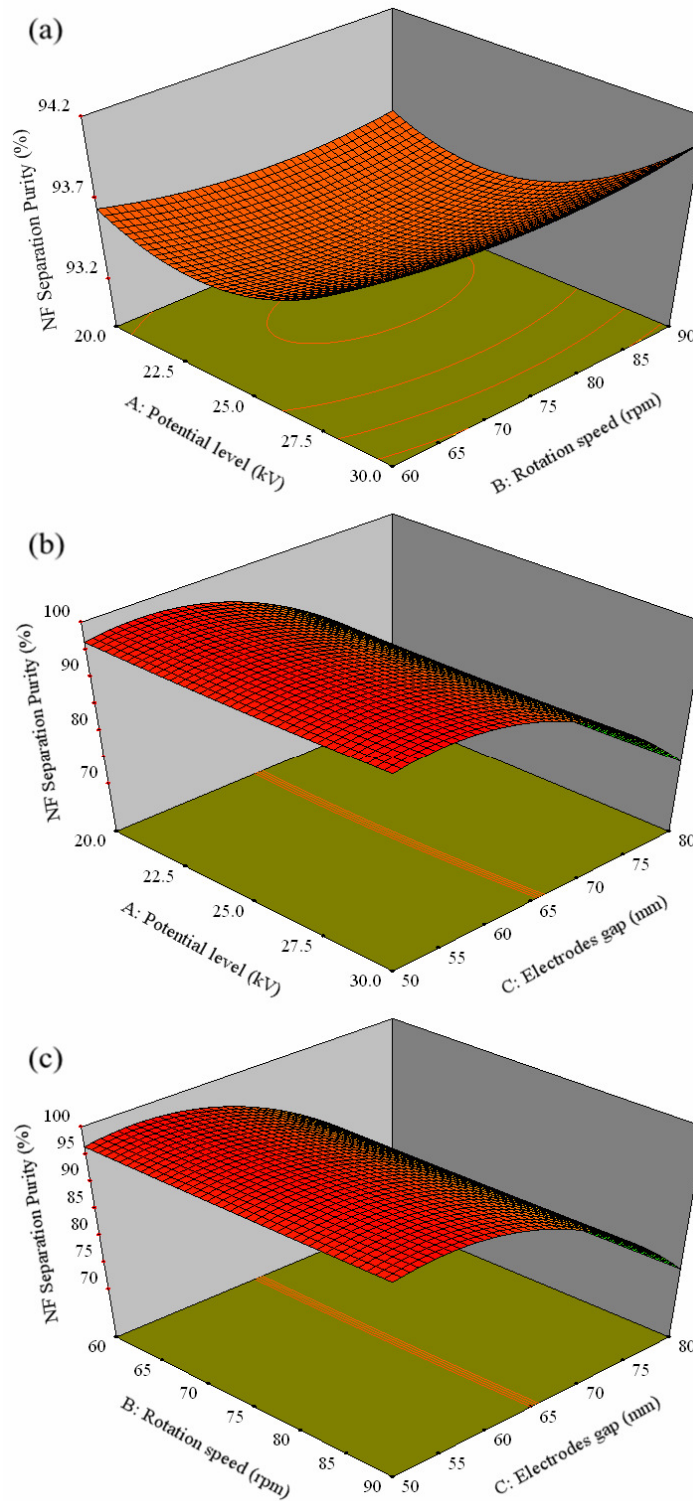
Figure 4.19: Surface plots for combined effects of two independent factors on

NF separation purity (a) Potential level and rotation speed (electrodes gap = 65

mm); (b) Potential level and electrodes gap (rotation speed = 75 rpm); (c)

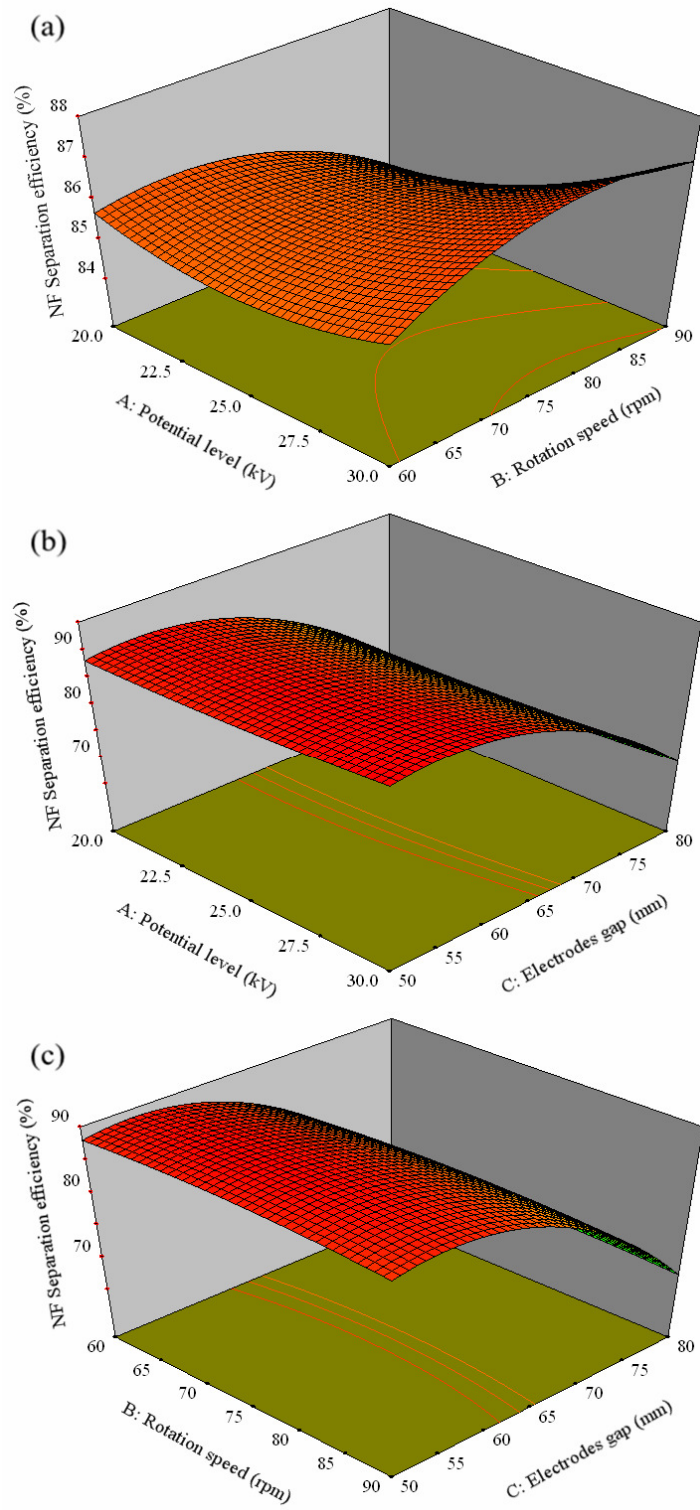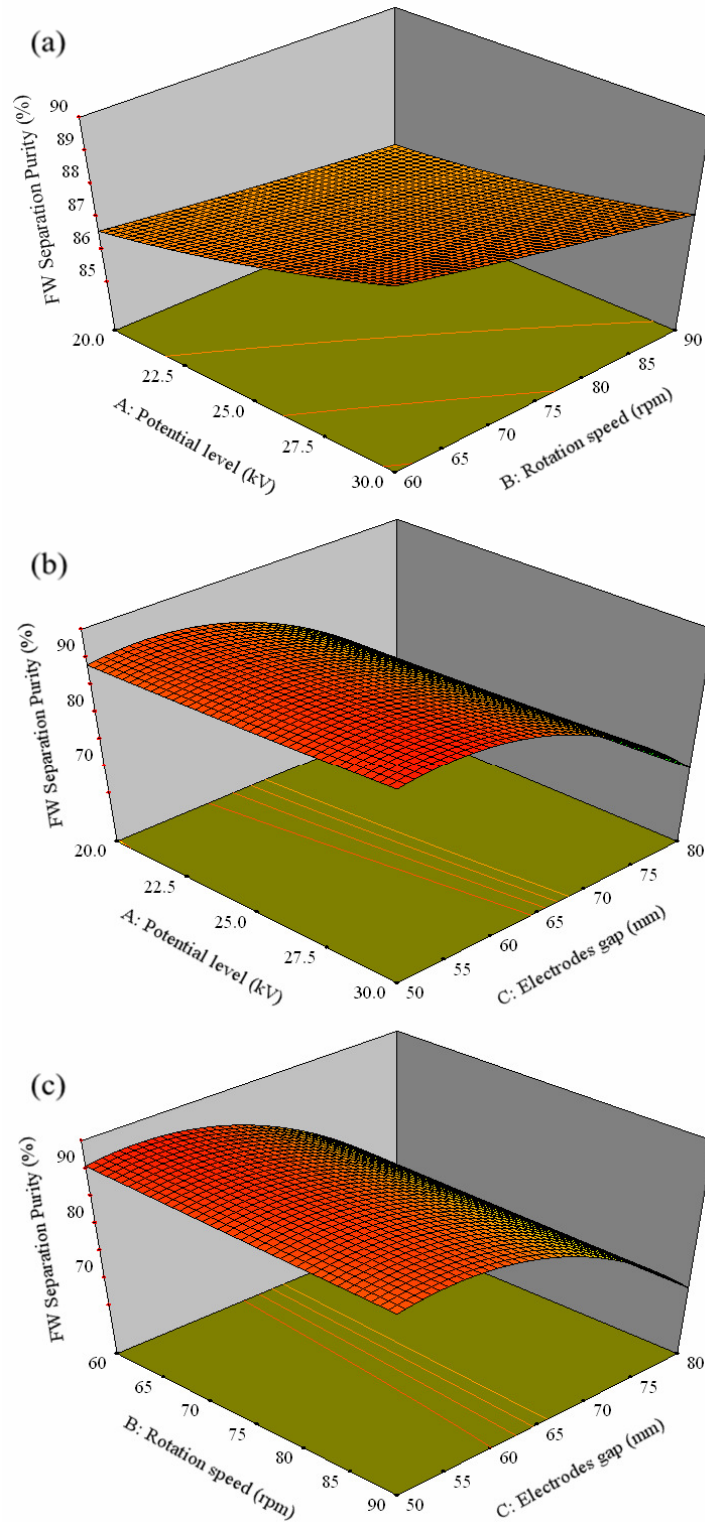Rotation speed and electrodes gap (potential level = 25 kV)

4.3.3   Model optimisation and validation

Optimisation was performed to identify the optimum operational conditions for electrostatic separation. This study defined the optimal separation conditions so as to have maximisation models of the separation efficiency (S_1, S_2) and purity (P_1, P_2). This allows the minimisation of unsorted and misclassified products. Based on the design range tabulated in Table 4.9, the optimal conditions were found at the potential level of 30 kV, roller rotation of 60 rpm and electrode gap of 54 mm. The minimum middling percentage of 12.7% (volume 100g) was also obtained. In order to validate the statistical experimental strategies, a triplicate set of experiments was performed at the specified optimum conditions and an average FW separation efficiency of 84.2% was achieved. A comparison between the observed and predicted values was summarised in Table 4.15. The experimental value agreed well with the predicted value. It indicated the validity of the model and the success of RSM in optimising the FW separation from waste mixture.

Table 4.15: Comparison results of observation and prediction.

Model	Observed value (%)	Predicted value (%)	Percentage of error (%)
FW separation efficiency	84.20	83.88	0.38
NF separation efficiency	88.70	89.51	0.91
FW separation purity	93.00	92.89	0.12
NF separation purity	98.50	97.97	0.54

4.3.4 Summary

The response surface methodology was used to optimise the separation conditions and to decide on the significant terms. Prior to optimisation, the PB screening procedure was applied to conclude that the separation conditions were mainly influenced by three factors (in the order of statistical significance): electrode gap, rotation speed and electrical potential level. Thus, the determination of optimal conditions was performed by employing the CCD approach. The CCD design shown that the three factors, namely A-potential level, B-rotation speed and C-electrode gap were statistically significant to the separation efficiency, whereas the C-electrode gap and its second-order effect played a key role for the separation purity. The optimum separation conditions were potential level / rotation speed / electrode gap = 30 kV / 60 rpm / 54 mm, and the maximum FW efficiency / NF efficiency / FW purity / NF purity was 84.2% / 88.7% / 93.0% / 98.5% with a minimum middling product of 12.7%. The quality control concerning the predictability of the model is very satisfactory.

CHAPTER FIVE

CONCLUSION AND FURTHER WORKS

5.1   Introduction

The work has extended the knowledge from electrostatic separator and provided discussion on improved separator configurations, which enhances the separation quality of food waste and non-food particles. The force model analysis which includes the centrifugal force, electrostatic force and corona image force was elucidated. The influential effects of the parameters on the separation efficiency have been described, and the variations of undesired random factors have been investigated. A mathematical surface model has been derived in this study, and the optimal operational condition was calculated from the model. Overall speaking, the results of this study have contributed to the fundamental knowledge required for future utilisation of practical electrostatically driven food waste separator.

5.2   Conclusion

The main findings of the study are summarised as follows:

1. Based on the force model, the applied voltage and rotation speed are the dominant factors of the separation process. Theoretically,

the increment of either or both factors enhances the separation efficiency of food waste at a predetermined angle of the corona electrode, γ. For non-food separation, the change of the applied voltage is associated with the value of the rotation speed, assuming the surface charge density and corona electrode angle are fixed.

2. Above the applied voltage of 15 kV, the separation efficiency and purity of both food and non-food particles enhanced with the increment of voltage. The recovered mass of food particles positively correlates to higher voltage and shorter angular position of electrodes, whereas the middling mass decreases in the same manner. The effect of the rotation speed is not able to predict from the parametric study.

3. The size and moisture of the particles affect the density, conductivity and surface resistivity, which in turn influent the separation results. Thus, the values of hard-to-control parameters of the particles should be fixed so as to minimise their impacts on the analysis of the system design factors.

4. The prediction from the response surface methodology confirms that the maximal separation result could be achieved at high voltage level under the optimal speed and angle. Although one may be able to further enhance the efficiency by utilising higher voltage, the optimisation model provides an alternative to reduce

the dependent on the costly power supply for generating a comparable outcome.

5.3   Further Work

The recommendations for further works are concluded as follows:

1. The electrostatic separator research could be extended to evaluate and recover other waste samples, e.g. food grain in order to reduce the waste disposal into the landfill. The relevant integrator system shall thus be studied.

2. The separation efficiency may be improved by employing a double roller design separator, or re-depositing the separated particles onto the roller for a second round of process.

3. The Life-Cycle Assessment could be performed to assess the balance point within the energy usage of the high voltage, energy generation of the biogas from the separated food waste, and also the return on investment of developing a large scale of separator based on the electrostatical method as described.

LIST OF REFERENCES

Aggarwal, A., Singh, H., Kumar, P. and Singh, M., 2010. Optimizing power consumption for CNC turned parts using response surface methodology and Taguchi's technique – A comparative analysis. *Journal of Materials Processing Technology*, 200, pp. 373-384.

Aman, F., Morar, R., Kohnlechner, R., Samuila, A. and Dascalescu, L., 2004. High-voltage electrode position: a key factor of electrostatic separation efficiency. *IEEE Transactions on Industry Applications*, 40(3), pp. 905-910.

Aravind, J., Lenin, C., Nancyflavia, C., Rashika, P. and Saravanan, S., 2015. Response surface methodology optimization of nickel (II) removal using pigeon pea pod biosorbent. *International Journal of Environmental Science and Technology*, 12, pp. 105-114.

Badgie, D., Samah, M.A.A., Manaf, L.A. and Muda, A.B., 2011. Assessment of municipal solid waste composition in Malaysia: Management, practice and challenges. *Polish Journal of Environmental Studies*, 21, pp. 539-547.

Basavarajappa, S., Chandramohan, G. and Davim, J.P., 2008. Some studies on drilling of hybrid metal matrix composites based on Taguchi techniques. *Journal of Materials Processing Technology*, 1(3), pp. 332-338.

Bashir, M.J.K., Aziz, H.A., Yusoff, M.S., Aziz, S.Q. and Mohajeri, S., 2010. Stabilized sanitary landfill leachate treatment using anionic resin: Treatment optimization by response surface methodology. *Journal of Hazardous Materials*, 182, pp. 115-122.

Bashir, M.J.K, Aziz, H.A., Yusoff, M.S. and Adlan, M.N., 2010. Application of response surface methodology (RSM) for optimizatio of ammoniacal nitrogen removal from semi-aerobic landfill leachate using ion exchange resin. *Desalination*, 254, pp. 154-161.

Bendaoud, A., Tilmatine, A., Medles, K., Rahli, M., Huzau, M. and Dascalescu, L., 2008. Charaterization of dual corona-electrostatic electrodes for electrostatic processes applications. IEEE Transactions on Industry Applications, 44(3), pp. 692-698.

Besseris, G.J., 2014. Multi-response non-parametric profiling using Taguchi's qualimetric engineering and neurocomputing methods: Screening a foaming process in a solar collector assembly. *Applied Soft Computing*, 22, pp. 222-237.

Calin, L., Neamtu, V., Morar, R., Iuga, A., Samuila, A. and Dascalescu, L., 2008. Tribocharging of granular plastic mixtures in view of electrostatic separation. *IEEE Transactions on Industry Applications*, 44(4), pp. 1045-1051.

Camposeco-Negrete, C., 2013. Optimization of cutting parameters for minimizing energy consumption in turning of AISI6061 T6 using Taguchi methodology and ANOVA. *Journal of Cleaner Production*, 53, pp. 195-203.

Chang, J.S., Crowley, J.M. and Kelly, A.J., 1995. *Handbook of Electrostatic Processes*, Marcel Dekker Inc.: New York.

Chian, E.S. and De Walle, F.B., 1976. Sanitary landfill leachates and their treatment. *Journal of Environmental Engineering (ASCE)*, 102, pp. 411-431.

Chiang, M.Y. and Hsieh, H.H., 2009. The use of the Taguchi method with grey relational analysis to optimize the thin-film sputtering process with multiple quality characteristic in color filter manufacturing. *Computers & Industrial Engineering*, 2, pp. 648-661.

Chou, C.S., Ho, C.Y. and Huang, C.I., 2009. The optimum conditions for combination of magnetic particles driven by a rotating magnetic field using the Taguchi method. *Advanced Powder Technology*, 20(1), pp. 55-61.

Christensen, T.H., Kjeldsen, P., Bjerg, P.L., Jensen, D.L., Christensen, J.B., Baun, A., Albrechtsen, H.J. and Heron, G., 2001. Biogeochemistry of landfill leachate plumes. *Applied Geochemistry*, 16, pp. 659-718.

Chua, K.H., Sahid, E.J.M., Leong, Y.P., 2011. Sustainable municipal solid waste management and GHG abatement in Malaysia. *Green and Energy Management*, 04-02, pp. 1-8.

Comakli, K, Simsek, F., Comakli, O. and Sahin, B., 2009. Determination of optimum working conditions R22 and R404A refrigerant mixtures in heat-pumps using Taguchi method. *Applied Energy*, 86(11), pp. 2451-2458.

Dascalescu, L., Samuila, A., Mihalcioiu, A., Bente, S. and Tilmatine, A., 2005. Robust design of electrostatic separation process. *IEEE Transactions on Industry Applications*, 41(3), pp. 715-719

Dascalescu, L., 2008. Robust corona-electrostatic separation method for solid waste recycling. *International Journal of Environment and Waste Management*, 2(4/5), pp. 423-435.

Davidson, M.J., Balasubramaniam, K. and Tagore, G.R.N., 2008. Experimental investigation on flow-forming of AA6061 alloys a Taguchi approach. *Journal of Materials Processing Technology*, 1(3), pp. 283-287.

Desideri, U., Di Maria, F., Leonardi, D. and Proietti, S., 2003. Sanitary landfill energetic potential analysis: A real case study. *Energy Conversion and Management*, 44, pp. 1969-1981.

Elder, J., Yan, E. and Raiser, G., 2003. eForce - Newest generation of electrostatic separator for the mineral sands industry. In: Heavy Minerals Conference. South Africa Institute of Mining and Metallurgy.

FAOSTAT, 2012. *Food Balance Sheets 2009*. [online] Available at: <http://faostat.fao.org/site/354/default.aspx> [Accessed 20 August 2012].

Galway Country Council, 2013. Waste Management. [online] Available at: <http://www.galway.ie/en/Services/Environment/WasteManagement/> [Accessed 22 March 2013].

Garnett, T., 2006. *Fruit and vegetables and UK greenhouse gas emissions: Exploring the relationship*. UK: Food and Climate Research Network, University of Surrey.

Gustavsson, J., 2010. *The Climate Change Impact of Retail Waste from Horticultural Products*. MSc. University of Gothenburg, Sweden.

Harper, W.R., 1967. *Contact and frictional electrification. Monographs on the Physics and Chemistry of Materials*. Clarendon Press: Oxford.

Holm-Nielsen, J.B., Al Seadi, T., Oleskowicz-Popiel, P., 2009. The future of anaerobic digestion and biogas utilization. *Bioresource Technology*, 100, pp. 5478-5484.

Hou, S., Wu, J., Qin, Y and Xu, Z., 2010. Electrostatic separation for recycling waste printed circuit board: a study on external factor and a robust design for optimization. *Environmental Science & Technology*, 44, pp. 5177-5181.

Hsu, W.H., Chao, C.K., Hsu, H.C., Lin, J. and Hsu, C.C., 2009. Parametric study on the interface pullout strength of the vertebral body replacement cage using FEM-based Taguchi method. *Medical Engineering & Physics*, 31(3), pp. 287-294.

Iuga, A., Morar, R., Dascalescu, L., Samuila, A. and Rafiroiu, D., 1993. A new type of corona electrode for high-tension separators. *Magnetic and Electrical Separation,* 4, pp. 75–90.

Iuga, A., Morar, R., Samuila, A. and Dascalescu, L., 2001. Electrostatic separation of metals and plastics from granular industrial wastes. *IEE Proceedings - Science, Measurement and Technology*, 148(2), pp. 47–54.

Iuga, A., Cuglesan, I., Samuila, A., Blajan, M., Vadan, D. and Dascalescu, L., 2004. Electrostatic separation of muscovite mica from feldspathic pegmatics. *IEEE Transactions on Industry Applications*, 40(2), pp. 422-429.

Jaffrin, A., Bentounes, N., Joan, A.M. and Makhlouf, S., 2003. Landfill biogas for heating greenhouses and providing carbon dioxide supplement for plant growth. *Biosystems Engineering*, 86, pp. 113-123.

Kathirvale, S., Muhd Yunus, M.N., Sopian, K. and Samsuddin, A.H., 2004. Energy potential from Municipal Solid Waste in Malaysia. *Renewable Energy*, 29(4), pp. 559-567.

Keles, O., 2009. An optimization study on the cementation of silver with copper in nitrate solutions by Taguchi design. *Hydrometallurgy*, 95, pp. 333-336.

Kiewiet, C., Bergougnou, M.A. and Brown, J.D., 1978. Electrostatic separation of fine particle in vibrates fluidized beds. *IEEE Transactions on Industry Applications*, 6, pp. 526-530.

Kjeldsen, P., Barlaz, M.A., Rooker, A.P., Baun, A., Ledin, A. and Christensen, T.H., 2002. Present and long-term composition of MSW landfill leachate: A

review. *Critical Reviews in Environmental Science and Technology*, 32, pp. 297-336.

Kofoworola, O.F., 2007. Recovery and recycling practices in municipal solid waste management in Lagos, Nigeria. *Waste Management*, 27, pp. 1139-1143.

Lawver, J.E. and Dyrenforth, W.P., 1973. *Electrostatic separation in electrostatics and its applications*. New York: Wiley.

Le Man, H., Behera, S.K. and Park, H.S., 2010. Optimization of operational parameters for ethanol production from Korean food waste leachate. *International Journal of Environmental Science and Technology*, 7, pp. 157-164.

Lee, C.-Y. and Lee, Z.-J., 2012. A novel algorithm applied to classify unbalanced data. *Applied Soft Computing*, 12(8), pp. 2481-2485.

Li, J., Lu, H., Guo, J., Xu, Z. and Zhou, Y., 2007. Recycle technology for recovering resources and products from waste printed circuit boards. *Environmental Science and Technology*, 41, pp. 1995-2000.

Lin, C.S.K., Pfaltzgraff, L.A., Herrero-Davila, L., Mufobu, E.B., Abderrahim, S., Clark, J.H. et al., 2013. Food waste as a valuable resource for the production of chemicals, materials and fuels. Current situation and global perspective, *Energy & Environmental Science*, 6(2), pp. 426-464.

Lin, Y.C., Chen, Y.F., Wang, D.A. and Lee, H.S., 2009. Optimization of machining parameters in magnetic force assisted EDM based on Taguchi method. *Journal of Materials Processing Technology*, 7, pp. 3374-3383.

Lindmark, J., Leksell, N., Schnürer, A. and Thorin, E., 2012. Effects of mechanical pre-treatment on the biogas yield from ley crop silage. *Applied Energy*, 97, pp. 498-502.

Lu, H., Li, J., Guo, J., Xu, Z., 2008. Movement behavior in electrostatic separation: Recycling of metal materials from waste printed circuit board. *Journal of Materials Processing Technology*, 197, pp. 101-108.

Magdalena, V. and Dana, A., 2014. Can vegetation indicate a municipal solid waste landfill's impact on the environment? *Polish Journal of Environmental*

Studies, 23(2), pp. 501-509.

Mahapatra, S.S., Patnaik, A. and Satapathy, A., 2008. Taguchi method applied to parametric appraisal of erosin behaviour of GF-reinforced polyester composites. *Wear*, 1(2), pp. 214-222.

Manaf, L.A., Samah, M.A.A., Zukki, N.I.M., 2009. Municipal Solid Waste management in Malaysia: Practice and challenges. *Waste Management*, 29, pp. 2902-2906.

Masui, N., 1982. Electrostatic separation for removal from green tea of stems and from food of impurities. *Proceedings of the IEJ*, 6(3), pp.159-162.

McMilan, J.D., 1997. Bioethanol production: status and prospects. *Renewable Energy*, 10, pp. 295-302.

Meen-Chee, H. and Narayanan, S., 2006. Restoring the shine to a pearl: Recycling behaviour in Penang, Malaysia. *Development and Change*, 37, pp. 1117-1136.

Mohabuth, N. and Miles, N., 2005. The recovery of recyclable materials from waste electrical and electronic equipment (WEEE) by using vertical vibration separation. *Resources, Conservation and Recycling*, 45(1), pp. 60-69.

Moukamnerd, C., Kawahara, H. and Katakur, Y., 2013. Feasibility study of ethanol production from food Wastes by consolidated continuous solid-state fermentation. *Journal of Sustainable Bioenergy Systems*, 3, pp. 143-148.

Murata, Y., Masui, N., Miyazawa, S. and Inculet, I.I., 1982. Non-uniform AC field electrostatic separator. In: Conference paper of the IEJ, pp. 293-294.

National Solid Waste Management Department, 2013. [online] Available at: <http://www.kpkt.gov.my/jpspn_en_2013/main.php> [Accessed 11 June 2013].

Parfitt, J., Barthel, M. and Macnaughton, S., 2010. Food waste within food supply chains: quantification and potential for change to 2050. *Philosophical Transactions of the Royal Society*, 365, pp. 3065-3081.

Periathamby, A., Hamid, F.S. and Khidzir, K., 2009. Evolution of solid waste management in Malaysia: Impacts and implications of the solid waste bill, 2007. *Journal of Material Cycles and Waste Management*, 11, pp. 96-103.

Ravishankar, S.A. and Kolla, H., 2009. Chemical enhanced electrostatic separation. In: 7th International Heavy Mineral Conference 'What next', The South African Institute of Mining and Metallurgy, pp.203-206.

Renou, S., Givaudan, J.G, Poulain, S., Dirassouyan, F. and Moulin, P., 2008. Landfill leachate treatment: Review and opportunity. *Journal of Hazardous Materials*, 150, pp. 468-493.

Rezouga, M., Tilmatine, A., Ouiddir, R. and Medles, K., 2009. Experimental modelling of the breakdown voltage of air using design of experiments. *Advances in Electrical and Computer Engineering*, 9, pp. 41-45.

Ruan, J. and Xu, Z., 2012. Approaches to improve separation efficiency of eddy current separation for removing aluminium from waste toner cartridges. Environmental Science and Technology, 46, pp. 6214-6221.

Saeed, M.O., Hassan, M.N. and Mujeebu. M.A., 2009. Assessment of municipal solid waste generation and recyclable materials potential in Kuala Lumpur, Malaysia. *Waste Management*, 19, pp. 2209-2213.

Samsudin, M.D.M. and Don, M.M., 2013. Municipal solid waste management in Malaysia: Current practices, challenges and prospect, *Jurnal Teknologi*, 62(1), pp. 95-101.

Samuila, A., Urs, A., Iuga, A., Morar, R., Aman, F. and Dascalescu, L., 2005. Optimization of corona electrode position in roll-type electrostatic separators. *IEEE Transactions on Industry Applications*, 41(2), pp. 527-534.

Schütze, A., James, Y.J., Steven, E.B., Park, J.Y., Gary, S.S. and Robert, F.H., 1998. The atmospheric pressure plasma jet: A review and comparison to other plasma sources. *IEEE Transactions on Plasma Science*, 26(6), pp. 1685-1694.

Senthilkumar, K., Senthikumaar, J.S. and Srinivasan, A., 2013. Reducing surface roughness by optimising the turning parameters. *The South African Journal of Industrial Engineering*, 24(2), pp. 78-87.

Srinu Naik, S. and Pydi Setty, Y., 2014. Optimization of parameters using response surface methodology and genetic algorithm for biological denitrification of wastewater. *International Journal of Environmental Science and Technology*, 11, pp. 823-830.

Stuart, T., 2009. *Waste - Uncovering the global food scandal*. New York: W.W. Norton and Company.

Tagaris, E., Sotiropoulou, R.E.P., Pilinis, C. and Halvadakis, C.P., 2003. A methodology to estimate odors around landfill sites: The use of methane as an odor index and its utility in landfill sitting. *Journal of the Air and Waste Management Association*, 53, pp. 629-634.

Taguchi, G., 1986. *Introduction to quality engineering: designing quality into products and processes*. Tokyo: Asian Productivity Organization.

Taherzadeh, M.J. and Karimi, K., 2008. Pretreatment of lignocellulosic wastes to improve ethanol and biogas production: a review. *International Journal of Molecular Sciences*, 9, pp. 1621–1651.

Tammemagi, H.Y. and Tammemagi, H., 1999. *The waste crisis: landfills, incinerators, and the search for a sustainable future*. New York: Oxford University Press.

Toraguchi, M. and Haga, K., 1982. Electrostatic separation of coal. *Proceedings of the IEJ*, 6(3), pp.139-147

Van Wyk, J.P.H, 2001. Biotechnology and the utilization of biowaste as a resource for bioproduct development. *Trends in Biotechnology*, 19(5), pp. 172-177.

Vavouraki, A.I., Volioti, V. and Kornaros, M.E., 2014. Optimization of thermo-chemical pretreatment and enzymatic hydrolysis of kitchen wastes. *Waste Management*, 34, pp. 167-173.

Veit, H.M., Diehl, T.R., Salami, A.P., Rodrigues, J.S., Bernardes, A.M. and Tenorio, J.A.S., 2005. Utilization of magnetic and electrostatic separation in the recycling of printed circuit boards scrap. *Waste Management*, 25, pp. 67-74.

Vlad, I., Campeanu, A., Enache, S. and Petropol, G., 2014. Operation

characteristics optimization of low power three-phase asynchronous motors. *Advances in Electrical and Computer Engineering*, 14, pp. 87-92.

Wagenaars, E., 2006. *Plasma breakdown of low-pressure gas discharges*. PhD, Technische Universiteit Eindhoven, Eindhoven.

Wang, Q., Ma, H., Xuc, W., Gong, L., Zhang, W. and Zou, D., 2008. Ethanol production from kitchen garbage using response surface methodology. *Biochemical Engineering Journal*, 39, pp. 604-610.

Weitz, K.A., Thorneloe, S.A., Nishtala, S.R., Yarkosky, S. and Zannes, M., 2002. The impact of municipal solid waste management on greenhouse gas emissions in the United States. *Journal of the Air and Waste Management Association*, 52(9), pp. 1000-1011.

Whalen, S.C., Reeburgh, W.S. and Sandbeck, K.A., 1990. Rapid methane oxidations in a landfill cover soil. *Applied and Environmental Microbiology*, 56, pp. 3405-3411.

Wu, J., Li, J. and Xu, Z., 2008. Electrostatic separation for multi-size granule of crushed printed circuit board waste using two-roll separator. *Journal of Hazardous Materials*, 159, pp. 230-234.

Xu, C., Chen, W. and Hong, J., 2014. Life-cycle environmental and economic assessment of sewage sludge treatment in China. *Journal of Cleaner Production*, 67, pp. 79-87.

Xu, Z.M., Li, J., Lu, H.Z. and Wu, J., 2009. Dynamics of conductive and nonconductive particles under high-voltage electrostatic coupling fields. *Sciences in China Series E: Technological Sciences*, 52(8), pp. 2359-2366.

Xue, M., Li, J. and Xu, Z., 2012. Environmental friendly crush-magnetic separation technology for recycling metal-plated plastics from end-of-life vehicles. Environmental Science and Technology, 46, pp. 2661-2667.

Yamane, L.H., de Moraes, V.T., Espinosa, D.C.R. and Tenório, J.A.S., 2011. Recycling of WEEE: Characterization of spent printed circuit boards from mobile phones and computers. *Waste Management*, 31(12), pp. 2553-2558.

Younes, M., Tilmatine, A., Medles, K., Rahli, M., and Dascalescu, L., 2007.

Numerical modeling of conductive particle trajectories in roll-type corona-electrostatic separators. *IEEE Transactions on Industry Applications*, 43(5), pp. 1130-1136.

Zarei, M., Niaei, A., Salari, D. and Khataee, A., 2010. Application of response surface methodology for optimization of peroxi-coagulation of textile dye solution using carbon nanotube-PTFE cathode. *Journal of Hazardous Materials*, 173 (1–3), pp. 544–551.

LIST OF ORIGINAL PUBLICATIONS

Journal publications:

1. **KoonChun Lai**, SooKing Lim, PehChiong Teh, KimHo Yeap (2015). Modeling and optimization of biowaste segregation from MSW: An approach of landfills treatment and reduction, *Research Journal of Applied Sciences, Engineering and Technology*. (Scopus indexed, in press)

2. **KoonChun Lai**, SooKing Lim, PehChiong Teh (2015). Optimization of electrostatic separation process for maximizing biowaste recovery using Taguchi method and ANOVA, *Polish Journal of Environmental Studies*, 24(3). DOI: 10.15244/pjoes/30927 (ISI indexed, in press)

3. **KoonChun Lai**, SooKing Lim, PehChiong Teh, Kimho Yeap (2014). Key factors of the electrostatic separator for solid waste segregation, *ScienceAsia*. (ISI indexed, in press)

4. **KoonChun Lai**, SooKing Lim, PehChiong Teh (2014). Electrostatic separation in recovering the food from solid waste, *World Applied Sciences Journal*, 32(7): 1296-1303. (Scopus indexed)

Conference papers:

1. **KoonChun Lai**, SooKing Lim, PehChiong Teh (2014). Optimization of the electrostatic separator for food waste segregation, *International Conference on Mathematics, Engineering and Industrial Applications (ICoMEIA 2014)*, Penang, Malaysia, 28 – 30 May 2014. (Paper ID 211)

2. **KoonChun Lai**, SooKing Lim, PehChiong Teh (2013). Application and optimization of a plasma discharge bubble jet for water treatment, *Proceedings of 6th International Engineering Conference, Energy and Environment (ENCON 2013)*, Sarawak, Malaysia, 1 – 4 July 2013, ISBN: 978-981-07-6059-5, pp. 187 – 192.

3. **KoonChun Lai**, SooKing Lim, PehChiong Teh, KimHo Yeap, YunThung Yong (2013). Study of a plasma discharge bubble jet: Design and optimization in water treatment, *8th International*

Conference on Multiphase Flow (ICMF), Jeju, South Korea, 26 – 31 May 2013.

4. **Lai Koon Chun**, Lim Soo King, Aissa Boudjella and Yeap Kim Ho (2011). Protection against human body electrostatic discharge in manufacturing, *Advanced Process and System in Manufacturing (APSIM)*, Kuala Lumpur, Malaysia, 14 – 15 December 2011, Paper AP62.